Activity of Bifunctional Motoneurons during Fictive Locomotion:

A Computational Modeling Study

A Thesis

Submitted to the Faculty

of

Drexel University

by

Khaldoun Chaouki Hamade

in partial fulfillment of the

requirements for the degree

of

Doctor of Philosophy

August 2010

Dedications

Dedicated to my parents

for their commitment, understanding, and continued encouragement.

Acknowledgments

I would like to thank my research supervisor Dr. Ilya Rybak for his support, supervision, guidance and patience. His advice and help made this research possible. I would also like to express my gratitude to Dr. Natalia Shevtsova and Dr. Sergey Markin for their help and guidance in conducting my research.

I owe Dr. Rahamim Seliktar, my academic adviser, a great deal of appreciation for keeping me on track with my academic requirements and helping me with my career decisions since the day I applied to Drexel University.

I would also like to thank Dr. Karen Moxon for her advice and help.

Table of Contents

List of Tables

List of Figures

Abstract
Activity of Bifunctional Motoneurons during Fictive Locomotion:
A Computational Modeling Study
Khaldoun Chaouki Hamade
Ilya A. Rybak, Ph.D

More than 90 years ago, Graham Brown demonstrated that the cat spinal cord can generate a locomotor rhythm in the absence of input from higher brain centers and afferent feedback, and proposed a general schematic for the spinal central pattern generator (CPG) generating rhythmic alternating activity of flexor and extensor motoneurons during locomotion, the "half-center" model. Since that time, the half-center concept has been used as the basis in many CPG models. Despite many advantages, classical half-center models of the locomotor CPG have been so far unable to reproduce and explain the generation of more complex activity patterns expressed during locomotion by some bifunctional motoneurons actuating muscles controlling more than one joint, such as posterior biceps and semitendinosus (PBSt) and rectus femoris (RF), which were found to be active within a portion of one phase or generated activity during both phases. During normal locomotion, the activity patterns of PBSt and RF are modulated by supra-spinal inputs and afferent feedback and vary with gate and locomotor conditions. However, even during fictive locomotion in the absence of afferent feedback and patterned supra-spinal inputs, PBSt and RF demonstrate a variety of complex activity patterns, similar to those observed in real locomotion under different conditions. This suggests that the complex patterns of bifunctionals are defined by the intrinsic spinal CPG organization. The non-trivial activity profiles expressed by bifunctional motoneurons have been considered as a strong argument against a bipartite half-center

organization of the spinal locomotor CPG. The challenging task of this study was to find and propose a neural organization of the spinal locomotor CPG that is able to reproduce the full repertoire of PBSt and RF activities observed during fictive locomotion within the framework of the bipartite organization of the locomotor CPG, implement it in a computational model, and validate the model by reproducing the behavior of bifunctional motoneurons during various types of deletions occurring during fictive locomotion. This study represents a significant step towards understanding the organization of the mammalian spinal locomotor CPG, shaping complex patterns of bifunctional motoneurons, and offers a mechanism for their control by afferent feedback.

Chapter 1: Introduction

1.1 Central Pattern Generators

Various rhythmic or repetitive actions are observed in animals, such as respiration, scratching, chewing and locomotion (flying, swimming and walking). Most of these motor behaviors are controlled by specialized neural networks called central pattern generators (CPGs). The term CPG is used to refer to a network of neurons whose collective activity produces and controls specific rhythmic motor activity such as locomotion (Stuart 2007). CPGs are activated and controlled by higher brain centers, but their rhythmogenic mechanisms are defined by intrinsic properties of neurons comprising each CPG and the network architecture of their interactions. Moreover sensory input and afferent feedback can modulate and/or modify the CPG operation and the rhythmic pattern generated to adjust the latter to the particular motor task and the environment.

Each CPG has a specific network organization, and the connections between neural populations within the CPG appear to be genetically determined (Selverston 2005). Though, these connections' weights are not fixed and can be altered to modify the activity of the CPG to fit the particular task or conditions. These alterations can be achieved through various neuromodulators affecting the properties of different pre and post-synaptic ionic channels (Selverston 2005).

The rhythmicity generated by a CPG is the result of intrinsic bursting properties of some or all of the individual neurons forming the CPG, or the result of the network architecture and specific interactions between non bursting neurons. It also may be the result of an interplay between both of these mechanisms (Selverston 2005). Intrinsic bursting of neurons occurs due to certain types of ionic channels, such as persistent

sodium and voltage activated calcium channels, which are responsible for burst initiation, and maintenance of the neuron's depolarized state throughout the burst duration such that spiking is maintained. Bursting activity can end due to spike adaptation, which results from slow changes to certain ionic channels' dynamics, leading to reduced activity and eventually termination. It can also be triggered through intrinsic mechanisms such as calcium dependant potassium channels, which are activated by increased concentrations of calcium within the neuron (Bellingham 1998). Finally, a burst's duration can also be intrinsically controlled with a transient potassium current (I_A) (Av-Ron 1994). Network architecture determined rhythmicity, on the other hand, operates mainly through excitatory connections among neurons, or populations of neurons, that are expected to be coactive (agonists), while burst termination and phase switching occurs as a result of reciprocal inhibition between antagonistic neurons or populations (Selverston 2005). Therefore two antagonistic populations within a CPG can at the same time play a role in determining each other's activity profile, in addition to each of them controlling one of a pair of antagonistic muscles. Reciprocal inhibition can also play a role in maintaining the timing of CPGs relative to each other, whether in phase or out of phase, for example the reciprocal inhibition between CPGs controlling two limbs that operate out of phase with each other.

CPGs, which are responsible for controlling a range of motor activities in several non mammalian and invertebrate species, have been extensively studied and fully or partially described, such as the CPGs responsible for the control of swimming in crayfish (Stein 1971), tritonia (Getting 1975), lamprey (Grillner 2003), and leeches (Kristan and Weeks 1983); the CPG controlling flight in locusts (Robertson and Pearson 1985); CPGs

controlling walking in insects (Buschges *et al.* 2008) and turtles (Stein 2005). Additionally, CPGs responsible for the control of digestion, respiration, cardiac activity, and swimming have been described in crustaceans (Hooper and DiCaprio 2004). The studies of such systems have played an essential role in expanding the understanding of the cellular and network bases of similar systems responsible for rhythmic motor activity in vertebrates. For example, the isolated spinal cord of a lamprey was found to be able to produce well coordinated locomotor activity in the absence of sensory feedback (Grillner *et al.* 1995; Grillner *et al.* 1998; Grillner and Wallen 2002). Furthermore, a neural model of the lamprey's spinal circuitry coupled with a mechanical model of the lamprey's body was able to reproduce swimming motion at different speeds, and realistic turning movements when simulated with variable descending inputs from supra-spinal centers (Ekeberg 1993; Ekeberg *et al.* 1995). That said, a lot remains to be unraveled when it comes to more complex systems such as the locomotion of rats, cats, primates and humans, seeing as in these cases the circuitry underlying the locomotory rhythm has not yet been fully described. And even though we believe that systems described in invertebrates can offer great insights into the organization of networks controlling locomotion in vertebrates it is reasonable to assume that the circuitry in higher order animals is likely to be much more complex than the one found in invertebrates, such as the lamprey, due to the involvement of more than one limb, multiple segments per limb, and the degree of coordination that operating such a system requires. The locomotor system of a lamprey is simpler; it is limited to a small number of neurons controlling each body segment such that when one side of a segment contracts the opposite side relaxes. Body segments are interconnected with each other and coordinated in such a way that

creates a travelling wave of contractions and relaxations that propel the animal forward, backwards or steers the animal in the desired direction (Grillner 2003). The coordination between body segments is achieved by having a delay of activity between the leading segment and the ones following it, with the delay increasing the farther away a body segment is from the leading end, creating a lag in the activation of consecutive body segments. The speed of a travelling wave of activity, whether towards or away from the head, determines the movement speed in the corresponding direction, such that the faster the wave propagates, the faster the lamprey moves, and the shorter the delay is between consecutive segments' activation (Grillner 2003). Clearly the control system required for propelling a bi-pedal or quadra-pedal vertebrate has to be much more complex than that, additionally such a control system has to deal with maintaining the body's stability and prevent it from falling off to one side.

In mammals, several neural networks have been identified within the central nervous system that control different repetitive rhythmic motor activity (Guertin and Steuer 2009), these CPG networks include: (1) The CPG controlling respiration, which studies suggest is located in the ventral part of the medulla in a region referred to as the pre-Bötzinger complex (Smith *et al.* 1991). Similar networks controlling respiratory motor activity have also been identified in mollusks (Syed *et al.* 1990). (2) The CPG controlling mastication, or chewing, located in the brainstem (Nakamura and Katakura 1995), not only controls the motion of the jaws but also the various facial and tongue muscles involved in the mastication process. In addition to chewing, data from several studies suggests that swallowing is produced by the rhythmic activity of a CPG located in the medulla (Jordan *et al.* 1992). Modulation of these basic rhythms is achieved through

sensory feedback relaying the properties of the food being chewed and proprioception of the jaws, tongue and face. (3) The process of ejaculation results from rhythmic activity of the pedundal motoneurons. This rhythmic activity originates in a network of neurons called the lumbar spinothalamic (LSt) neurons, located in lumbar L3 and L4 segments of the spinal cord and forming a CPG referred to as the spinal generator of ejaculation (SGE) (Truitt and Coolen 2002). In addition to projecting to the pedundal motoneurons, the SGE also projects its activity to the forebrain and receives sensory inputs from the sexual organs through the pedundal and dorsal nerves of the penis (Schroder 1985). Stimulation of these nerves has been shown to elicit an ejaculatory response in low-thoracic transected rats (McKenna *et al.* 1991). Similar data has also been reported in men (Wieder *et al.* 2000). (4) Another process that relies on rhythmic activity generated by a CPG is macturition, or urination. Elimination of urine involves the coordination of the activity of several muscles in the urinary bladder, bladder neck, urethra, and urethral sphincter (Nadelhaft and Vera 1995). Several studies have suggested that the CPG responsible for the control of the macturition process is located in the thoracolumbar and lumbosacral regions of the spinal cord (Sugaya *et al.* 1997; Vizzard *et al.* 1995). (5) The CPG controlling the scratch mechanism. Scratching is characterized by an animal bringing its hind limb forward towards the region triggering the scratch response, and then following that with repetitive rhythmic movements of the hind limb against the animal's body (Stein 2008). Studies have shown that the scratch CPG is located in the L7-S1 region of the spinal cord (Barajon *et al.* 1992), moreover it was suggested that an overlap between the scratch and locomotion CPGs exists, particularly since both processes involve the activation of similar muscle synergies (Berkowitz 2008). Yet

recordings of premotor neurons active during scratch but not during locomotion have been obtained in turtles, pointing towards only a partial overlap between the scratch and locomotion CPGs (Berkowitz 2002).

1.2 Neural Control of Locomotion

The generation and control of the locomotor rhythm has been mainly studied in animal models although there is mounting evidence for the existence of a CPG controlling locomotion in humans (Hultborn and Nielsen 2007; Minassian *et al.* 2007). The mammalian locomotor CPG components and organization remain mostly unknown; however it is believed that the CPG is mainly located in the thoracolumbar segments (Cina and Hochman 2000; Dimitrijevic *et al.* 1998; Gerasimenko *et al.* 2008; Nishimaru *et al.* 2000) of the spinal cord.

Early in the study of locomotion in vertebrates, during the latter part of the 19th century and the first half of the 20th century, the prevailing hypothesis for the control of stepping was that it resulted from reflex reactions, suggesting that sensory and proprioceptive stimulations played a central role in the control of locomotion. It was believed that reflex stepping was generated as a result of afferent stimulations the limbs receive during locomotion in addition to muscular proprioceptors that generate signals relaying the position of the limbs and muscle properties (Stuart and Hultborn 2008). However at the same time, in 1874, spinal cord transected dogs, held over ground level, were shown to generate short episodes of locomotor activity after one of their limbs was dropped from a flexed position (Freusberg 1874), revealing that the spinal cord was capable of generating a locomotor rhythm on its own. Comparable observations were

made by Philippson (1905), who also studied rhythmic air stepping of dogs' hind limbs held off the ground, and concluded that locomotion was the result of both, central and reflex mechanisms (Clarac 2008). Philippson (1905) was able to map the sequence of reflex stimulations that he believed were behind the stepping reaction, even though he did note that there might be an additional central mechanism contributing to stepping that he was not able to identify. At the time, little attention was paid to Freusberg's and Philippson's findings, concerning the probability of a central mechanism contributing to the control of locomotion (Clarac 2008), which challenged the widely accepted reflex stepping theory of that time.

Another scientist during that time, who argued for stepping being a reflex reaction, was Charles Sherrington. His extensive work on spinal cord transected cats and dogs provided evidence suggesting that the basic motor pattern of walking was the result of reflex actions from proprioceptors acting on spinal centers (Sherrington 1910a). Following transection of the spinal cord, and after a period of spinal shock, the hind limbs were capable of executing reflex stepping movements which strikingly resembled those of natural step. Sherrington studied different reflex reactions that were elicited through various types of stimulus; he determined which muscles were involved in each reflex reaction and the strength of the responses that they produced (Sherrington 1910a). He then went on to determine which of the reflex reactions the he was able to produce could possibly play a role in the locomotion process. Finally, Sherrington compared the reflex reactions that he thought were responsible for producing the locomotor rhythm in different types of preparations (intact, decerebrate, and spinal) and pointed out the similarities and difference.

Even though in several of Sherrington's papers and studies there was evidence pointing towards a central mechanism being involved in the control of stepping, and even though Sherrington himself mentioned the possibility of the existence of such a mechanism, he continued to argue for the reflex reaction concept and peripheral control of locomotion. Sherrigton believed that similarities between hind limb stepping and scratching existed (Sherrington 1910b, c), and although he had previously shown that deafferentation of the limb involved in scratch did not abolish scratching, rather it left the rhythm unchanged (Sherrington 1906), he maintained that stepping was the result of a reflex reaction. Sherrington held that the locomotor rhythm was produced due to cyclic input from proprioceptors of the hip flexor muscles in addition to other reflexes, because rhythmic stepping was not eliminated even after cutting all hind limb cutaneous nerves. Moreover, on the issue of air stepping, where the animal is lifted off the ground during the observed locomotor rhythm, Sherrington disagreed with the views of Philippson (1905), he argued that although the lack of contact with the ground meant that limbs received no cutaneous stimulus, but muscular propioceptors remained active and were capable of producing afferent feedback signals that reached the spinal cord and induced the stepping rhythm (Clarac 2008). Sherrington believed that muscular and cutaneous afferents played a major role in the control of stepping.

Sherrington (1910a) also discovered that the stepping reaction elicited through limb stimulation may have a frequency different to that of the stimulus being applied. He reacted to his discovery by remarking: *"... the rhythm is therefore central in seat"*. Sherrington also suggested that certain specialized neurons in the spinal cord can transform tonic peripheral inputs into basic central stepping motor commands, since

locomotion could be elicited through continuous stimulation of the skin or the spinal cord; yet he maintained his position that the locomotor rhythm was mainly the result of a reflex mechanism. Nevertheless, Sherrington had a change of heart towards the end of his career, he conceded to a friend that he no longer believed that control of locomotion laid peripherally (Stuart and Hultborn 2008), and that he thought that reflex stepping as a theory did not explain the complexity of the stepping action. Sherrington, considered reflex stepping a useful concept initially, but as researchers uncovered more details in the field of stepping and locomotion it could no longer offer the desired explanations.

1.3 Thomas Graham Brown and the Half-Center CPG

The first scientist to clearly argue for central control of locomotion was Thomas Graham Brown. He was also the first to develop the idea of a spinal half-center rhythm generator that is at the heart of the control of locomotion (Clarac 2008). Based on his experiments showing that the basic pattern for stepping was generated entirely in the spinal cord in the absence of peripheral afferent input, in spinal cord transected cats, rabbits and guinea-pigs (Graham Brown 1911a, 1914), Brown developed his half-center concept of the spinal mechanism responsible for the control of locomotion. This idea, which is currently widely accepted, did not receive much acceptance during Brown's time and up until the 1960's (Delcomyn 1980; Stuart and Hultborn 2008). Brown, who was a student of Sherrington, also saw a similarity between the control of hind limb stepping and scratching in guinea pigs and rabbits (Graham Brown 1910, 1911b). Along with Sherrington, Brown demonstrated that scratching was preserved after deafferentation of the hind limbs. Unlike Sherrington though, Brown found that this

observation held a clue to the control of stepping, namely that stepping, like scratching, is probably controlled by a central spinal mechanism (Graham Brown 1911a). Brown went further in trying to prove his hypothesis, he experimented with cats that were decerebrated, transected (at segment T12), deafferented (by severing most of the dorsal and lumbar roots exiting the hind limb), and paralyzed with an anesthetic. The animals were lying on one side when stepping movements in the hind limbs was spontaneously evoked (narcosis progression). The level of anesthetic used was shown to abolish proprioceptive and exteroceptive reflexes but not locomotor activity; Brown was able to record rhythmic alternating flexor-extensor activation patterns in the hind limbs (Graham Brown 1911a). The rhythmic bursts that Brown observed were in nerve fibers carrying motoneuron signals to a flexor muscle (tibialis anterior) and an extensor muscle (gastrocnemius) (Clarac 2008). This proved that the source of activity that Brown observed in hind limb motoneurons was neither supra-spinal, nor was it the result of stimulations experienced by limbs during locomotion, nor did it depend on the state or position of the muscles involved in the stepping action. Rather, Brown's work suggested that control of hind limb stepping lay with the central mechanism located in the lumbar part of the spinal cord (Graham Brown 1911a). Leading Brown to propose his half-center model consisting of two groups of spinal neurons mutually inhibiting each other and capable of producing the basic stepping rhythm (Fig. 1). Functionally, the two half-centers are antagonistic, when one is active the other is silent. This idea of mutual inhibition in the spinal cord was not new at the time, Sherrington had proposed it earlier, but had suggested that mutual inhibitory connections were under the control of proprioceptive feedbacks (Stuart and Hultborn 2008). Brown suggested that a locomotor

rhythm was generated in the following way: (1) Activity in the first group of neurons (half-center) activates motoneurons innervating extensor muscles, and simultaneously inhibits the opposite half-center preventing the activity of antagonist muscles. (2) Phase switching occurs when the active group of neurons becomes fatigued allowing the opposite group of neurons to escape its inhibition, or the opposite group, on its own, manages to overcome the inhibition.

Brown also experimented with removing half of the lumbar cord along the antero-posterior axis in decerebrate and spinal rabbits, guinea pigs and cats, and observing any remaining rhythmic activity (Graham Brown 1913). He performed these experiments under light anesthesia, which allowed sensory afferents to provide enough general excitation to lumbar centers to activate them. Brown observed normal stepping movements of the hind limb ipsilateral to the intact spinal cord, while the contralateral hind limb, on the side of the damaged spinal cord, showed no movement. These finding offered further insights into the organization of the spinal centers controlling stepping. Namely, it suggested that each hind limb is controlled by a separate half-center CPG that may function in or out of phase relative to the CPG controlling the opposite hind limb (Stuart and Hultborn 2008).

As for the role of afferents, whether muscle proprioceptives or cutaneous feedbacks, Brown thought that these mechanisms had an important role to play in the control of locomotion. This role however was not in the generation of the basic rhythm; rather it was in the regulation and augmentation of the centrally produced rhythm (Graham Brown 1911a). Therefore, according to Brown, afferent feedbacks can play a

role in dynamically modifying the locomotor rhythm depending on environmental conditions and the state of the hind limbs.

In summary, Brown's findings can be summarized in the following five points (Graham Brown 1911a): (1) The locomotor rhythm is composed of three stages that repeat in the following order: flexion, balance between flexion and extension, and extension. (2) Spinal cord stimulation in an animal with all limb muscles deafferented and paralyzed (other than the muscles being recorded), produces an alternating flexor-extensor muscle rhythm. (3) The rhythm observed in a deafferented animal is similar to the rhythm observed before the afferents were cut. (4) The locomotor rhythm is the result of central spinal mechanisms with intrinsic phasic oscillations that do not depend on external phasic inputs or peripheral stimulations. (5) In an intact animal, where afferents are preserved, proprioceptive feedbacks play a regulatory role that is not essential to the production of the locomotor rhythm.

As mentioned earlier, Brown's ideas were not widely accepted during his time and received little appreciation from his educator Sherrington. While Sherrington did find validity in the idea of a mechanism intrinsic to the spinal cord capable of controlling the stepping rhythm, he did not accept the idea that afferent feedbacks and reflexes only played a regulatory role (Sherrington 1913). Therefore, the half-center concept remained in obscurity until the 1960s when Andreas Lundberg brought it back to light and gave it the acceptance that it deserved (Clarac 2008).

1.4 Alternative CPG Models

Several other organizations of the circuitry responsible for locomotion have been proposed. Here we offer a brief description of these hypotheses. First, the Miller and Scott model (1977), which proposed that Renshaw cells are responsible for the alternation between flexion and extension. Increased activity in one motoneuron pool gradually causes its own inhibition by the corresponding Renshaw cell population. Simultaneously, that Renshaw cell population facilitates the activity of the antagonistic motoneuron pool by inhibiting the corresponding Ia interneuron population which would otherwise inhibit the activity of the antagonistic motoneuron pool. This model fails to clearly explain how the basic rhythm is generated, furthermore it has been demonstrated that the activity of Renshaw cells is not essential for the generation of a basic locomotor rhythm (Pratt and Jordan 1987). More evidence against the Miller and Scott model comes from studies with nicotinic antagonist mecamylamine (MEC), which greatly reduces Renshaw cell activity. It was shown that the basic locomotor pattern and Ia interneuron activity persists even after the application of MEC (Noga *et al.* 1987).

Another CPG model that has been proposed is the flexor burst generator model (Duysens 1977; Pearson and Duysens 1976) which consists of a rhythmically bursting activity generator that directly drives flexor motoneurons, and inhibits extensor motoneurons indirectly through an inhibitory interneuron. Extensor motoneurons are excited by a tonic drive, which allows them to be active as long as the flexor burst generator is silent. The issue with the flexor burst generator concept is that the evidence for an asymmetric organization of the CPG is underwhelming (Duysens 2006). Moreover, such an organization fails to explain several characteristics of fictive

locomotion, namely non-resetting deletions in which extensor activity is maintained (tonic) while flexor activity is abolished (silent) (McCrea and Rybak 2008) (spontaneous deletions are discussed in greater details in later sections of this study). On the other hand, mounting evidence, based on studies of spontaneous deletions occurring during fictive locomotion and scratch, suggest that the locomotor CPG has a symmetrical organization (Lafreniere-Roula and McCrea 2005).

A ring model has also been suggested as a possible organization of the locomotor CPG (Gurfinkel and Shik 1973; Szekely *et al.* 1969). The architecture of the ring CPG is composed of at least five groups of neurons, two pure extensors, two pure flexors, and one bifunctional, that directly or indirectly project to motoneuron pools. The sequence of activity of the CPG groups and hence motoneuron pools, is determined by a propagated inhibitory drive that flows around the ring at a variable speed depending on the particular phase duration. This model organization has failed to gain wide acceptance, and remains a conceptual model.

The last CPG organization discussed here is that of the unit burst generator, UBG. Due to the difficulty in separating motoneuron activity into one of two groups, pure flexor or pure extensor, it was suggested that the locomotor CPG does not produce alternating flexor-extensor activity (Grillner and Zangger 1974, 1979). Rather, it was proposed that the CPG produces a delicate pattern where all motoneuron activity is initiated and terminated at precise moments in the step cycle; this includes delays in onsets and offsets of motoneuron pools active in the same phase, and the activity of some motoneurons during both phases of locomotion. This idea led to the suggestion that the CPG was comprised of UBG modules, where each UBG controls only a few of the limb's

motoneuron pools (Grillner 1981). Individually, each UBG is a half-center oscillator, and the activity of the UBGs making up a CPG is coordinated by a number of excitatory and inhibitory interconnections between the different UBGs. This organization has several weaknesses: (1) it has not yet provided an explanation of how complex bifunctional motoneuron activity patterns can be generated (McCrea and Rybak 2008); (2) considering that it is a single level architecture, it fails to explain some of the observed affects of afferent stimulation, in addition to non-resetting deletions, where activity deletion is observed in all agonist motoneuron pools yet somehow the phase of the locomotor rhythm is maintained (McCrea and Rybak 2008).

Chapter 2: Control of Locomotion

Further evidence of the ability of the neural circuitry, found in the spinal cord of vertebrates, to control rhythmic locomotor movement regardless of any other rhythmic input into the spinal cord has been presented by several researchers. Mammals, in addition to lower vertebrates, whose cerebral cortex had been removed, have been found capable of reproducing complex locomotor patterns that are usually observed in intact animals (Grillner 1985). The spinal cord contains the neural circuitry necessary for generating the locomotor rhythm through recruiting and controlling the level of activation of various muscles involved in stepping and locomotion (Grillner 1985). An isolated spinal cord from a newborn rat can produce locomotor-like alternating rhythmic activity in hind limb motoneurons and muscles if an NMDA receptor agonist is introduced to the isolated spinal cord (Kudo and Yamada 1987; Smith and Feldman 1987). It has also been shown that locomotor activity, resembling that observed in intact animals, can be induced by 5-HT, dopamine, and 5-HT in combination with NMDA (Kiehn and Kjaerulff 1996). The application of pharmacological agents is generally used to mimic the effects of descending supra-spinal drive from the brain to the locomotor CPG to continuously activate it (Kiehn and Butt 2003). The role of supra-spinal inputs, into this spinal circuitry, does not exceed that of an activator signal. For example, neonatal cats that had their cortex removed, can, once physically competent, move around in a fashion that is very similar to an intact normal cat (Bard and Macht 1958; Bjursten *et al.* 1976). In these neonatal cats, if the basal ganglia are left intact, the animal is capable of initiating and carrying out complex locomotor patterns. It was also shown that repetitive low strength electrical stimulation applied to a particular region of a decerebrate cat's brainstem (the

mesencephalic locomotor region (MLR)), was enough to elicit walking movement (Shik *et al.* 1966a; Shik and Orlovsky 1976). Additionally, the strength of the stimulation could be used to control the speed of the locomotor rhythm, such that if the stimulus' strength was increased gradually, the animal would start with a slow walk and gradually speed up to a trot and finally start to gallop (Grillner and Wallen 1985), suggesting that the brainstem plays an essential role in the initiation of locomotion. The function of the brainstem can thus be reproduced through direct stimulation of particular regions in the mesencephalon that usually have to be activated in order for the locomotor rhythm to be initiated, namely the MLR.

As in decerebrate cats, spinalized and deafferented cats have also been shown capable of producing walking movements. It has been demonstrated that a cat spinalized at the T12 level and completely deafferented (L3-S4), can walk if the animal is either tonically stimulated at the L6 dorsal root level, or if Nialamide and L-DOPA were administered to the spinal cord region (Grillner and Zangger 1974, 1979). Moreover, a transected spinal cord at the mid-thoracic region can still generate locomotor movements in a cat placed on a treadmill, if sensory afferents are left intact (Forssberg *et al.* 1980; Shurrager and Dykman 1951), suggesting that sensory afferents have an initiatory role to play in a transected animal even though they do not directly create the rhythm. Similarly, deafferented cats whose spinal cord has been left intact, when stimulated at the brainstem level, specifically at the MLR, reproduce the basic locomotor pattern (Grillner and Zangger 1975, 1984). Therefore, supra-spinal inputs into the locomotory regions of the spinal cord are not essential for producing the basic locomotor rhythm, just like afferent

sensory feedback from the limbs; the source of rhythmicity is the neural circuitry within the spinal cord.

2.1 Location of Locomotor CPG

Several components of the locomotor CPG have been recently identified and partially characterized (Brownstone and Wilson 2008; Kiehn *et al.* 2008), the cellular and genetic organization is no longer a complete mystery. Researchers have used activity dependent labeling to locate spinal neurons active during locomotion. These studies have revealed neurons in the lumbar area of the spinal cord of rabbits and cats which are rhythmically active during locomotion (Dai *et al.* 2005; Viala *et al.* 1988). Kjaerulff et al. (1994) used sulforhodamine-101, an activity dependent marker, to reveal rhythmic CPG neuron candidates *in vitro* isolated spinal cord preparations of rats. Labeled cells were discovered in L1–L6 segments, bilaterally near the central canal and in the medial intermediate zone. Similarly, Cina and Hochman (2000), using sulforhodamine and a fictive locomotion preparation, discovered that a limited number of neurons, mainly in segments L1–L5, were labeled and therefore rhythmically active during fictive locomotion. The amount of rhythmic neurons they found was less than 0.1% of all cells constituting these segments, which led them to predict that the locomotor CPG is likely composed of a relatively small number of neurons (Cina and Hochman 2000). Moreover, spinal cord sectioning in combination with pharmacological blocking agents have been used to reveal that the hind limbs CPG network in neonatal rats and mice extends from the lower thoracic (Th11-Th13) down to the lumbar region (L1-L6) of the spinal cord (Kiehn and Butt 2003). However, it has been suggested that the rostral parts (Th11-L2) of

the CPG network in neonatal rats are more involved in the rhythm generation process compared to caudal parts (Kjaerulff and Kiehn 1996). In addition, other studies have revealed that key CPG components are probably present in the upper lumbar cord segments (Christie and Whelan 2005; Dimitrijevic *et al.* 1998; Kiehn 2006; Nishimaru *et al.* 2000). This pattern is not consistent across all species since there is evidence that in cats (Langlet *et al.* 2005) key CPG components are located at a more caudal position, in the mid-lumbar segments. As for the transversal distribution of rhythmic interneurons within the segments of the spinal cord, activity dependant labeling points to a ventro-medial distribution (Carr *et al.* 1995; Kjaerulff *et al.* 1994). In particular research findings suggest that all CPG elements are located in laminae VIII, X and the medial parts of lamina VII of the thoracic and lumbar spinal cord (Kjaerulff and Kiehn 1996).

2.2 Role of Afferent Inputs

Based on all data available to us we are aware that the locomotor CPG is capable producing rhythmic activity on its own without any phasic input or afferent feedback, but that does not mean that sensory feedbacks have no role to play during locomotion of intact animals. A spinal cord isolated from all brain structures can generate a locomotor rhythm, if afferent feedbacks from hind limbs are left intact (Shik and Orlovsky 1976). Afferents also provide the necessary regulation of step cycle period and stability control. An experiment showing how hind limb afferents can affect the function of the CPG is one where a spinal cat performs treadmill locomotion (mentioned in the previous section). The transected cat maintains the ability to adjust its stepping speed, therefore if the treadmill's speed is varied positively or negatively, the cat's locomotor speed changes

such that it matches the speed of the treadmill (Andersson *et al.* 1981; Forssberg *et al.* 1980; Grillner 1975; Grillner and Wallen 1982; Pearson and Duysens 1976; Shurrager and Dykman 1951). Therefore afferents inputs are responsible for controlling the locomotor CPG and setting its rhythm. Furthermore, if the treadmill's speed is increased beyond a certain point, the two hind limbs' movement becomes synchronized (as opposed to out of phase at slower speeds of locomotion) and the stepping rhythm becomes similar to that usually observed during galloping (Forssberg *et al.* 1980; Shurrager and Dykman 1951). Since supra-spinal inputs, that in normal cases provide activating drive to the locomotor CPG, are not present in the spinal animal, therefore it is safe to suggest that the animal would not walk were it not for afferent inputs into the locomotor CPG. Hence, afferents can play a role in the initiation of the locomotor CPG in a spinal animal; moreover, they also play a role in determining phase durations and period length of the CPG due to their phasic nature. When the treadmill's speed increases, the hind limb flexor muscles get stretched earlier during the stance phase, this results in the CPG switching from extension to flexion, due to afferent feedback, earlier than it would have, thereby decreasing the period of the CPG and increasing the speed of locomotion. On the other hand, when the treadmill slows down, the limb now requires more time to reach the latter part of the stance phase where it would usually provide an afferent signal from flexor muscles being stretched. This signal, which in spinal animals controls the switching from extension to flexion, now prolongs the extension phase and increases the duration of the CPG's period.

In an intact animal, the locomotor CPG switches from flexion to extension and *vice versa* on its own, the basic alternating rhythmicity of the locomotor rhythm is

centrally generated, yet afferent inputs remain important for foot positioning, maintenance of coordination, and overall stability during locomotion (Rossignol *et al.* 2008). Even though sensory afferents are not essential for producing the basic locomotor rhythm, they are important for accurate adaptable locomotion, allowing the CPG to quickly adjust to perturbations. Sensory feedbacks alone cannot produce a robust locomotor pattern, but they are essential when considering locomotion on an uneven surface with possible obstacles; in such a situation they offer the necessary modulation of the CPG, required for successfully walking across a bumpy surface (Grillner 1985).

2.3 Role of MLR

Descending supraspinal inputs that are believed to initiate rhythmic locomotor activity in the spinal CPG, originate from the MLR. The term MLR refers to a region of the brainstem, close to the caudal part of the nucleus cuneiformis, containing reticulospinal neurons (Garcia-Rill and Skinner 1987) responsible for, or contribute to, the initiation of locomotion once stimulated. The MLR has also been found to elicit walking in primates as well as reptiles and swimming in bony, cartilaginous, and cyclostome fish (Eidelberg *et al.* 1981; Grillner and Wallen 1985; Shik *et al.* 1966b, 1967; Shik and Orlovsky 1976). The MLR structure has been identified in several species so far, in lampreys, fish, reptiles, birds and primates (Grillner *et al.* 2008; Jordan 1991) and it was found to be evolutionary conserved. Electrical stimulation (20-60Hz, 20-100μA) or chemical stimulation of the MLR elicits locomotion in mesencephalic and thalamic cats (Orlovsky 1969; Orlovsky *et al.* 1999; Shik *et al.* 1966b) as well as in lightly anesthetized cats (Sirota and Shik 1973). In mesencephalic cats, MLR stimulation

allows the animal to walk on its own free of any support, however the locomotion is machine-like and if obstacles are placed in the cat's trajectory, it fails to avoid them (Shik and Orlovsky 1976).

Evidence suggests that in an intact animal, tonic MLR activity promotes locomotion at different speeds depending on the strength of activity of the MLR (Shik and Orlovsky 1976); at rest MLR activity is inhibited by other brain centers. When the MLR is stimulated, depending on the strength of the stimulation, a tetrapod, such as a cat, may exhibit walking, trotting or galloping (Grillner *et al.* 2008). Stimulation of the MLR produces variable locomotor speeds, the stronger the stimulation the faster the speed of progression (Mori 1987; Mori *et al.* 1991; Sirota and Shik 1973).

The MLR is not a necessary structure; locomotion can be initiated and maintained even if the MLR is destroyed (Orlovsky 1969; Sirota and Shik 1973). It determines the intensity of muscle contractions, or the power produced by the animal during locomotion. The speed of walking and frequency of stepping are indirectly controlled depending on the power developed by the muscular system and external conditions, such as the slope of the surface (Orlovsky *et al.* 1999). In mesencephalic cats, stronger MLR stimulation was found to produce a higher propulsive force when the speed of the treadmill was kept constant (Shik *et al.* 1966b).

Chapter 3: Analysis of Locomotor Activity

3.1 Fictive Locomotion

The ability of the CPG to generate a locomotor rhythm in the absence of rhythmic supra-spinal inputs and afferent feedback was verified through studying fictive locomotion in decerebrate and deafferented immobilized cat preparations (Burke *et al.* 2001; Edgerton *et al.* 1976; Grillner and Zangger 1979; Noga *et al.* 2003; Shik and Orlovsky 1976). In this reduced experimental preparation, cortical descending inputs, rhythmic proprioceptive afferents and other sensory afferent feedbacks are absent (McCrea 2001). CPG activity is therefore triggered by tonic stimulation of the MLR (Rossignol 1996), or by pharmacological agents introduced into the spinal cord that mimic the actions of descending pathways (noradrenergic agonists, L-DOPA (Jankowska *et al.* 1967a, b; Lundberg 1981)). Activity produced by the CPG can be recorded in nerve fibers as elctroneurograms (ENGs), as well as through interneuron recordings of specific motoneurons in the spinal cord.

The spinal circuitry operating during fictive locomotion is a subset of the locomotor system that functions during normal locomotion in intact animals. Yet, the rhythm observed during fictive locomotion experiments resembles that of normal locomotion with regards to the sequence of motoneuron activation and the frequency of the step cycle (Rossignol 1996). Fictive locomotion experiments are particularly important when studying the pure CPG operation, free from any modulations due to influences external to the CPG. They offer greater insights into the operation of the CPG and the role of afferent and supra-spinal inputs, compared to the study of normal locomotion only. For instance, if an activity pattern of a certain motoneuron pool,

observed during normal locomotion, remains unchanged in a fictive locomotion preparation, this suggest that this particular activity pattern is centrally generated by the CPG, but we cannot draw any conclusions regarding the role of afferents in this situation. On the other hand, if a particular motoneuron pool activity pattern disappears entirely during a fictive locomotion experiment, compared to normal locomotion, in this case it is difficult to determine what the role of the afferent is. The afferent might be influencing the generation of the motoneuron activity in different ways: (1) The particular motoneuron activity might be entirely created by the afferent signal, and therefore when the signal is eliminated so is the activity; (2) The activity is centrally generated by the CPG but the afferent signal is necessary for the generation of the motoneuron activity, because (a) the afferent plays a "permissive role", for example by preventing a certain inhibition within the central network; or (b) it provides the necessary additional excitation for the activity to be generated (Grillner 1985).

3.2 Comparison of Fictive and Real Locomotion

It is beneficial to consider motoneuron and muscle synergies when investigating the organization of the CPG since it has been suggested that the limb is controlled as a whole during its stereotyped movement in locomotion, rather than at the single muscle or joint level (Shik and Orlovsky 1976). There is a close similarity in activity profiles and synergies of motoneurons innervating one-joint muscles during fictive locomotion and the corresponding muscles during normal locomotion. The use of fictive locomotion preparations of decerebrate cats offers a unique opportunity to examine patterns of motoneuron activation and synergies formed by the CPG in the absence of afferent

feedback and patterned supra-spinal signals. During normal locomotion, afferent feedback may change these activation patterns and muscle synergies to adjust locomotor behavior to constantly changing external environment conditions and limb mechanics. Recent studies (Markin *et al.* 2007; Markin *et al.* 2008) have demonstrated a significant similarity in the activity of several motoneuron pools (and their corresponding muscle synergies) between fictive and normal locomotion, and identified specific differences in the activity of other motoneuron pools innervating two-joint muscles. These findings provided important insights into the organization and operation of the spinal CPG.

3.2.1 Bifunctional Motoneurons

During normal locomotion, the activities of extensor and flexor motoneurons are locked to the corresponding extension or flexion phase. In contrast, bifunctional motoneurons activating muscles spanning more than one joint (biarticular), such as posterior biceps semitendinosus (PBSt) (hip extensor/knee flexor) and rectus femoris (RF) (hip flexor/ knee extensor) express different activity patterns depending on the gait of the animal, speed of locomotion or locomotor conditions (Carlson-Kuhta *et al.* 1998; Halbertsma 1983; Smith and Carlson-Kuhta 1995). For example, the activity of PBSt during locomotion can be described as flexor or extensor related, depending on the primary muscle group it is co-active with, or biphasic. PBSt has commonly been considered to be a flexor, as it is mostly flexor related during trot or level walking (Grillner 1981; Halbertsma 1983). However, when walking upslope or galloping on level ground PBSt is purely extensor related (Smith and Carlson-Kuhta 1995). It has also been observed expressing double bursts when walking on level ground (depending on speed),

upslope, downslope, trotting, and crouching (Smith *et al.* 1998), and the duration of its activity in either phase varies depending on gait or posture (Carlson-Kuhta *et al.* 1998). RF shows similar variability in activity during locomotion depending on gait and locomotor conditions (Pratt *et al.* 1996; Smith and Carlson-Kuhta 1995).

While afferent feedback and supra-spinal inputs contribute to the formation of multiple patterns of PBSt and RF activity during real locomotion, these motoneurons demonstrate a variety of behaviors during fictive locomotion in decerebrate cats in the absence of sensory feedback and supra-spinal inputs. Different patterns of PBSt and RF activities, during fictive locomotion in different experimental preparations, have been previously reported (Grillner and Zangger 1979; Guertin *et al.* 1995; Orsal *et al.* 1986; Perret and Cabelguen 1980; Perret 1983). For example, PBSt was flexor related in drug induced locomotion in acute spinal cats (Grillner and Zangger 1979), extensor related during spontaneous locomotion in some decerebrate fictive preparation (Perret and Cabelguen 1980) and also expressed biphasic activity with short flexor and prolonged extensor bursts (Grillner and Zangger 1984). With peripheral stimulation during fictive locomotion, PBSt activity was reportedly altered from being flexor related to extensor related (Perret 1983) while RF activity changed from biphasic to extensor related (Orsal *et al.* 1986).

In a recent qualitative comparison of ENG patterns obtained during fictive locomotion with the corresponding EMG patterns observed during normal locomotion (Fig. 2) showed striking similarities in the profiles of one-joint flexors and extensors, however, some differences could be identified (Markin *et al.* 2008). In contrast to the one-joint muscles and their corresponding motoneurons, the activity profiles of nerves

innervating two-joint muscles (PBSt and RF) (Fig. 2A) clearly differed from the EMG activity of these muscles recorded during normal locomotion (Fig. 2B) (Markin *et al.* 2008). Specifically, (1) during fictive locomotion, PBSt motoneuron activity never exhibited a short second burst at the end of flexion (swing) similar to that recorded from PBSt during normal locomotion, (2) during normal locomotion, PBSt did not express a typical extensor activity like the one exhibited by PBSt motoneurons during fictive locomotion, and (3) during normal locomotion, RF motoneurons never exhibited a flexor burst similar to the one observed during fictive locomotion, and the onset of its late extensor burst was delayed relative to that observed during fictive locomotion.

3.2.2 Motoneuron Synergies

Finding groups of motoneuron synergies during fictive locomotion studies, without the influence of afferent feedback, allowed for the identification of possible synergies hardwired into the spinal locomotor CPG for control of locomotion. Comparison of this classification with ones done during normal locomotion (Krouchev *et al.* 2006; Markin *et al.* 2008) showed similarity in the classification of most synergies; especially for motoneurons of one-joint muscles.

The question was whether afferent feedback directly controls the rhythm generator and hence affects motoneurons via synergies engaged by the CPG, or it uses synergies independent of the CPG to directly control the activity of individual motoneuron populations. If activity profiles and groups of synergists identified during fictive and normal locomotion were the same, then it could be suggested that afferent feedback does nothing more than control the locomotor cycle and phase durations, i.e.

only controls the operation of the rhythm generator, defining timing of phase transitions and durations of the locomotor cycle and its phases. On the other hand, differences in the activity of synergist groups between fictive and normal locomotion would suggest a possible direct effect of afferent feedback on the activity of these synergist groups.

Analysis of the differences in the activity profiles of most one-joint flexors and extensors during fictive and normal locomotion (Fig. 2) revealed that their behavior was very similar. Therefore, activity of these synergist groups is most likely controlled by the CPG and/or by afferent feedback via the CPG (synergies inherent to the CPG organization). In contrast, the behavior of two-joint motoneurons and muscles, such as PBSt, RF, EDL and FDL, were different. Therefore, activity of these motoneuron pools seems to be largely determined by afferent feedback acting at a location different from the rhythm generator. This suggestion about a possible role for motion-dependent feedback in regulating activity of two-joint muscles is consistent with results of previous studies of fictive locomotion (Perret and Cabelguen 1980) and different forms of normal locomotion in which two-joint muscles demonstrated mutable activity patterns, whereas one-joint extensors and flexors typically maintained similar reciprocal activity.

Nevertheless the activity patterns exhibited by bifunctional motoneurons, such as PBSt and RF, during fictive locomotion, differed from one experiment to another even though no afferent stimulus was present. Therefore it is reasonable to suggest that the locomotor CPG does indeed include neural components that produce these patterns observed during fictive locomotion. Moreover, it can also be suggested that afferent inputs can directly interact with these component networks to determine appropriate bifunctional motoneuron profiles necessary for the successful completion of a locomotion

task. Therefore, in the absence of afferent feedback and supra-spinal control, the activity patterns of PBSt and RF motoneurons during fictive locomotion are expected to be solely defined by the activity of the locomotor CPG and neural interactions within it. Thus studying PBSt and RF behavior during fictive locomotion may provide better insights into the organization of the locomotor CPG.

3.3 Analysis of the Half-Center Model Performance

The bipartite half-center organization of the locomotor CPG was originally proposed by Brown (1914) and expanded by Lundberg, Jankowska and their colleagues (Jankowska *et al.* 1967a, b; Lundberg 1981; Stuart and Hultborn 2008). Brown provided the first evidence that the basic locomotor rhythm is generated by mechanisms intrinsic to the spinal cord. These and later investigations led to the widely accepted concept of CPGs which reside within the central nervous systems of invertebrates and vertebrates and control various rhythmic movements. Brown (1914) also proposed a general schematic for the spinal CPG generating rhythmic alternating activity of flexor and extensor motoneurons during locomotion, the half-center model. His ideas were embraced by Lundberg and his colleagues in their description of how spinal interneurons involved in flexion reflexes could serve as the basic building block of the circuitry responsible for mammalian locomotion (Jankowska *et al.* 1967a, b; Lundberg 1981). The key points of the half-center CPG organization shown in Fig. 1 are: (1) Each limb is controlled by a separate CPG; (2) Each CPG contains two groups of excitatory interneurons (i.e., the half-centers) that directly project to, and control the activity of, flexor and extensor motoneurons; (3) Mutual inhibitory interconnections between the

half-centers ensure that only one can be active at a time; (4) An undefined "fatigue" process gradually reduces excitation in the active half-center; (5) Phase switching occurs when the reduction in the excitability of one half-center falls below a critical value and the opposing center is released from inhibition; (6) Inhibition of antagonist motoneurons is tightly coupled to the excitation of agonists.

The appeal of the half-center hypothesis for the control of locomotion includes corroborating evidence on the organization and activity of lumbar interneurons during locomotor-like flexor and extensor motoneuron activity. Systemic administration of the noradrenergic precursor, L-DOPA, evokes spontaneous alternating activity of flexors and extensors (Grillner 1969; Grillner and Zangger 1979; McCrea and Rybak 2008). Intracellular motoneuron recordings during L-DOPA induced locomotion revealed strong mutual inhibitory interactions between interneuronal pathways to flexors and extensors (Jankowska *et al.* 1967b). Also interneuron recordings showed a strong reciprocal organization of interneurons that were rhythmically active in the absence of sensory stimulation and were also part of the reorganization of flexion reflexes that occur in these preparations (Jankowska *et al.* 1967a). A key feature of the half-center hypothesis is that there is an intrinsic spinal organization of interneuron populations with strong (mutual) inhibition between them. Alternating activity in flexor and extensor motoneurons results from alternating activity of interneurons that may also be activated by a variety of sensory afferents (Lundberg 1981).

The important role that mutual inhibition plays in the functioning of the locomotor CPG was highlighted by an experiment where strychnine or bicuculline was used to block inhibitory synaptic transmissions (Kiehn 2006). It was found that once

inhibition was abolished, synchronized rhythmic activity of flexor and extensor motoneurons emerged. In addition, studies conducted in fictive locomotion setups (Burke *et al.* 2001) revealed that flexor and extensor parts of the CPG were capable of independent rhythmic activity. These findings suggest that each of the CPG's half-centers possess rhythmogenic intrinsic properties and can therefore independently generate oscillations under certain conditions and when inhibition is blocked. Furthermore, the synchronization of flexor and extensor activity after the blockade of inhibitory connections is most likely due to weak excitatory interconnections between the CPG half-centers (Rybak *et al.* 2006a), these interconnections' effects become more pronounced once inhibition is eliminated.

3.4 The Two-Level CPG Organization Concept

3.4.1 Motoneuron Activity Inconsistent with the Half-Center CPG Concept

The half-center architecture can only accommodate producing a strictly alternating pattern of flexor and extensor activity with all motoneurons having to fall under these two groups. During locomotion, however, all motoneurons cannot be strictly classified into only these two groups. Even though a group of motoneurons, responsible for activating either a group of flexor or extensor muscles, can generally be regarded as being either a pure flexor or extensor, in reality these motoneurons most likely have to be separated into several groups when considering the development of a model that can reproduce all the intricacies of the act of progression and motoneuron activity during fictive and/or real locomotion. For instance, the activity onset and offset of motoneurons belonging to either phase of locomotion do not always match; the activity of two flexor

or extensor motoneuron pools might be initiated and/or terminated at different instances relative to each other (Markin *et al.* 2007; Markin *et al.* 2008; Rossignol 1996). Furthermore, certain motoneuron pools, particularly those activating biarticulate muscles spanning two joints, exhibit variable activity where they might be active during either phase of locomotion, or during both phases at the same time (two bursts per cycle). Such motoneurons can neither be classified as extensors nor flexors, instead they are commonly referred to as bifunctional motoneurons.

It has been suggested that proprioceptive afferent inputs were responsible for converting simple flexor-extensor activity into more complex behaviors (Engberg and Lundberg 1969), where motoneuron activity can be shifted or occur during both phases. However, the persistence of these complex activity patterns following bilateral deafferentation of the hind limbs in decerebrate cats (Grillner and Zangger 1975) suggests otherwise. Specifically, it suggests that the locomotor CPG does not generate a simple alternating activity pattern of flexors and extensors, rather it produces a more elaborate pattern that involves the sequential activation of different motoneuron pools at the appropriate instance; moreover, the CPG, independent of afferent inputs, produces complex activity patterns necessary for the activation of bifucntional motoneurons.

3.4.2 Effects of Afferent Stimulations

Several studies have revealed further weaknesses in the simple half-center CPG model hypothesis; for example, investigations of the effect of stimulation of hind limb sensory afferents on motoneuron activity and step cycle timing (Guertin *et al.* 1995; McCrea 2001; Perreault *et al.* 1995; Rybak *et al.* 2006b; Stecina *et al.* 2005). These

studies showed that in many cases, afferent stimulations can delay or cause premature phase switching within the ongoing step cycle without affecting the timing of the subsequent step cycles. These observations are difficult to explain within the framework of a simple half-center CPG and point towards a more complex organization of the locomotor CPG.

3.4.3 Spontaneous Deletions

Several studies have focused on investigating deletions occurring during fictive locomotion experiments. Deletions are spontaneous errors in the rhythmic activity of motoneurons occurring during fictive locomotion, they are characterized by brief periods of inactivity (missing bursts) affecting a group of agonist motoneurons (flexors or extensors) (Grillner and Zangger 1979; Jordan 1991; Lafreniere-Roula and McCrea 2005). Deletions have also been observed during treadmill locomotion in cats (Duysens 1977) and during scratch reflex in turtles (Stein and Grossman 1980; Stein 2005). During a deletion, motoneuron activity fails simultaneously in synergist motoneuron pools while antagonist motoneurons exhibit tonic, or maintain rhythmic, activity (McCrea and Rybak 2008). The widespread effect of deletions on the activity of multiple motoneuron pools throughout the limb is strong evidence that they are produced by failures in the operation of some common spinal circuitry, such as the CPG, and are not the result of local perturbations affecting the excitability of particular motoneurons.

An analysis of motoneuron activity before and following a deletion revealed that some deletions, called "resetting deletions", are accompanied by a shift in the phase of the re-emerging rhythm relative to the rhythm preceding the deletion (Lafreniere-Roula

and McCrea 2005; Rybak *et al.* 2006a). Such rhythm resetting or phase shifting after a deletion can be easily explained within the framework of the classical half-center CPG organization (Fig. 1). For example, because of reciprocal inhibition between the half-centers, a spontaneous temporary increase in the excitability of one half-center would cause an inhibition of the antagonist half-center, resulting in a deletion of the activity of the corresponding antagonist motoneuron pools. As the duration of the perturbation causing the deletion is arbitrary, the rhythm following the perturbation would generally be accompanied by a phase shift of the post-deletion rhythm relative to the pre-deletion rhythm. However, most spontaneous deletions observed during fictive locomotion in decerebrate cats are characterized by phase maintenance; such deletions are called "non-resetting deletions" (Lafreniere-Roula and McCrea 2005; Rybak *et al.* 2006a). Thus bursts of motoneuron activity that re-emerge after a deletion often occur at an integer number of the missing locomotor periods. These observations suggest that the internal structure of the CPG can 'remember' and maintain the locomotor cycle period when motoneuron activity falls silent. Such rhythm and phase maintenance is inconsistent with the classical half-center CPG organization, in which a single network is responsible for both rhythm generation and motoneuron activation; therefore suggesting that there should exist an additional circuitry responsible for rhythmic depolarization and hyperpolarization of motoneurons that is separate from the circuitry involved in rhythm generation.

It has been proposed that the locomotor rhythm can be maintained, during a deletion, by CPGs of other limbs, but observations suggest otherwise. Specifically, during fictive locomotion, even when only one limb's motoneurons exhibit a locomotor

rhythm (while other limb motoneurons are either silent or exhibit non-locomotor activity), non-resetting deletions still occur (Rybak *et al.* 2006a). Hence, reinforcing the hypothesis that the CPG contains separate circuitries for rhythm generation and motoneuron activation, and that non-resetting deletions occur due to failures within the CPG itself and are not due to influences beyond the CPG.

3.4.4 Control of Locomotor Rate and Motoneuron Activation

Another characteristic of locomotion that the half-center CPG models fails to explain is how the frequency of stepping and the level of activation of motoneurons can be controlled separately. It has been suggested (McCrea and Rybak 2008; Orlovsky *et al.* 1999) that the frequency of the half-center CPG can be modulated through the level of activation it receives, where increased excitatory drive results in higher step cycle frequency, and as a secondary affect leads to higher activity levels during each phase considering that individual neuron's spiking frequency increases. Based on the simple half-center model, excitatory interneurons generating the locomotor rhythm are directly connected to motoneurons that they activate; consequently any changes in excitability of the half-centers should simultaneously affect both cycle timing and motoneuron activity. However, this creates a problem as to how stepping frequency can be independently altered without affecting the activation level of motoneurons; and similarly, how activation level of motoneurons can be increased or decreased independent of the frequency of the half-center. To resolve this problem, several researchers (Burke *et al.* 2001; Jordon 1991; Kriellaars 1992; McCrea and Rybak 2008; Perret *et al.* 1988) have suggested that additional neural circuitry should exist in the locomotor CPG between the

rhythm generating half-center and motoneuron populations. This extra circuitry would regulate the activation level of motoneurons independent of the half-center activity. This also allows for the modulation of the frequency of locomotor activity through altering the drive to the half-center populations without affecting motoneuron activation levels.

3.5 Two-Level CPG

To overcome the inconsistencies of the simple half-center model, several attempts have been made, some of which included proposing fundamentally different concepts and hypotheses on how the locomotor rhythm is generated and controlled. Several of these ideas have been already discussed earlier, such as the flexor burst generator, ring model, and unit burst generator. Other more conservative approaches to the issue have also been taken, such solutions focused on maintaining the half-center architecture as the central component of the locomotor CPG and evolving the CPG by introducing additional neuron populations and circuitry to explain all the different behaviors observed in different types of locomotion that a simple half-center architecture fails to explain. The main intent of the additional neuron populations is to have a layer of circuitry interposed between the half-center rhythm generator and motoneuron populations. The basic concept is to have rhythm generation and motoneuron recruitment performed by separate neuronal populations.

Based on insights gained from studies of non-resetting deletions and sensory afferent stimulations, it can be ascertained that the CPG is capable of maintaining the period and phase of oscillation even during situations of external perturbations. Therefore, it has been suggested that a CPG with separate rhythm generation and pattern

formation networks can realistically reproduce many experimental phenomena including spontaneous deletions and the effects of afferent stimulation (Fig.3A) (Burke *et al.* 2001; Jordan 1991; Kriellaars *et al.* 1994; McCrea and Rybak 2008; Rybak *et al.* 2006a). Pattern formation (PF) network, refers to the extra neuron populations and circuitry added between the half-center oscillator, or rhythm generator (RG), and motoneuron pools; the PF network's activity, controlled by the RG, projects to flexor and extensor motoneuron populations. A CPG with separate RG and PF networks, or levels, is generally called a two-level CPG.

In support of this concept is the ability of the two-level CPG to explain and reproduce situations where sensory stimulation could alter the locomotor cycle timing, such as speeding up or slowing down the rhythm's frequency, without affecting the amplitude of motoneuron activity (Kriellaars *et al.* 1994). Hence the two-level CPG allows sensory inputs to separately control the degree of motoneuron recruitment and timing of the locomotor rhythm (Orsal *et al.* 1990). Moreover, a two-level CPG organization can easily explain and reproduce the effects of afferent stimulation on phase switching without shifting of the post-stimulus phase (McCrea and Rybak 2008), however, this observation is difficult to explain within the framework of the simple half-center organization.

Rybak and McCrea have recently suggested a two-level organization of the locomotor CPG (Rybak *et al.* 2006a) (Fig. 3A), containing a half-center RG, performing a "clock" function, and an intermediate PF network that distributes and coordinates the activities of multiple motoneuron populations (Fig. 3A). The RG defines the locomotor rhythm and durations of the flexor and extensor phases, it also controls the activity of the

PF network interposed between the RG and motoneurons. The PF network, on the other hand, contains multiple interneuron populations projecting to multiple synergist motoneuron populations and reciprocally inhibiting other populations within the PF network. This organization was implemented in a computational model which describes the interactions populations of interneurons and motoneurons (Fig. 3B). Briefly, the model's RG consists of a homogeneous population of excitatory interneurons with mutual excitatory interconnections. These neurons are divided into two populations, RG-E and RG-F, representing the half-centers of the RG. Reciprocal inhibition between the RG half-centers is mediated by inhibitory interneuron populations, Inrg-E and Inrg-F. The PF network is similarly organized but has a lower capacity for rhythmogenesis (Rybak *et al.* 2006a), it is also composed of excitatory interneuron populations coupled by reciprocal inhibition (via Inpf-E and Inpf-F). The PF populations PF-E and PF-F operate under the control of the RG, receiving strong inhibitory inputs from Inrg-F and Inrg-E and weak excitation from RG-E and RG-F, respectively. PF populations project directly to motoneuron populations and are responsible for the phasic excitation of motoneurons during locomotion. Phasic inhibition of motoneurons during locomotion is provided by an additional set of inhibitory interneurons, Ia-E and Ia-F, driven by the PF network. The model also incorporates connections between and among the inhibitory Ia interneurons, Renshaw cells and motoneurons based on the description provided by Jankowska (1992).

The model has been developed to simulate motoneuron activity recorded during fictive locomotion evoked by continuous electrical stimulation of the MLR. Locomotion in the model is therefore initiated and terminated through the application and removal of

excitatory tonic MLR drives to the RG and PF networks (Rybak *et al.* 2006a; Rybak *et al.* 2006b). The RG generates a biphasic rhythm with alternating bursts of RG-E and RG-F populations. The rhythmogenic mechanism operating in the RG is based on a combination of intrinsic cellular properties (activation of the slowly inactivating persistent sodium current, I_{NaP}) and reciprocal inhibition between the RG-E and RG-F half-centers. During normal locomotor operation, the onset of activity bursts is determined mostly by the activation of the intrinsic I_{NaP} excitatory mechanism, on the other hand burst termination is determined by reciprocal inhibition. Alternating bursting activity in the PF network follows that in the RG and produces phasic excitation of the corresponding motoneuron pools.

The two-level organization of the CPG provides the ability to differentially regulate locomotor speed at the RG level and the level of motoneuron activity at the PF level. By changing MLR drive to the RG half-centers, locomotor phase durations and step cycle periods can be independently regulated (McCrea and Rybak 2007; Rybak *et al.* 2006a) over ranges that encompass those occurring during fictive locomotion in decerebrate cats (Yakovenko *et al.* 2005) and during treadmill locomotion in intact cats (Halbertsma 1983). Since the PF populations receive their own MLR input, the degree of motoneuron activation can be controlled independent of RG activity. Consequently, sensory signals or spontaneously occurring perturbations may affect CPG operation at the RG level, altering the locomotor rhythm (e.g. producing a phase shift or rhythm reset) or act at the PF level, altering the pattern of motoneuron activation without resetting the rhythm or shifting the phase (Rybak *et al.* 2006a; Rybak *et al.* 2006b).

3.6 Activity of Bifunctional Motoneurons and the Two-Level CPG

According to the classical half-center CPG architecture, the activity of all motoneurons should be locked either to the extensor or flexor phase, however bifunctional motoneurons activating muscles spanning more than one joint, such as PBSt (hip extensor and knee flexor) and RF (hip flexor and knee extensor), express different and often more complex activity patterns which depend on the gait of the animal and/or locomotor conditions (Carlson-Kuhta *et al.* 1998). These observations are true during both normal and fictive locomotion, as described in section 3.2.

The complex non-trivial profiles of activity expressed by bifunctional motoneurons have been considered a strong argument against the bipartite organization of the locomotor CPG. This was one of the factors motivating researchers to look for alternative concepts for the CPG organization. To overcome some of the inherent limitations of a simple bipartite CPG organization and provide for a variety of motoneuron patterns, Grillner (1981) suggested that the locomotor CPG consists of multiple coupled UBGs controlling motoneurons operating at each joint (see section 1.4). Although the UBG architecture looks potentially more flexible compared to the bipartite CPG organization, no attempts have been made so far to develop a computational model of a UBG-based CPG that could reproduce the complex patterns of bifunctional motoneurons and their state-dependent changes.

At the same time, Perret and his colleagues (Orsal *et al.* 1986; Perret and Cabelguen 1980; Perret 1983; Perret *et al.* 1988) attempted to solve the problem within the framework of the bipartite locomotor CPG. They put forward a schematic for the pathways that may be involved in the generation of PBSt and RF patterns and their

variations (see Fig. 4). The principal suggestion was that PBSt and RF motoneuron pools receive both excitatory and inhibitory inputs from both flexor and extensor half-centers of the CPG oscillator. Superimposed upon excitation of PBSt and RF motoneurons are periods of inhibition that shape their final pattern (Orsal *et al.* 1986). This inhibition is produced by the half-center rhythm generator through activation of inhibitory reflex pathways, and is facilitated by afferent feedbacks. Perret and his colleagues suggested that the proposed inhibitory pathways are in fact an additional neural network interposed between the half-center rhythm generator and bifunctional motoneuron pools (Orsal *et al.* 1986; Perret 1983; Perret *et al.* 1988) solely responsible for spontaneously, or due to afferent stimulation, shaping the variable PBSt and RF activity patterns. Therefore, this additional network receives both descending and ascending inputs that contribute to its function in shaping PBSt and RF activity patterns. Specifically, the effect of these additional interneuron populations on PBSt and RF is controlled or facilitated by tonic afferent feedbacks or by variations in the level of central activity. However, our experiments have shown that the whole variety of PBSt and RF activity patterns can be observed in fictive locomotion preparations of decerebrate immobilized cats, i.e. without the influence of sensory afferent inputs. Furthermore, the CPG organization that was proposed by Perret and his group cannot account for all the different types of PBSt and RF behaviors observed during fictive locomotion; the model lacks a mechanism for controlling the length and timing of a burst of PBSt or RF activity relative to the phase of locomotion during which the burst occurs. It is worth noting that Perret's group (Orsal *et al.* 1986) observed that characteristics (time course and amplitude) of PBSt motoneuron activity were inversely correlated with those of RF motoneurons, when both were

simultaneously observed together. This finding led them to suggest that the same part of the locomotor CPG was responsible for shaping PBSt and RF activity, such that it inhibits PBSt at the same time and with the same amplitude that it excites RF, and *vice versa* (Orsal *et al.* 1986).

Another study (Burke *et al.* 2001) presented a generalized model of the circuitry controlling flexor digitorum longus (FDL) motoneurons, which also exhibit biphasic activity and innervate the FDL muscle which spans the digits and ankle joints. However, an exact structure or organization of the FDL CPG model was not defined in this study. To our knowledge, no computational model has yet been developed and tested to suggest a network organization responsible for the generation of complex and variable patterns of bifunctional motoneuron pools.

3.7 Extended Model of the Two-Level CPG

The study presented here is based on the recently proposed concept of a two-level CPG organization, suggesting that the spinal locomotor CPG contains a bipartite half-center RG and specially organized PF networks (see Fig. 3, and section 3.5) (McCrea and Rybak 2007, 2008; Rybak *et al.* 2006a; Rybak *et al.* 2006b). The suggested two-level architecture of the CPG allows for the separate control of the locomotor rhythm (at the RG level) and the patterns of motoneuron activations (at the PF level). According to this concept, the RG defines the locomotor rhythm and durations of the flexor and extensor phases. Whereas the PF network interposes between the RG and motoneurons, and depending on the input from the RG level and the interactions within the PF network, each PF population is activated during a particular phase of the step cycle producing a

phase-specific synchronized activation of the corresponding group of synergetic motoneuron pools.

A computational model of the two-level CPG architecture, controlling two antagonist motoneuron pools, flexor and extensor, was developed (Rybak *et al.* 2006a) (Fig. 3B). The model generated a realistic locomotor rhythm and produced alternating activity of the pair of flexor and extensor motoneuron pools. It was also able to reproduce many characteristics of fictive locomotor patterns, including spontaneous deletions of synergist motoneurons, occurring with and without rhythm resetting, as well as various effects of afferent stimulations on the locomotor phase durations and phase transitions (for details see, McCrea and Rybak 2007, 2008; Rybak *et al.* 2006a; Rybak *et al.* 2006b). However, this original CPG model is a reduced one; it has been primarily developed to demonstrate the advantages of the two-level CPG organization. It simulates the control of only two motoneuron pools and does not consider the activity and control of bifunctional motoneurons, such as PBSt and RF.

Even though Perret and his colleagues (Perret *et al.* 1988) believed that the variability of PBSt and RF activity patterns is the result of interactions between the central locomotor drive and afferent influences, recent fictive locomotion studies of decerebrate cats in the absence of sensory feedback (Markin *et al.* 2007; Markin *et al.* 2008), and research done as part of this study indicate that the full repertoire of PBSt and RF non-trivial behaviors can in fact be generated by the CPG alone. The concept that excitatory and inhibitory inputs from both extensor and flexor parts of the bipartite locomotor rhythm generator are involved in shaping PBSt and RF activity patterns, as suggested by Perret and his colleagues (Orsal *et al.* 1986; Perret and Cabelguen 1980;

Perret 1983; Perret *et al.* 1988), has not been implemented so far in a computational model. However, this CPG organization, incorporating additional neuronal networks for shaping PBSt and RF activities, provides only an explanation for biphasic PBSt and RF patterns but does not explain the complete variety of PBSt and RF profiles observed during fictive locomotion and their specific behaviors during spontaneous deletions.

The major objective of this study was to demonstrate that complex patterns of bifunctional motoneurons, specifically the variety of PBSt and RF patterns, can be generated within the framework of the two-level CPG with a bipartite RG. Analyzing PBSt and RF activity patterns observed during fictive locomotion we proposed and incorporated in the model (at the PF level of the CPG) a hypothetical network of interneuron populations that provided for the full repertoire of the PBSt and RF activity profiles and explained the various behaviors they exhibit during deletions. The architecture of this network was explicitly evolved from the analysis of PBSt and RF behaviors during deletions. We systematically analyzed and classified patterns of PBSt and RF activities recorded during fictive locomotion in decerebrate immobilized cats. We also analyzed the behavior of PBSt and RF motoneurons during deletions representing spontaneous errors in the rhythmic activity. During deletions, the behavior of PBSt and RF motoneurons is fairly complex, and in most instances cannot be predicted based on their patterns exhibited before and after a deletion We believe that the complex behaviors of PBSt and RF occurring during fictive locomotion and spontaneous deletions provides clues to the organization of the neuronal networks in the locomotor CPG participating in shaping PBSt and RF activity.

Chapter 4: Methods

4.1 Experimental Recordings

The experimental data pertaining to motoneuron activity used in the present study was collected over several years in Drs. David McCrea's and Larry Jordan's laboratories at the University of Manitoba and examined PBSt and RF activity during fictive locomotion, in decerebrate deafferented cats, induced by midbrain stimulation. No new animals were used to collect data for the present study. Instead we used the existing experimental database available at the Spinal Cord Research Center, in the University of Manitoba. Surgical and experimental protocols for the above experiments were performed in compliance with the guidelines set out by the Canadian Council on Animal Care and the University of Manitoba. Anaesthetized cats were precollicular-postmammillary decerebrated such that all cortex and rostral brainstem regions were removed before discontinuing the anesthetic. Fictive locomotion was evoked by unilateral or bilateral electrical stimulation of the MLR with 0.5ms duration current pulses (50-500mA, 10-20Hz) following neuromuscular blockade. During each experiment, the activities of several (4-9) hind limb ipsilateral nerves were simultaneously recorded after the nerves were dissected and mounted on conventional hook electrodes. ENG records were rectified and integrated before digitization at 500Hz (for further details see, Lafreniere-Roula and McCrea 2005). For this study, experimental recordings containing PBSt, RF, or both, were chosen.

Fig. 5 provides a schematic representation of the location of all muscles controlled by the motoneuron pools used in this study. During fictive locomotion, both the total duration of the locomotor cycle and the duration of flexion and extension phases

exhibited substantial variability between preparations. Therefore, building a full table of all major motoneuron activities from many experiments required the development and implementation of special normalization and averaging procedures.

The full list of motoneurons used as part of this research along with their name abbreviations is presented here: EDL - extensor digitorum longus (ankle flexor); LG - lateral gastrocnemius (ankle extensor); LGS - LG combined with soleus; MG - medial gastrocnemius (ankle extensor); GS - combined LGS and MG; Plant - plantaris (ankle extensor); PB - posterior biceps (hip flexor/knee extensor); St - semitendinosus (hip flexor/knee extensor); PBSt - PB combined with St (hip flexor/knee extensor); RF - rectus femoris (hip extensor/ knee flexor); Sart - sartorius (hip/knee flexor); SmAB - semimembranosus combined with anterior biceps; TA - tibialis anterior (ankle flexor); VA - vastus (knee extensor).

4.2 Data Processing

During fictive locomotion, PB (posterior biceps) and St (semitendinosus) motoneurons, if recorded separately, demonstrated similar activity patterns and similar behavior during spontaneous deletions. This is illustrated in Fig. 6 for PB and St flexor related (Fig. 6A), extensor related (Fig. 6B), and biphasic (Fig. 6C) activity types. Fig. 6C shows PB and St behavior during three successive deletions. Both PB and St are biphasic before and after the deletions, and become silent during extensor deletions with tonically active flexor (Sart) (first and third deletion episodes in Fig. 6C) and tonically active during flexor deletion with tonically active extensor (SmAB) (second deletion episode in Fig. 6C). Because of their similarity during most experiments where they were

simultaneously recorded, we considered the combined PB and St ENG activity (PBSt) in our analysis.

During fictive locomotion, both the total duration of the step cycle and the duration of flexion and extension phases exhibited substantial variability between preparations. Therefore, to obtain averaged patterns for similar profiles of PBSt, RF and other motoneurons, normalization was used. Each ENG pattern was normalized for both amplitude and phase duration. The custom software developed at the Spinal Cord Research Center, in the University of Manitoba, and running under the Linux operating system was used to detect the onset and offset of bursts in the pre-processed recorded ENGs. The step cycle period in each experimental record was defined as the average time between two consecutive flexor or extensor bursts. The burst onset of Sart was considered to be the beginning of flexion and the burst onset of SmAB was considered to be the beginning of extension. Because the locomotion cycle and phase durations substantially varied between preparations, the durations of flexor and extensor phases were normalized separately over all experiments. The duration of the normalized step cycle was set to 1s, and because in fictive locomotion experiments there was no definite phase dominance between flexion and extension, the duration of the normalized flexor and extensor phases was set to 0.5s for both. The normalized timing for onset and offset of ENG activity for all motoneurons were presented relative to the corresponding (flexor or extensor) phase, and motoneuron activities, normalized and averaged within each phase, were then connected together in the proper sequence; for biphasic ENG patterns, each phase was separately processed.

ENG patterns for each step cycle were linearly interpolated before being normalized. This is illustrated in Fig. 7 for one ENG burst that is mainly located in the flexor phase. Normalization was performed as follows. Let $\vec{S}^j$ be a j-th pre-processed ENG recording ($j = 1, 2,..., N$), where N is the total number of records for all experiments. The corresponding normalized pattern $\vec{S}^j_{norm}$ can be presented as vector $\vec{S}^j_{norm} = \{(\tau_i^j, a_i^j)\}$, $i = 1, 2, ..., M$, where M is the number of crossing points between the original signal $\vec{S}^j$ and amplitude levels A_i^j which are evenly distributed in the range $[0, A_{max}^j]$, where A_{max}^j is the maximal amplitude of the original pattern $\vec{S}^j$; a_i^j is the normalized value of the original pattern at time t_i^j when the signal crosses the i-th amplitude level; τ_i^j is the normalization of time t_i^j relative to the current phase duration (T_F^j or T_E^j). The components of normalized vector $\vec{S}^j_{norm} = \{(\tau_i^j, a_i^j)\}$ were calculated as follows:

$$\tau_i^j = \begin{cases} 0.5 \cdot \dfrac{t_i^j - t_F^j}{T_E^{j-1}}, & if \quad t_i^j \in [t_E^{j-1}, t_F^j); \\[3mm] 0.5 \cdot \dfrac{t_i^j - t_F^j}{T_F^j}, & if \quad t_i^j \in [t_F^j, t_E^j); \\[3mm] 0.5 + 0.5 \cdot \dfrac{t_i^j - t_E^j}{T_E^j}, & if \quad t_i^j \in [t_E^j, t_F^{j+1}); \\[3mm] 1.5 \cdot \dfrac{t_i^j - t_F^{j+1}}{T_F^{j+1}}, & if \quad t_i^j \in [t_F^{j+1}, t_E^{j+1}). \end{cases}$$

$$a_i^j = \frac{A_i^j}{A_{max}^j}.$$

where t_F^j is the onset time for the flexor phase, and t_E^j is the onset time for the extensor phase (see Fig. 7).

Averaged ENG patterns for all experiments were obtained using the following process: (1) each original pattern (extensor, flexor, PBSt and RF) was normalized for both its amplitude and phase duration over several consecutive step cycles (as described above); (2) normalized PBSt and RF patterns were classified according to their activity profiles; (3) all normalized patterns were averaged over several different experiments (different types of PBSt and RF activities were averaged separately). The normalized patterns of flexor and extensor motoneurons, and each type of PBSt and RF activity profile were averaged for all experiments, according to the following equation:

$$\vec{S}_{ENG} = \{(\bar{\tau}_i, \bar{a}_i)\} = \begin{cases} \bar{\tau}_i = \dfrac{\sum_j \tau_i^j}{N} \\[4mm] \bar{a}_i = \dfrac{\sum_j a_i^j}{N} \end{cases} \quad j = 1,2,..N \; .$$

where N is the total number of normalized patterns through all experiments , $\bar{\tau}_i$ and $\bar{a}_i$ are the averaged time and amplitude of the averaged pattern $\vec{S}_{ENG}$.

Only stable records (with less than 20% variability in both amplitude and step cycle period during not less than 10 successful step cycles) containing ENGs of PBSt (n=67) or RF (n=23) were selected for processing of PBSt and RF patterns in this study.

To analyze PBSt and RF behaviors during spontaneous deletions, experimental recordings with deletions and with recordings of PBSt and/or RF ENGs were divided into groups according to the following criteria: (1) the type of agonist motoneuron pools with activity missing during the deletion episode (flexor or extensor); (2) the type of deletion (resetting/non-resetting/rhythmic flexors) (see, Lafreniere-Roula and McCrea 2005;

Rybak *et al.* 2006a); (3) the type of PBSt or RF activity pre and post-deletion; (4) the type of PBSt or RF behavior during the deletion (silent/tonic/rhythmic).

4.3 Modeling

4.3.1 Basic Concept and Network Architecture

The model of the spinal locomotor CPG proposed here is an extension of the previous model developed by Rybak *et. al*. (2006a; 2006b) (Fig. 3B). Similar to the preceding model, the extended model is based on a two-level CPG concept (Fig. 3A); therefore, the locomotor CPG includes a half-center RG (identical to that found in the previous model) and a PF network. The extended model maintains all neural populations and their interconnections that were present in the preceding model. To maintain the analogy with experimental data on fictive locomotion, locomotor activity in the model is initiated by an external tonic "MLR drive" to excitatory neural populations of the CPG. The locomotor rhythm generation at the RG level is based on a combination of intrinsic (persistent sodium current) properties of excitatory RG neurons and reciprocal inhibition between the two half-centers (the RG-E and RG-F populations) mediated by inhibitory populations Inrg-E and Inrg-F[1] (described in detail in, Rybak *et al.* 2006a). The alternating busting activities of the RG-E and RG-F populations define the extensor and flexor phases of the locomotor cycle. The principal PF populations (PF-E and PF-F), in addition to the tonic excitatory drive from MLR, receive excitatory and inhibitory inputs from RG populations and inhibitory inputs from interneuron populations within the PF (Inpf-E and

---

[1] Note that for consistency with the current work we reversed the names of inhibitory interneuron populations Inrg-E, Inrg-F, Inpf-E and Inpf-F compared to the basic model (Rybak *et al.* 2006a; Rybak *et al.* 2006b). The 'E' or 'F' in each interneuron population's name now corresponds to the phase in which that particular population is active.

Inpf-F). The principal PF populations (PF-E and PF-F) finally transmit rhythmic activities to extensor (Mn-E) and flexor (Mn-F) motoneuron populations and to the inhibitory Ia interneuron populations (Ia-E and Ia-F), representing a third level of reciprocal inhibition in the system and rhythmically inhibiting motoneuron populations during the inactive phase of the step cycle (see Fig. 3B). The model also includes populations of Renshaw cells (R-E, and R-F) that receive collateral excitatory input from the corresponding motoneuron populations (Mn-E and Mn-F) and provide feedback inhibition to the homonymous motoneuron population, and populations of Ia inhibitory neurons (Ia-E and Ia-F).

In this extended model, we incorporated additional populations of PBSt and RF motoneurons (Mn-PBSt and Mn-RF), corresponding populations of Renshaw cells (R-PBSt and R-RF), and additional circuitry at the PF level to provide the desired PBSt and RF motoneuron activity. Specifically, we have suggested that at the PF level of the CPG there are populations specifically responsible for generating the PBSt and RF motoneuron activity. This suggestion was based on evidence showing that both PBSt and RF, of all types, demonstrate variable behavior during spontaneous deletions that is sometimes dissimilar from motoneuron populations corresponding to the type of activity of the bifunctional motoneuron pool before and after a deletion (see Table 4). Therefore, we included in the PF network populations PF-PBSt and PF-RF which: (1) receive "MLR" drive, similar to PF-F and PF-E populations; (2) receive excitatory inputs from extensor and flexor parts of the CPG; and (3) directly project to and control the activities of the corresponding motoneuron pools, Mn-PBST and Mn-RF. We also incorporated additional inhibitory interneuron populations (In-E, In-F, In-lE, In-lF, In-eE, and In-eF)

which shape the activity of PF-PBSt and PF-RF populations (Fig. 10). In addition, we had to, (1) define inputs to PF-PBST and PF-RF from extensor and flexor parts of the CPG (e.g., decide whether these inputs came from the RG or PF level of the CPG); (2) decide if In-F and In-lF shaping PBSt activity during flexion (or In-E and In-eE shaping RF activity during extension) comprise one population; and (3) construct circuits (connections and additional neural populations if necessary) that would provide the appropriate activities of interneuron populations involved in shaping PF-PBSt and PF-RF activities under different conditions.

It is important to note that there might be several network architectures that would reproduce the full repertoire of PBSt and RF activity. However, if the behavior of PBSt and RF during deletion experiments is taken into consideration, then this greatly limits the possibilities of probable network organizations. Therefore, in the construction of PF level networks, we took into consideration the behavior of PBSt and RF during deletions, in addition to their various activity types during fictive locomotion, to arrive at the most realistic model possible.

4.3.2 Modeling Single Motoneurons and Interneurons

All neurons were modeled in the Hodgkin-Huxley style. Interneurons were simulated as single compartment models. Motoneurons had two compartments: soma and dendrite and were described based on the previous model (Booth *et al.* 1997; Rybak *et al.* 2006a). In accordance with these models, the following ionic currents (with the corresponding channel conductances) have been included: fast sodium (I_{Na} with maximal conductance $\bar{g}_{Na}$); delayed rectifier potassium (I_K with maximal conductance $\bar{g}_K$);

calcium-N (I_{CaN} with maximal conductance $\bar{g}_{CaN}$); calcium-L (I_{CaL} with maximal conductance $\bar{g}_{CaL}$), calcium-dependent potassium ($I_{K,Ca}$ with maximal conductance $\bar{g}_{K,Ca}$), and leakage (I_L with constant conductance g_L) currents. In addition, based on evidence of the presence of persistent (slowly inactivating) sodium current (I_{NaP}) in spinal cord interneurons and motoneurons (Darbon *et al.* 2004; Lee and Heckman 2001; Streit *et al.* 2005), this current has been also included in our neuron models (with maximal conductance $\bar{g}_{NaP}$). Also, based on evidence for the presence of a transient (rapidly inactivating) potassium current in the spinal cord interneurons and motoneurons (Safronov and Vogel 1995) this current has been also included in our motoneuron models (I_A with maximal conductance $\bar{g}_A$). The above ionic currents are described as follows:

$$I_{Na} = \bar{g}_{Na} \times m_{Na}^3 \times h_{Na} \times (V - E_{Na});$$
$$I_{NaP} = \bar{g}_{NaP} \times m_{NaP} \times h_{NaP} \times (V - E_{Na});$$
$$I_K = \bar{g}_K \times m_K^4 \times (V - E_K);$$
$$I_A = \bar{g}_A \times (0.6 \times m_{A1}^4 \times h_{A1} + 0.4 \times m_{A2}^4 \times h_{A2}) \times (V - E_K);$$
$$I_{CaN} = \bar{g}_{CaN} \times m_{CaN}^2 \times h_{CaN} \times (V - E_{Ca});$$
$$I_{CaL} = \bar{g}_{CaL} \times m_{CaL} \times (V - E_{Ca});$$
$$I_{K,Ca} = \bar{g}_{K,Ca} \times m_{K,Ca} \times (V - E_K);$$
$$I_L = g_L \times (V - E_L),$$

where V is the membrane potential of the corresponding neuron compartment (soma, $V_{(S)}$, or dendrite, $V_{(D)}$) in two-compartment models, or the neuron membrane potential V in one-compartment models; E_{Na}, E_K, E_{Ca}, and E_L are the reversal potentials for sodium, potassium, calcium, and leakage currents, respectively; variables m and h with indexes indicating ionic currents represent, respectively, the activation and inactivation variables

of the corresponding ionic channels. The descriptions of activation and inactivation variables for each channel can be also found in Table 1.

The reversal potential values in the model are as follows: E_{Na}=55mV; E_K=-80mV; E_{Ca}=80 mV; E_L=-64±0.64mV in RG neurons, E_L=-65±0.325mV in Inrg interneurons and motoneurons, and E_L=-68±0.34mV in all other neurons.

The dendrite-soma coupling currents (with conductance g_C) for soma $I_{C(S)}$ and dendrite $I_{C(D)}$ are described following the Booth et al. (1997) model:

$$I_{C(S)} = \frac{g_C}{p} \times (V_{(S)} - V_{(D)});$$

$$I_{C(D)} = \frac{g_C}{1-p} \times (V_{(D)} - V_{(S)}),$$

where p is the parameter defining the ratio of somatic surface area to total surface area (p=0.1); g_C=0.1mS/cm^2.

The synaptic excitatory (I_{synE} with conductance g_{synE} and reversal potential E_{SynE}=-10mV) and inhibitory (I_{synI} with conductance g_{synI} and reversal potential E_{SynI}=-70mV) were also incorporated into the model and described as follows:

$$I_{SynE} = g_{SynE} \times (V - E_{SynE});$$
$$I_{SynI} = g_{SynI} \times (V - E_{SynI}).$$

The kinetics of intracellular Ca^{2+} concentration (Ca, described separately for each compartment) is modeled according to the following equation (Booth et al. 1997):

$$\frac{d}{dt} Ca = f \times (-\alpha \times I_{Ca} - k_{Ca} \times Ca),$$

where f defines the percentage of free to total Ca^{2+}, α converts the total Ca^{2+} current, I_{Ca}, to Ca^{2+} concentration, and k_{Ca} represents the Ca^{2+} removal rate.

In accordance with the two compartment motoneuron model (Booth *et al.* 1997; Rybak *et al.* 2006a), the membrane potentials of the motoneuron soma ($V_{(S)}$) and dendrite ($V_{(D)}$) are described according to the following differential equations:

$$C \times \frac{dV_{(S)}}{dt} = -I_{Na(S)} - I_{K(S)} - I_{A(S)} - I_{CaN(S)} - I_{K,Ca(S)} - I_{L(S)} - I_{C(S)} ;$$

$$C \times \frac{dV_{(D)}}{dt} = -I_{NaP(D)} - I_{CaN(D)} - I_{CaL(D)} - I_{K,Ca(D)} - I_{L(D)} - I_{C(D)} - I_{SynE} - I_{SynI} ,$$

where C ($C=1\mu F/cm^2$) is the membrane capacitance and t is time. With the following maximal conductances for the soma compartment: $\bar{g}_{Na}=120mS/cm^2$; $\bar{g}_K=100mS/cm^2$; $\bar{g}_A=200\pm40mS/cm^2$; $\bar{g}_{CaN}=14mS/cm^2$; $\bar{g}_{K,Ca}=2mS/cm^2$; $g_L=0.51mS/cm^2$. And the following maximal conductances for the dendrite compartment: $\bar{g}_{NaP}=0.1mS/cm^2$; $\bar{g}_{CaN}=0.3mS/cm^2$; $\bar{g}_{CaL}=0.33mS/cm^2$; $\bar{g}_{K,Ca}=0.8mS/cm^2$; $g_L=0.51mS/cm^2$. Subscripts S and D indicate the soma or dendrite compartments, respectively.

For simplicity and because of the lack of specific data, all interneurons (single compartment models) except RG and PF neurons contain only a minimal set of ionic currents:

$$C \times \frac{dV}{dt} = -I_{Na} - I_K - I_L - I_{SynE} - I_{SynI}$$

with the following maximal conductances: $\bar{g}_{Na}=120mS/cm^2$; $\bar{g}_K=10mS/cm^2$; $g_L=0.51mS/cm^2$.

The excitatory neurons of the RG and PF levels and populations In-eE and In-eF include the persistent (slowly inactivating) sodium current, I_{NaP}, which has been suggested to play an important role in the intrinsic rhythmogenesis in spinal interneurons

(Darbon *et al.* 2004; Streit *et al.* 2005). The membrane potential of these interneurons is described as follows:

$$C \times \frac{dV}{dt} = -I_{Na} - I_{NaP} - I_K - I_L - I_{SynE} - I_{SynI}$$

with maximal conductances for neurons in these populations as follows: g_L=0.51mS/cm^2; $\bar{g}_{Na}$=150mS/cm^2 in RG neurons and 120mS/cm^2 in both PF populations and In-eE and In-eF populations; $\bar{g}_{NaP}$=1.25mS/cm^2 in both RG populations and In-eE and In-eF populations and 0.1mS/cm^2 in both PF populations; $\bar{g}_K$=5mS/cm^2 in RG populations and 10mS/cm^2 in both PF populations and In-eE and In-eF populations.

Activation m and inactivation h of voltage-dependent ionic channels (e.g., Na$^+$, Na$_P^+$, K$^+$, K$_A^+$, Ca$_N^{2+}$, Ca$_L^{2+}$) are described by the following differential equations:

$$\tau_{mi}(V) \times \frac{d}{dt} m_i = m_{\infty i}(V) - m_i;$$
$$\tau_{hi}(V) \times \frac{d}{dt} h_i = h_{\infty i}(V) - h,$$

where i identifies the name of the channel, $m_{\infty i}(V)$ and $h_{\infty i}(V)$ define the voltage-dependent steady-state activation and inactivation respectively, and $\tau_{mi}(V)$ and $\tau_{hi}(V)$ define the corresponding time constants (see Table 1). Activation of sodium channels is considered to be instantaneous ($\tau_{mNa}=\tau_{mNaP}=0$) (Booth *et al.* 1997; Butera *et al.* 1999).

Activation of the Ca^{2+} dependent potassium channels is also considered instantaneous and described as follows (Booth *et al.* 1997):

$$m_{K,Ca} = \frac{Ca}{Ca + K_d},$$

where Ca is the Ca^{2+} concentration within the corresponding compartment or neuron, and K_d defines the half-saturation level of this conductance.

Excitatory (g_{SynE}) and inhibitory synaptic (g_{SynI}) conductances are equal to zero at rest and may be activated (opened) by the excitatory or inhibitory inputs respectively:

$$g_{SynEi}(t) = \bar{g}_E \times \sum_j \sum_{t_{kj}<t} S\{w_{ji}\} \times \exp(-(t - t_{kj})/\tau_{SynE}) + \bar{g}_{Ed} \times \sum_m S\{w_{dmi}\} \times d_{mi};$$

$$g_{SynIi}(t) = \bar{g}_I \times \sum_j \sum_{t_{kj}<t} S\{w_{ij}\} \times \exp(-(t - t_{kj})/\tau_{SynI}) + \bar{g}_{Id} \times \sum_m S\{-w_{dmi}\} \times d_{mi},$$

where the function $S\{x\}=x$, if $x\geq0$, and 0 if $x<0$. The excitatory and inhibitory synaptic conductances have two terms: the first term describes the integrated effect of inputs from other neurons in the network (excitatory and inhibitory respectively). The second term describes the integrated effect of inputs from external drives or stimulations d_{mi} (see also, Rybak *et al.* 1997; Rybak *et al.* 2003). Each spike arriving to neuron i from neuron j at time t_{kj} increases the excitatory synaptic conductance by $\bar{g}_E \times w_{ji}$ if the synaptic weight $w_{ji}>0$, or increases the inhibitory synaptic conductance by $-\bar{g}_I \times w_{ji}$ if the synaptic weight $w_{ji}<0$. $\bar{g}_E=0.05\text{mS/cm}^2$ and $\bar{g}_I=0.05\text{mS/cm}^2$ are the parameters defining an increase in the excitatory or inhibitory synaptic conductance, respectively, produced by one arriving spike at $|w_{ji}|=1$. $\tau_{SynE}=5\text{ms}$ and $\tau_{SynI}=15\text{ms}$ are the decay time constants for the excitatory and inhibitory conductances respectively. The second terms of the equations, $\bar{g}_{Ed} = \bar{g}_{Id}=1\text{mS/cm}^2$ are the parameters defining the increase in the excitatory synaptic conductance, produced by external input drive $d_{mi}=1$ with a synaptic weight of $|w_{dmi}|=1$.

4.3.3 Modeling Neural Populations

In the present model, each functional type of interneuron is represented by a population of 20 neurons, and each type of motoneuron by a population 40 neurons. Connections between populations were established such that if population A was assigned to receive an excitatory or inhibitory input from population B or external drive D, then each neuron in population A receives the corresponding excitatory or inhibitory synaptic input from each neuron in population B or from drive D, respectively. All connections were randomly distributed to provide heterogeneity of individual neuron behavior in populations. The mean weights of synaptic connections between the neural populations in our model are shown in Table 2. Standard deviations of the synaptic weights varied from 10% to15% of mean value.

In addition to the random distribution of inputs, the heterogeneity of neurons within each population was provided by a random distribution of reversal potential of leak channel, E_L, and initial conditions for values of membrane potential, calcium concentrations and some channel conductances. In all simulations, initial conditions were chosen randomly from a uniform distribution for each variable, and a settling period of 20s was allowed before data was collected. Each simulation was repeated 20-30 times, and demonstrated qualitatively similar behavior.

4.4 Computer Simulations

All simulations were performed on an Intel Core i7$^{(tm)}$ 2.8GHz/4GB with a Windows XP operating system using a special simulation package NSM 2.1 RC2, developed at Drexel University by I. A. Rybak, S. N. Markin, and N. A. Shevtsova using

Microsoft Visual C++. Differential equations were solved using the exponential Euler

integration method (MacGregor 1987) with a step of 0.1 ms (Rybak *et al.* 2006a; Rybak

et al. 2003).

Chapter 5: Activity Patterns of PBSt and RF during Fictive Locomotion

5.1 Classification of PBSt and RF Activity Patterns

Prior to extending the previous two-level CPG model, data pertaining to PBSt and RF motoneuron activity during fictive locomotion was collected, classified and analyzed. This data of motoneuron ENGs, during MLR stimulation evoked fictive locomotion, were obtained from the experimental database of the Spinal Cord Research Center at the University of Manitoba. All motoneuron recordings were performed in fictive locomotion preparations, with activity evoked in decerebrate immobilized cats through electrical stimulation of the MLR. Recordings were carried out in several nerve fibers during each experiment; recordings used for this particular research project included ones that had at least one of PBSt or RF ENGs, or both. Analyzed data included 98 records from 48 cats (with 35 step cycles on average in each record). The locomotor cycle duration in different experiments varied from 400 to 1800ms and was 690ms on average. Averaged and normalized profiles of motoneuron activities during fictive locomotion are shown in Fig. 2A. The activity of all one-joint motoneuron pools (both flexor and extensor) fully corresponded to their function, i.e. all flexor motoneurons were active during the flexor phase and silent during the extensor phase and all extensor motoneurons were active only during extension. In contrast, two-joint and multi-joint motoneurons (i.e. those activating muscles spanning more than one joint), such as PBSt and RF, demonstrated a variety of activity patterns depending on the preparation.

Patterns of PBSt and/or RF were classified as either flexion or extension related, depending on the primary muscle group with which they were co-active, or as biphasic if

they were active during both phases of the locomotor cycle. Activity patterns of PBSt motoneurons were qualitatively classified under three distinct types:

1. A flexor-type PBSt profile, where PBSt motoneurons were active only during the flexion phase (Fig. 8A, B, G and H). In the majority of recordings of flexor-type PBSt (more than 75 %), PBSt showed only a short burst of activity at the onset of flexion (less than one third of the phase's duration) (Fig. 8A, G and H); and in the other 25% of the recordings, PBSt exhibited a longer burst of activity starting at the onset of flexion and continuing up to or more than half of the phase (Fig. 8B).

2. An extensor-type PBSt profile, where PBSt motoneurons were active during extension (Fig. 8C and D). In this case, PBSt was usually active for the entire phase.

3. A biphasic PBSt profile, where activity occurred during both phases of the locomotor cycle (Fig. 8E and F). Activity during flexion occurred at the onset of the phase and for only a short duration; activity during extension covered the entire phase. The amplitude of activity varied significantly between different experiments (compare Fig. 8E and F).

On the other hand, RF activity during fictive locomotion experiments was classified under two different types:

1. A flexor-type, where RF was active late in flexion with activity starting within the first half of the phase (rather than from the beginning of the phase) and ramping up until the end of flexion (Fig. 8G).

2. A biphasic profile, where RF activity was comprised of two components, a short burst at the end of extension and a longer burst at the end of flexion (Fig. 8H).

5.2 Normalized Profiles of PBSt and RF Activity

Records classified as belonging to the same type of PBSt or RF where normalized and averaged within each category. Fig. 9A shows the normalized and averaged profiles for the three types of PBSt patterns (panel Ab) and the two types of RF patterns (panel Ac), corresponding to the classifications described above, and with respect to the normalized activity of typical flexor (Sart) and extensor (SmAB) motoneurons (panel Aa). The data presented in Fig. 9A was averaged over 49 recordings for flexor-type PBSt (type 1), 6 recordings for extensor-type PBSt (type 2); 12 recordings for biphasic PBSt (type 3); 13 recordings for flexor-type RF (type 1); and 10 recordings for biphasic RF (type 2).

Analysis of PBSt and RF activities from experiments where they were simultaneously recorded revealed that they were never simultaneously active together. Fig. 9B illustrates the averaged and normalized RF patterns with respect to three types of PBSt behavior for experiments with simultaneous recording of PBSt and RF ENGs.

1. When PBSt demonstrated flexor-type activity (i.e. type 1), RF was either biphasic (type 2) or flexor-type with delayed activity increasing towards the end of flexion (type 1) (Fig. 9Ba).

2. When PBSt activity was extensor related (type 2) or biphasic (type 3), RF displayed flexor-type activity (type 1) (Fig. 9Bb and Bc).

5.3 Discussion

After analyzing the data available on PBSt and RF behavior, no consistent relationships between PBSt and RF activity patterns and the locomotor period and/or

phase dominance were found. For example, the locomotor rhythm is flexor dominated in the recordings shown in Fig. 8A and B, and PBSt demonstrates flexor-type behavior in both cases, however in each case PBSt demonstrates a different length of the flexor related burst; a short burst at flexion onset in Fig. 8A, and a longer burst in Fig. 8B that lasts for the majority of the phase's duration. Furthermore in Fig. 8C and D, even though the locomotor rhythm is extensor dominated in Fig. 8C and flexor dominated in Fig. 8D, in both cases PBSt is of the extensor-type. Finally, in Fig. 8E and F, even though the locomotor rhythm is symmetric in Fig. 8E and extensor dominated in Fig. 8F, PBSt demonstrates biphasic activity in both instances. Therefore, we concluded that the particular pattern expressed by PBSt or RF was dependent on the preparation and remained unchanged during the course of the absolute majority of the experiments, even during experiments where the locomotor period, phase durations, or burst amplitude spontaneously varied. Furthermore, if deletions spontaneously occurred, PBSt and RF activity re-emerged after the deletions unchanged and had the same profile as before the deletion.

Analysis of simultaneous activity of PBSt and RF during fictive locomotion indicated some reciprocal relationships between these motoneuron populations. When PBSt was active during extension (i.e., expressed an extensor-type or biphasic profile), RF never exhibited any extension related activity and was only active during flexion. And *vice versa*, if RF exhibited a biphasic profile, PBSt was only active during flexion. However, we did not classify PBSt and RF as direct antagonists since their activity is not always antagonistic and both can be silent at the same time in some instances (for example, during extension, when both have flexor-type activity; or early in flexion, when PBSt

exhibits extensor-type activity and RF exhibits flexor-type activity). These findings are similar to, and agree with, what has been previously reported (Perret 1983) of PBSt and RF activity when they were simultaneously recorded in fictive locomotion preparations, where late flexor RF activity appeared only with extensor and biphasic PBSt activity; and late extensor RF activity appeared only when PBSt was active during flexion.

The relationship between PBSt and RF during fictive locomotion appears to be complex or indirect, and may therefore involve interactions with circuits controlling other motoneuron pools. During real locomotion, more direct relationships between PBSt and RF motoneuron pools may be additionally established through sensory afferents (e.g., at the level of the reciprocal Ia interactions). A study of such possible interactions will require a detailed analysis of the effects of various afferent stimulations on the activity of PBSt and RF, as well as an analysis of intracellular motoneuron recordings.

5.4 Activity of Bifunctional Motoneurons and Organization of the Locomotor CPG

The study of the activity of bifunctional muscles, such as PBSt and RF, during fictive locomotion experiments is an approach for understanding the organization of the locomotor CPG. The first attempt at explaining the complex and non-trivial behavior of PBSt and RF motoneurons during fictive locomotion, in terms of the bipartite locomotor CPG organization, was made by Perret and his colleagues (Orsal *et al.* 1986; Perret 1983; Perret *et al.* 1988). The chief idea of their proposal was that bifunctional motoneuron pools of PBSt and RF receive excitatory and inhibitory inputs from both flexor and extensor CPG half-centers and that some additional interneural network is responsible for shaping the activity profiles of bifunctional motoneurons. The results presented as part of this

current research confirm these suggestions. First, during fictive locomotion experiments, we found that PBSt and RF may exhibit activity during both locomotor phases. This clearly suggested that both PBSt and RF receive excitatory inputs from both extensor and flexor parts of the locomotor CPG. Second, as mentioned earlier (see section 5.2 and Fig. 9B), PBSt and RF can be simultaneously active during flexion, each during just a part of the phase; PBSt during the earlier part and RF during the latter part of flexion. This confirmed Perret's suggestion that the activity of both PBSt and RF is regulated by inhibitory influences originating from additional inhibitory interneurons. Since the basic half-center CPG concept does not account for any inhibitory influences that can have such an effect on PBSt and RF activity, Perret (1988) suggested that this additional neuronal network is controlled by afferent feedbacks, and demonstrated how PBSt and RF patterns can be altered through tonic afferent inputs from the ipsilateral hindlimb. However, we found that during fictive locomotion, with all afferent feedbacks abolished, PBSt and RF activity patterns were still being shaped by inhibitory influences.

Available experimental data suggested that inhibitory circuitry responsible for shaping PBSt and RF activity during fictive locomotion can operate independent of any afferent feedbacks and is therefore directly controlled by the CPG. Furthermore, the hypothetical inhibitory interneuron populations making up this inhibitory circuitry must be part of the locomotor CPG for them to continue to operate in a fictive locomotion setup. On the other hand, afferent inputs to this additional circuitry would still be able to shape PBSt and RF activity during afferent stimulation, as was shown in Perret's experiments (Perret *et al.* 1988), and during real locomotion. Therefore, the interplay of excitatory and inhibitory influences is responsible for shaping PBSt and RF activity.

5.5 Shaping the Profiles of PBSt and RF Activity

Our goal was to expand the basic two-level CPG model (McCrea and Rybak 2007; Rybak *et al.* 2006a) to account for PBSt and RF behavior while maintaining the half-center organization of the rhythm generation level. Therefore, new inhibitory interneuron populations hypothesized to exist within the CPG, as discussed in the previous section, had to be incorporated at the pattern formation level. We previously suggested that both PBSt and RF receive excitatory inputs from both extensor and flexor parts of the CPG, as was also proposed by Perret and his colleagues for PBSt and RF motoneurons (Perret and Cabelguen 1980; Perret 1983); in addition we proposed that PBSt and RF should also receive excitatory tonic drives similar to pattern formation level interneuron populations controlling the activity of flexor and extensor motoneurons (McCrea and Rybak 2007; Rybak *et al.* 2006a) (Fig. 10B and D); excitatory connections and tonic input drives are represented by arrows. Therefore, PBSt and RF populations receive total excitatory inputs representing some weighted sum of the activities of the flexor and extensor parts of the CPG and tonic drive. The total excitatory inputs are shown schematically as lightly shaded areas in the third traces in Fig. 10A and C. The differences between the total excitatory inputs and the observed PBSt and RF profiles (darker profiles in the third traces in Fig. 10A and C) are shown in the bottom traces of Fig. 10A for PBSt and Fig. 10C for RF. We suggested that these "extra activations" (represented by the bottom traces in Fig. 10A and C) are eliminated by inhibition from hypothetical inhibitory interneuron populations, illustrated in Fig. 10B for PBSt and Fig. 10D for RF, which allows PBSt and RF to exhibit the different activity profiles.

Considering the different activity patterns of PBSt and RF during fictive locomotion experiments, we proposed additional interneuron populations that can shape these patterns at the PF level of the CPG. Specifically, we suggested that three inhibitory interneuron populations shape the activity of PBSt (see Fig. 10B; inhibitory connections are represented by lines terminating with a circle). The first (In-E_{PBSt}), active throughout the extensor phase, is responsible for inhibiting or shaping the extensor component of the PBSt profile. The second, (In-F), is active throughout the entire flexor phase, it is responsible for inhibiting the flexor component of PBSt when PBSt exhibits extensor-type activity. The third, (In-lateF, or In-lF), is active during late flexion with increasing activity towards the end of the phase, it is responsible for shaping the flexor component of the PBSt profile if PBSt is active during flexion. The strength of In-lF's activity determines the duration of PBSt's activity during early flexion; the weaker the activity of In-lF, the longer PBSt is active in flexion.

These additional inhibitory interneuron populations function in the following way to shape PBSt's activity: (1) if the activity of In-E_{PBSt} is strong (Fig. 10Ba), then the extensor component of the PBSt profile is fully inhibited, and the duration of PBSt flexor activity is regulated through the activity of In-lF, resulting in the expression of a flexor-type (type 1) PBSt activity (see dark profile in the third row of Fig 10Aa). (2) And if the activity of In-E_{PBSt} is moderate or weak (Fig. 10Bc), then PBSt maintains a low amplitude extensor component and exhibits a biphasic (type 3) pattern (dark profile in the third row of Fig. 10Ac). (3) Finally, if In-E_{PBSt} is inactive and the activity of In-F is strong enough to completely suppress the flexor component of PBSt (Fig. 10Bb), then

PBSt exhibits an extensor-type (type 2) profile (dark profile in the third row of Fig 10Ab).

Similarly, we suggested that three inhibitory interneuron populations shape the activity profile of RF (Fig. 10D). The first, In-E$_{RF}$, is active throughout the extensor phase, it is responsible for inhibiting the extensor component of RF when RF exhibits flexor-type activity. The second, (In-earlyE, or In-eE), is active at the beginning of the extensor phase, it is responsible for shaping the extensor component of the RF profile. The third, (In-earlyF, or In-eF), active during early flexion with decrementing activity, is responsible for shaping the flexor component of the RF profile. Similar to In-lF discussed above, the strength of activity of In-eF and In-eE determines the duration of RF's activity during late flexion and late extension, respectively; the weaker the activity of In-eF or In-eE, the longer RF is active in flexion or extension, respectively. Therefore: (1) If the activity of In-E$_{RF}$ is strong, then the extensor component of RF is fully inhibited (Fig. 10Da), and RF only exhibits flexor-type (type 1) activity, shaped by In-eF (see dark profile in the third row of Fig 10Ca). (2) And if In-E$_{RF}$ is inactive, and the activity of In-eE is moderate (Fig. 10Db), then RF is active in both phases and it exhibits biphasic (type 2) activity (dark profile in third row of Fig. 10Cb). In this case In-eE shapes the extensor component of the activity profile of RF and determines its onset and duration. In addition, in both types of RF profiles, the activity of In-eF shapes and determines the onset and duration of the flexor component of the RF profile.

It should be noted that In-lF, when considering PBSt, (or In-eE, when considering RF) may behave like In-F (or In-E$_{RF}$) if strongly active. In other words, exhibit activity for the entire duration of flexion (or extension), therefore inhibiting PBSt (or RF) for the

duration of the corresponding phase. Hence one may suggest that In-lF and In-F (or In-eE and In-E_{RF}) may possibly be one and the same, and therefore comprise the same interneuron population.

Relying only on the analysis of activity patterns of PBSt and RF during fictive locomotion is not enough to propose a comprehensive organization of the connections within the CPG and to establish whether In-F and In-lF should be merged into one population (in the case of PBSt), or In-E_{RF} and In-eE should be merged (in the case of RF). Hence, in the following sections we demonstrate how the behavior of PBSt and RF during different types of spontaneous deletions was used to gain further insights into the organization of the CPG circuitry and thus allowed us to propose an extended CPG model that would realistically reproduce all behaviors of PBSt and RF during fictive locomotion.

Chapter 6: Behavior of PBSt and RF during Spontaneous Deletions

We analyzed the behavior of PBSt and RF during deletions, which are characterized by brief periods of inactivity lasting for several step cycles and occurring simultaneously in multiple synergist motoneuron pools (e.g., flexors or extensors), while the activity of antagonist motoneuron pools usually becomes tonic or remains rhythmic (Lafreniere-Roula and McCrea 2005; Rybak *et al.* 2006a). Deletions with tonic activity of antagonistic motoneuron pools were previously classified under two types: resetting deletions, which are accompanied by a shift in the phase of the post deletion rhythmic activity, relative to the pre-deletion rhythm; and non-resetting deletions, after which the rhythm reappears without a phase shift of the post-deletion activity (Lafreniere-Roula and McCrea 2005; Rybak *et al.* 2006a). It was previously suggested that resetting deletions result from perturbations affecting the rhythm generation level of the locomotor CPG, whereas non-resetting deletions as well as deletions with rhythmic activity of antagonistic motoneuron pools occur when spontaneous perturbation affect the CPG at lower level circuits (pattern formation level) without influencing the rhythm generation level (Rybak *et al.* 2006a).

6.1 Results

The behaviors of both PBSt and RF during deletions of flexor and extensor activities were variable. This is illustrated for flexor-type PBSt in Fig. 11A-C showing records from three different experiments. All of these deletion episodes are of extensor motoneurons with tonic flexors, and in each experiment PBSt demonstrates flexor-type activity (type 1) before and after the deletion. However, the behavior of PBSt during the

deletions was completely different in each of these experiments. In Fig. 11A, PBSt behaved like a flexor during the deletion, i.e. it was tonically active. In Fig. 11B, PBSt was silent during the deletion, similar to all extensors. In Fig. 11C, PBSt demonstrated rhythmic activity during the deletion, with an oscillation frequency that was not related to the locomotor frequency before and after the deletion. In all three experiments, the reemerging post deletion activity pattern was identical to that observed before the deletion; this was also the case for the absolute majority of deletion experiments.

Results of the analysis of PBSt and RF behaviors during spontaneous deletions are summarized in Table 4. This analysis included data from 36 experiments involving 34 different cats. In some experiments, several spontaneous deletions episodes occurred separated by periods of rhythmic locomotor activity. For some of the experiments used, the activities of PBSt and RF motoneurons were simultaneously recorded. Deletions were separated into two groups based on the type of deletion, non-resetting or resetting; the latter group also included recordings with variable locomotor cycle length, for which it was difficult to determine whether a phase shift occurred during a deletion. The numbers in parentheses, in Table 4, indicate the number of deletion episodes where the particular PBSt or RF behavior was observed, for a given deletion and PBSt/RF type combination.

The following observations were made with regards to PBSt. (1) There is an obvious difference between the behavior of flexor-type PBSt with a short flexor burst and with a longer flexor burst, during deletions. This resulted in the separation of flexor-type PBSt into two subtypes (type 1a and type 1b) depending on the length of the flexor burst (see Table 4). (2) During resetting extensor deletions, the behavior of biphasic PBSt with a short flexor burst (not exceeding 30% of the flexor phase) compared to that with a

longer flexor burst are completely different. Biphasic PBSt with a short flexor burst is silent like extensors during the deletion, while biphasic PBSt with a longer flexor burst is tonic like flexors during the deletion. Though no data was available for the behavior of biphasic PBSt with a long flexor burst for other types of deletions, we separated biphasic type PBSt patterns into two subtypes (type 3a and 3b) depending on the length of the flexor burst, similar to flexor type PBSt (see Table 4).

Even though we could not find any explicit relationships between the behavior of PBSt or RF during a deletion episode and their activity profile (before and after the deletion), analysis of the results presented in Table 4, pointed to certain tendencies which are summarized below, (numbers in parentheses indicate the number of deletion episodes in which an observation was made):

1. Flexor-type PBSt with short flexor burst (type 1a), was silent during most deletions (n=11) (see, for example, Fig. 11B). However, during non-resetting extensor deletions with either tonic (n=1) or rhythmic flexors (n=1), PBSt demonstrated irregular rhythmic activity where some bursts disappeared and the remaining ones had reduced activity amplitude. For the bursts with reduced activity, the frequency was identical to the frequency of PBSt activity before and after the deletions.

2. Flexor-type PBSt with long flexor burst (type 1b), often but not always, behaved like flexors during deletion episodes. During flexor deletions (n=4), it was silent. During extensor deletions with rhythmic flexor activity (n=6), it was rhythmic. During resetting extensor deletions, in most cases (n=4), it also behaved like flexors (i.e. was tonically active, see for example Fig. 11A), except for one

experiment (shown in Fig. 11C) in which PBSt exhibited rhythmic bursts with a frequency not related to the frequency of PBSt activity before and after the deletion. Finally, during non-resetting extensor deletions with tonic flexors (n=4), type 1b PBSt maintained rhythmic activity during the deletion in all available experiments, and therefore in this case behaved unlike flexors which were tonic for the duration of the deletion episode.

3. Extensor-type PBSt (type 2), behaved like extensors during most observed deletions. During extensor deletions (n=13), it was silent. During resetting flexor deletions (n=8), it was tonic. However, during non-resetting flexor deletions, it was silent during one experiment and exhibited low amplitude rhythmic activity in another.

4. Biphasic PBSt with short flexor burst (type 3a), like extensor type PBSt, mostly behaved like extensors during deletions. During extensor deletions (n=8), it was silent. During resetting flexor deletions (n=5), it was tonic. No experiments were found where type 3a biphasic PBSt was recorded during a non-resetting flexor deletion.

5. Biphasic PBSt with a long flexor burst (type 3b), was tonic during resetting extensor deletions (n=2), but there were no experiments in our records where type 3b PBSt was recorded during any other type of deletion.

6. Flexor-type RF (type 1), was tonic during resetting extensor deletions (n=5), rhythmic during non-resetting extensor deletions with either tonic (n=1) or rhythmic (n=3) flexors, and silent during all flexor deletions (n=7).

7. Biphasic RF (type 2), like type 1 RF, was tonic during resetting extensor deletions (n=5), and rhythmic during non-resetting extensor deletions with either tonic (n=7) or rhythmic (n=9) flexors; but we had no experimental records with type 2 RF during a flexor deletion. Remarkably, during all episodes of rhythmic activity during a deletion (n=16), biphasic RF lost its extensor component.

6.2 Discussion

The behavior of PBSt and RF motoneurons during the various deletion types was rather complex, and in many cases could not be predicted based on their patterns expressed before and after the deletions (Table 4). Therefore, broad generalizations were not possible for the following:

1. Short flexor-type PBSt (type 1a), was silent during most deletions, except during extensor deletions with either tonic or rhythmic flexors, where it remained rhythmic and had reduced activity amplitude.

2. Long flexor-type PBSt (type 1b), behaved like flexors during all flexor deletions, during some resetting extensor deletions with tonic flexors (4 of 5 records), and during all extensor deletions with rhythmic flexors. However, type 1b PBSt maintained rhythmic activity during non-resetting extensor deletions with tonic flexors.

3. Extensor-type PBSt (type 2), behaved like extensors during most deletions, except during non-resetting flexor deletions, where it was either silent or rhythmic.

4. Flexor-type RF (type 1), behaved like flexors during all deletions, except during non-resetting extensor deletions with tonic flexors, where it was rhythmic.

5. Biphasic RF (type 2), behaved like flexors during all deletions, except during non-resetting extensor deletions with tonic flexors, where it was rhythmic. (Note, we had no experiments where type 2 RF was recorded during any type of flexor deletion)

On the other hand, based on available experiments where PBSt and/or RF were recorded during deletion episodes, we were able to draw more solid conclusions for the following:

1. Biphasic PBSt with short flexor burst (type 3a), behaved like extensors during all observed deletions. (Note, we had no experiments where type 3a PBSt was recorded during a non-resetting flexor deletion)

2. Biphasic PBSt with long flexor burst (type 3b), was tonic during resetting extensor deletions, which was the only type of deletion, with type 3b PBSt, that we were able to find among our experimental records.

Further observations that are worth noting at this point: (1) In most cases the behavior of both PBSt and RF was different during resetting versus non-resetting deletions. (2) PBSt behavior during resetting extensor deletions seems to be predominantly determined by the presence and duration of PBSt activity during the flexor phase. In particular, both flexor and biphasic type PBSt with long flexor bursts (types 1b and 3b) were tonic during resetting extensor deletions, while both flexor and biphasic type PBSt with short flexor bursts (types 1a and 3a) were silent during deletions of the same type. (3) The behavior of both flexor and biphasic type RF is similar during most deletion types. (4) In all deletion records, where RF and PBSt were simultaneously recorded during a deletion episode, they never exhibited concurrent activity which is indicative

that some reciprocal relationship exists between these motoneuron pools; but, there were situations where both PBSt and RF were silent during a deletion, indicating that these two motoneuron pools cannot be considered as direct antagonists.

Chapter 7: CPG Model Construction

7.1 Circuits Controlling the Activity of PBSt and RF

The objective of this study was to extend the basic model (Fig. 3B) originally presented by Rybak and McCrea (2006a) by incorporating additional circuitry necessary for the generation of PBSt and RF motoneuron activity. To construct such a model we proposed that the PF level of the CPG should include two unique populations, PF-PBSt and PF-RF, similar to the populations PF-F and PF-E proposed by Rybak and McCrea in their two-level model (Fig. 3B), which directly project to PBST and RF motoneuron pools, Mn-PBSt and Mn-RF respectively. Furthermore, we suggested that the PF level should include additional interneuron populations with a special organization of connections that provides the shaping of PBSt and RF activity patterns (see section 5.5). The extended model had to produce all patterns of PBSt and RF motoneuron activity expressed during fictive locomotion, and replicate the behavior of PBSt and RF observed during various types of deletions, as discussed in the previous section.

Therefore, based on the previous suggestions, PF-PBSt and PF-RF populations had to receive excitatory inputs from both extensor and flexor parts of the CPG, in addition to tonic MLR drive. These inputs could potentially come either from the RG or PF level (i.e., from RG-E or PF-E, and from RG-F or PF-F populations). We also suggested that the PF network included inhibitory populations In-E$_{PBST}$ (active during extension), In-F (active during flexion), and In-lF (active during late flexion) which are responsible for shaping the activity patterns of PBSt. Also, the PF network included inhibitory populations In-E$_{RF}$ (active during extension), In-eE (active during early

extension), and In-eF (active during early flexion) which are responsible for shaping the activity patterns of RF (see Fig. 10).

Complimentary activity patterns of PBSt and RF during flexion could result from the complimentary activities of In-eF and In-lF. This may be achieved by having the interneurons which make up population In-eF include adaptive intrinsic properties, in addition to having populations In-eF and In-lF in a mutually inhibitory relationship. Furthermore, in some experiments where PBSt and RF were recorded simultaneously and PBSt was active during extension only, the activity of flexor type RF did not start from the beginning of the flexor phase (see for example Fig. 8C), this indicated that populations In-F and In-lF, which are responsible for shaping the flexor component of PBSt activity, were in fact two separate populations, as we had speculated earlier. The reasoning here was that PBSt being active only during extension indicated that In-F was strongly active and inhibiting PBSt during flexion, but there must have been another inhibitory population, namely In-lF, active late in flexion and inhibiting In-eF activity, permitting RF activity in late flexion. On the other hand, no similar data was found to suggest that population In-E$_{RF}$ and In-eE, which are responsible for shaping the extensor component of RF activity, were two different populations. Therefore, we proposed that only one inhibitory population, In-eE, is responsible for shaping the extensor component of RF activity. When In-eE is strongly activated it inhibits RF for the entire extension phase and when In-eE is moderately active it inhibits RF for only the earlier part of extension, resulting in a flexor-type RF in the first case and biphasic RF in the second. Eliminating an unnecessary interneuron population, based on all available data to us at

the time, was mainly done to keep the CPG model as simple as possible while still being able to reproduce all desired PBSt and RF activity.

In summary, shaping the activity patterns of PBSt is provided by three inhibitory interneuron populations: In-E (subscript PBSt can now be omitted), active throughout extension; In-F, active throughout flexion, and In-lF, active during the latter part of flexion. On the other hand, shaping of the activity patterns of RF is provided by two inhibitory interneuron populations: In-eE, active during the early part of extension, and In-eF, active during the early part of flexion.

The interneuron populations proposed to be present at the PF level could potentially receive inputs from either the RG or PF levels of the CPG or from other sources. To determine the source of inputs for PF-PBSt, PF-RF, and all other interneuron populations involved in shaping PBSt and RF activity at the PF level of the locomotor CPG, we considered PBSt and RF behavior during different types of deletions (Fig. 12). The construction of the extended PF circuitry (shown in Fig. 13), was carried out in a process that took into account the behaviors of PBSt and RF during deletions, in addition to their activity profile before and after these deletions. At each step of the process, the determination of which connections needed to be added and which needed to be excluded was consistent with the behavior of all motoneuron records obtained from the experimental deletion data. The construction of the extended model included all interneuron and motoneuron populations that were present in the basic two-level model. The behaviors of essential interneuron populations retained from the basic model, during different types of deletions, are summarized in Table 3. Note that during non-resetting deletions (without phase shift of post-deletion activity) all populations at the RG level of

the CPG remain rhythmically active since the perturbation causing the deletion is acting at the PF level. Also note that, during all types of deletions the behavior (silent, tonic or rhythmic) of flexor and extensor motoneurons is identical to the behavior of their corresponding PF level population (PF-F and PF-E).

7.1.1 Construction of the Circuit Controlling PBSt Activity

In Fig. 12Aa, a fictive locomotion ENG recording, we have an extensor deletion episode where extensor motoneurons SmAB and GS were silent for the duration of three step cycles, while flexors Sart and TA, PBSt, and RF remained active. The lack of phase shift in the remerging locomotor activity, after the deletion, indicated that this deletion was non-resetting and resulted from increased excitability of population PF-F. During such a deletion, population RG-E and RG-F would maintain their rhythmic activity, while PF-E becomes silent and PF-F shows sustained (possibly modulated) tonic activity (Table 3) (Rybak *et al.* 2006a). In this example, PBSt exhibited a flexor-type profile (type 1) of activity before and after the deletion (see shaded bars 1 and 5 in Fig. 12Aa), therefore, its activity should be shaped by populations In-E, inhibiting PF-PBSt during extension, and In-lF inhibiting PF-PBSt during the latter part of flexion (see Fig. 10 and Fig. 13Aa). During this deletion episode, flexors were not tonically active; TA showed modulated sustained activity, whereas Sart remained rhythmic and was inactive during intervals where extensor activity was expected to occur had there been no deletion (see shaded bars 2-4 in Fig. 12Aa). PBSt exhibited rhythmic activity during the deletion, however it was active during intervals where extensor activity was expected and continued into parts of the flexor intervals. PBSt activity, occurring in the flexor intervals

during the deletion, had reduced amplitude and duration relative to its activity during flexion before and after the deletion (see shaded bars 2-4 in Fig. 12Aa). This is more clearly demonstrated in the top trace of Fig. 12Ab, which shows an enlarged overlay of PBSt ENG activity before the deletion (black trace) and during the deletion episode (red trace). Here you can clearly see how the red trace's (during the deletion) activity starts during the extensor interval and ends earlier compared to the black trace (pre-deletion), furthermore the amplitude of the red trace is lower than that of the black one. This particular behavior of PBSt during the deletion indicated that, (1) PF-PBSt continued to receive excitatory inputs from both extensor and flexor parts of the CPG during the deletion; (2) population In-E, which inhibited PF-PBSt before and after the deletion during extension, became silent or at the very least its activity decreased during the deletion episode; and (3) populations In-F and In-lF, shaping PF-PBSt behavior during flexion, their activity was slightly increased during the deletion, however In-lF continued to be rhythmically active and inhibited PF-PBSt in late flexion. Thus, the analysis of PBSt behavior during this deletion episode and other similar recordings allowed for the following suggestions (see red connections in Fig. 13Aa):

1. Population PF-PBSt receives excitatory inputs from both RG-E and RG-F populations.

2. An excitatory input from PF-E activates In-E during extension, and In-E inhibits PF-PBSt pre and post-deletion during extension. During the deletion, PF-E is silent; therefore, the activity level of In-E decreases or is completely eliminated, thus allowing PF-PBSt, and by extension PBSt motoneuron population Mn-PBSt,

to become active within the intervals of expected extensor activity, as was demonstrated in Fig. 12A and 12Ab.

3. In-F and In-lF receive a weak excitatory input from PF-F. Therefore during the deletion, because PF-F activity increases, the activity of In-F and In-lF also increases, this causes a reduction in the amplitude (due to increased activity of In-F) and duration (due to increased activity of In-lF) of PBSt activity in the flexor interval during the deletion. The connections are weak, because otherwise In-F and In-lF would have completely inhibited PBSt during the flexor interval.

4. In-lF also receives excitatory tonic drive and is inhibited by Inrg-E. This guarantees that it remains rhythmic during non-resetting deletions like this one.

In Fig. 12Ba, we have another example of PBSt behavior during a non-resetting deletion, this time of flexor activity (Sart) with sustained tonic extensor activity (SmAB and GS). Such a deletion results from increased excitability of population PF-E, this causes it to become tonically active, while population PF-F is silent for the duration of the deletion. In this experiment, during the pre and post-deletion periods, PBSt had an extensor-type activity profile (active throughout the extension phase, type 2), hence we expect that population In-F was strongly active during flexion and inhibited PF-PBSt during that phase. On the other hand, during the deletion, PBSt was rhythmically active during the expected extensor intervals only (shaded bars 2-4 in Fig. 12Ba; and the overlay of the pre and during deletion traces of PBSt ENGs in Fig. 12Bb, top trace). This supports the above suggestion that PF-PBSt receives excitatory input from RG-E, but not from PF-E, since the latter is supposed to be tonic during the deletion (Table 3), while PBSt remains rhythmically active throughout the deletion. In addition, to allow for

rhythmic PBSt activity during this deletion, and to allow for any extensor activity of PBSt in general (profile types 2 and 3), there should be a mechanism to either reduce the activity of In-E or fully suppress it. Therefore the following changes were made to the PF level circuitry responsible for shaping PBSt (Fig. 13Ab):

1. An additional interneuron population In-T was introduced to the model. In-T receives tonic excitatory input and provides inhibition of population In-E. In other words, the activity of In-T determines whether PF-PBSt can be active only during flexion (PBSt types 1a and 1b, when In-T is silent and In-E is active during extension), can express activity for the entire duration of the extensor phase (PBSt type 2, when In-T is strongly active and In-E is silent), or have low amplitude extensor activity when PBSt is biphasic (PBSt types 3a and 3b, when In-T is moderately active and In-E is also moderately active during extension).

2. Population In-F should receive excitatory tonic drive, and should be inhibited during extension by populations Inrg-E and Inpf-E. During the deletion in Fig. 12Ba, PBSt was only active during the extensor intervals and remained silent during the flexor intervals. Based on the model's architecture, during this type of deletion PF-F is expected to be silent (see Table 3) and therefore cannot activate population In-F in order for it to inhibit PF-PBSt during the expected flexor intervals. Hence, to have In-F rhythmically active, in the flexor intervals during this deletion, we introduced tonic drive and inhibition by Inrg-E Inpf-E to it.

Finally in Fig. 12C we have an example of a spontaneous deletion of extensor activity (SmAB, MG and LGS) during which flexors (Sart and TA) remained rhythmic. This is an example of a non-resetting deletion, and since flexors remained rhythmic during the

deletion, this suggested that the deletion occurred due to the cessation of activity of population PF-E, while population PF-F continued to be rhythmically active. In this experimental recording, PBSt was of a flexor-type before and after the deletion and exhibited a long flexor burst lasting for more than half of the flexor phase (type 1b). To have PBSt active during the early part of flexion, PF-PBSt should be inhibited by In-lF during late flexion; and during extension, PF-PBSt should be inhibited by In-E, thus population In-T must be silent. During the deletion episode, like flexors, PBSt remained rhythmically active and only during the early portion of the flexor interval (see shaded bars 1 and 2 in Fig. 12C). To obtain such an activity profile for PBSt with the model that was achieved after the last step of construction (Fig. 13Ab), further changes had to be made to it (Fig. 13Ac). To reproduce the activity of PBSt in early flexion during the deletion, In-E had to continue expressing rhythmic extensor activity and inhibit PF-PBSt; but, during the deletion PF-E was silent and thus no longer capable of activating In-E. Therefore, an additional excitatory tonic drive was added to population In-E, and inhibition during flexion by populations Inrg-F and Inpf-F was added (Fig. 13Ac), this allows In-E to remain rhythmically active during the extension interval of the deletion and continue to inhibit PF-PBSt in that particular interval.

The PF level circuitry for PBSt presented in Fig. 13Ac is expected to shape and reproduce all activity of PBSt observed during fictive locomotion and its behavior during all types of spontaneous deletions. These claims were tested and verified, and the results are presented in chapter 8 of this study.

7.1.2 Construction of the Circuit Controlling RF Activity

To construct the neural circuitry that can reproduce the behavior of RF, we considered how RF acted during a selection of experimental ENG recordings that included deletion episodes. First, we considered the recording shown in Fig. 12Aa of a non-resetting deletion of extensor activity (SmAB and GS) while flexors (Sart and TA) remained active. As mentioned earlier, this type of deletion results from increased activity of population PF-F, which in turn suppresses the activity of population PF-E. In this experiment, RF exhibited a biphasic activity profile (type 2) comprised of two burst, a late flexor and a late extensor burst, during the pre and post-deletion period (see shaded bars 1 and 5 in Fig. 12Aa and the bottom black trace in Fig. 12Ab). To obtain such an activity profile, population PF-RF should be inhibited by populations In-eE and In-eF during early extension and early flexion, respectively. During the deletion episode, RF lost the extensor component of its activity and remained active only during the latter part of the flexion interval (see shaded bars 2-4 in Fig. 12Aa and the bottom red trace in Fig. 12Ab). This led to the following suggestions (Fig. 13Ba):

1. During this non-resetting extensor deletion, biphasic RF lost its extensor component. Considering that we expect RG level populations to remain rhythmic and population PF-E to become silent during such a deletion, we suggested that PF-RF receives excitatory input from population PF-E, and not from population RG-E. This allows biphasic RF to lose its extensor component during the deletion, as PF-E and all extensors became silent.

2. Continued rhythmic activity of RF in the latter part of the expected flexor intervals during the deletion indicated that PF-RF receives an excitatory input

from the RG level of the flexor side of the CPG, i.e. RG-F, which remains rhythmic during the deletion.

3. Also considering the activity of RF during the deletion and how it still occurred late in the flexor interval, similar to pre and post-deletion, this suggested that In-eF remains rhythmic during this type of deletion. To allow for that, we added an excitatory tonic drive to population In-eF, and provided it with inhibition from Inrg-E, which is active during extension and since it is an RG level population, it remains rhythmic during non-resetting deletions.

In another non-resetting deletion, shown in Fig. 12Ba, of flexor (Sart) with tonic extensors (SmAB and GS), RF expressed flexor-type activity (type 1) before and after the deletion episode, and during the deletion RF was silent similar to flexors (compare bottom black and red traces in Fig. 12Bb). This type of deletion occurs when population PF-E becomes tonically active thus causing population PF-F to become silent. To enable our model to replicate such behavior of RF further changes needed to be made (Fig. 13Bb):

1. Since we suggested in the previous construction step (Fig. 13Ba) that PF-RF receives excitatory input from PF-E, then we should expect PF-RF, and by extension RF motoneurons, to be tonically active during this type of deletion, but that was not the case, RF was silent during the deletion. Therefore, in the second step of the construction process (Fig. 13Bb) we added an excitatory connection to population In-eE from PF-E. This excitatory connection allows population PF-E, which is tonically active during this type of deletion, to activate In-eE for the

duration of the deletion, which in turn inhibits PF-RF during the deletion and produces the RF activity profile we observed (Fig. 12Ba).

2. RF exhibited a flexor-type activity profile before and after the deletion (Fig. 12Ba). To reproduce this profile type, PF-RF should be inhibited during the full duration of extension by In-eE, and shaped during flexion by In-eF. Since the presence of an extensor component for RF depends entirely on whether In-eE is strongly active (inhibits RF extensor component) or moderately active (allows RF to be active during late extension), there needs to be a way for the activity level of In-eE to be managed. Therefore we decided to add a tonic excitatory drive to population In-eE (Fig. 13Bb); RF activity during extension would be determined by the strength of this tonic drive.

3. With the tonic drive added to In-eE we now had to also provide In-eE with inhibition during flexion, to guarantee that it is active only during extension. That inhibition was provided from population Inpf-F, because during the deletion episode shown in Fig. 12Ba, Inpf-F is expected to be silent (Table 3) and therefore allows In-eE to be tonically active during the deletion and inhibit PF-RF for its duration.

7.2 Completing the Extended Model

In the process of constructing the neural circuitries responsible for the generation of PBSt and RF activity, we incorporated into the PF level of the CPG model special interneuron populations, in particular two, In-lF and In-eF, which we suggested were responsible for shaping PF-PBSt and PF-RF activity profiles, respectively, during the

flexor phase (see Fig. 10 and Fig. 13A). We suggested that population In-eF (early flexion) has a decrementing (adapting) activity pattern, with an activity peak at the beginning of flexion. On the other hand, population In-lF (late flexion) has an incrementing activity pattern with increased activity towards the end of the phase. To form such activity patterns we suggested that neurons with an "early" activity pattern must have intrinsic properties defining neuronal adaptation, and that neurons with a "late" pattern must be inhibited by populations of the "early" type. Therefore, we designed our model with the pair of In-eF and In-lF populations mutually inhibiting each other, and we explicitly implemented this in our model (see Fig. 14A and B). Moreover, mutual inhibitory interactions between populations In-eF and In-lF provide complimentary shaping of the activity profiles of PF-PBSt and PF-RF during flexion.

In Fig. 14B you can also see one further modification made to the RF circuitry, in particular the part of the model responsible for shaping the activity of PF-RF during extension. To control the activity of population In-eE, active at the beginning of extension, we incorporated into the PF network an additional population, In-lE, active in late extension. We also assumed that the interneurons making up population In-eE posses adaptive properties, similar to population In-eF. And we implemented mutual inhibition between In-eE and In-lE, just like we did for In-eF and In-lF. Furthermore, we suggested that population In-lE receives tonic excitatory drive and inhibition from population Inrg-F, which maintains the model's ability of reproducing all deletion types presented in Fig. 12. Finally, we suggested that population In-lE should be inhibited by population In-T, which is involved in shaping the activity of PF-PBSt during extension (see Fig. 13Ab and the corresponding text). This inhibition provides complimentary shaping

for the activity profiles of PF-PBSt and PF-RF during extension. For example, if In-T is active, then PF-PBSt is active during extension, and PF-RF is inhibited for the full duration of extension. The opposite is also true when In-T is inactive; this agrees with our findings in section 5.2 and Fig. 9B.

The complete proposed schematic of the extended model appears in Fig. 15. This schematic includes all hypothetical populations and circuitry incorporated into the PF network (see Figs. 13 and 14) to provide the full repertoire of PBSt and RF activity profiles observed during fictive locomotion and their behavior during spontaneous deletions. Tonic inputs to interneuron populations In-E, In-T, In-eE, In-lE, In-F, In-eF, and In-lF, in the extended model, participate in shaping PBSt and RF activity patterns and control their behavior during deletions. Mutual inhibition between populations In-eF and In-lF provides complimentary shaping for the activities of PBSt and RF during flexion. Population In-T, which simultaneously inhibits populations In-E and In-lE, provides complimentary control of PBSt and RF activity during extension. If strongly activated, In-T inhibits In-E, thus allowing PF-PBSt to exhibit activity during extension, and at the same time In-T inhibits In-lE, thus allowing In-eE to become active and inhibit PF-RF during the whole extensor phase. Conversely, if In-T is silent, then In-E is active and it inhibits PF-PBSt during extension; at the same time, In-lE will also be active and inhibit In-eE during the latter part of extension, this allows In-eE to be active in early extension and inhibit PF-RF, thus PF-RF will be active during late extension. This idea of having the same CPG component networks shape PBSt and RF's activity patterns in order to replicate these motoneuron pools' complimentary activity, is similar to Perret's (Orsal *et al.* 1986) suggestion although not exactly identical. Perret suggested that the same part of

the CPG activated one of PBSt or RF and at the same time activated an inhibitory population that inhibited the other, of PBSt or RF (Orsal *et al.* 1986). Our hypothetical CPG organization shares the idea of a common component network being responsible for shaping PBSt and RF, but the complementation of their activity is provided by the mutual inhibition that exists between the inhibitory interneuron populations shaping PBSt and RF's activity.

The extended model also incorporates additional motoneuron populations, Mn-PBSt and Mn-RF, and Renshaw cell populations, R-PBSt and R-RF, that receive collateral excitatory inputs from the corresponding motoneuron populations (Mn-PBSt and Mn-RF) and provide feedback inhibition to the homonymous motoneuron populations. No data is available to conclude which motoneurons could be considered as direct antagonists of PBSt or RF and whether reciprocal interactions exist between them and other motoneuron populations. Hence, in the current version of the extended model, the third level of reciprocal inhibition, mediated by Ia interneuron populations, is not included into the PBSt-RF circuitry. In Fig. 15, the additional populations and circuitry incorporated into the extended CPG model (and not present in the basic model in Fig 3B) are shown within the shaded rectangle outlined with a dashed border.

Chapter 8: Model performance

8.1 Generating PBSt and RF Activity Profiles

The extended CPG model, capable of replicating activity patterns of PBSt and RF, which was described in the previous sections, was tested and verified. Here we discuss results obtained from testing the extended model's components which make it possible to generate PBSt or RF patterns. Figs. 16 and 17 show component circuits of the extended model which are involved in the process of shaping PBSt and RF activity patterns, respectively, and illustrate how the interplay between tonic drives to interneuron populations added at the PF level works to shape specific patterns of PBST and RF activities. Figs. 16Aa, Ba, Ca and Da and 17Aa and Ba demonstrate how component circuitries participating in the shaping of each particular type of activity operate; dashed rectangles indicate whether particular interneuron populations within them participate in shaping the flexor or extensor component of PBSt or RF. Arrows between two populations are used to represent excitatory connections, and lines terminating with a circle represent inhibitory connections. Arrows pointing towards interneuron populations schematically represent excitatory input drives to these populations; the size of each arrow is a representation of the strength of the tonic drive, the larger the arrow size the stronger the input drive. Excitation level of each individual population is schematically represented by the size of the output connection, the greater the level of excitation, the larger the connection. Interneuron populations represented by an empty circle are inactive for that particular simulation and PBSt or RF type. Figs. 16Ab, Bb, Cb, and Db and 17Ab and Bb show examples of computer simulation outputs, for that particular input drive

distribution. For each simulation, activity of all populations is represented by histograms of the average activity of neurons within each population.

Similar to the basic original model (Rybak *et al.* 2006a), locomotor rhythm in the extended model is generated by the half-center RG level. Alternating rhythmic bursts of RG populations, RG-F and RG-E (top two traces in Figs. 16Ab, Bb, Cb, and Db and 17Ab and Bb) define the durations of extensor and flexor phases (indicated by dashed vertical lines) and hence the locomotor cycle period. At the PF level, populations PF-F and PF-E closely track the activity of corresponding RG populations (third and fourth traces in above figures). The next four traces are of histograms of interneuron populations involved in shaping PF-PBSt or PF-RF activity. Finally, the two bottom traces demonstrate resultant activity of the corresponding bifunctional PF populations (PF-PBSt or PF-RF) and motoneuron pools (Mn-PBSt or Mn-RF). Shaded bars highlight the time intervals during which Mn-PBSt or Mn-RF are active (for one locomotor cycle).

8.1.1 Flexor-Type PBSt

Figs. 16A and B demonstrate how flexor-type PBSt patterns (types 1a and 1b) are shaped by the extended model. To generate flexor-type activity patterns, PF-PBSt should be fully inhibited during extension by In-E, which therefore should have a high activity level; and PF-PBSt should be inhibited during the latter part of flexion by In-lF. Population In-F, in this case, should be silent or weakly active to allow PF-PBSt activity during flexion. In the model, excitability of In-E is controlled by the excitatory tonic drive it receives (D_E) and inhibition from population In-T. Therefore, if In-T is silent and D_E is strong enough (Fig. 16Aa and Ba), then In-E becomes highly active and fully

suppresses the activity of PF-PBSt (and hence Mn-PBSt) during extension (see traces in Fig. 16Ab and Bb showing the activity of In-E, PF-PBSt, and Mn-PBSt). Note that In-E itself is inhibited by Inrg-F (see Fig. 15) during flexion, thus it does not suppress PF-PBSt (and Mn-PBSt) activity during that phase. Inhibition of PF-PBSt activity during late flexion is provided by population In-lF, and the duration of the flexor component is determined by the activity level of In-lF. Relative excitability of In-lF and In-eF, mutually inhibiting each other during flexion, is determined by excitatory drives, D_{lF} and D_{eF}, to these populations, respectively (Fig. 16Aa and Ba). Therefore the stronger D_{lF} and/or the weaker D_{eF} is, the shorter the duration of PF-PBSt flexor burst (Fig. 16Ab), and *vice versa* (Fig. 16Bb).

8.1.2 Extensor-Type PBSt

Extensor-type PBSt pattern (type 2) is obtained using the method described in Fig. 16C. To have PF-PBSt active during extension, it should first receive minimal to no inhibition during extension, second, it should be completely inhibited during flexion. If input drive D_E to population In-E is relatively weak and input drive D_T to population In-T is strong enough to produce high activity within it, then In-T would fully inhibit In-E (Fig. 16Ca). Consequently, PF-PBSt would be disinhibited during extension allowing it (and Mn-PBSt) to be active for the duration of the phase (bottom two traces in Fig. 16Cb). To completely suppress PF-PBSt activity during flexion, population In-F has to be strongly activated by input drive D_F. Note that during extension, population In-F is inhibited by Inrg-E (see Fig.15), therefore it can only be active during flexion. Populations In-eF and In-lF do not participate in shaping PBSt activity in this case, hence

the nature of their activity is inconsequential. Fig. 16Cb shows the activities of populations In-E, In-F, In-eF and In-lF and the resulting extensor profile of PF-PBSt and Mn-PBSt activity.

8.1.3 Biphasic PBSt

Fig. 16D illustrates the generation of biphasic PBSt pattern (type 3) using the extended model. For this activity profile, PBSt usually demonstrates persistent activity (reduced, in many cases) during extension, followed by a short burst at the beginning of flexion. Reduced activity during extension is provided by moderate inhibition of PF-PBSt by population In-E. The strength of this inhibition is determined by the relative strengths of excitatory drive inputs D_E and D_T to populations In-E and In-T, respectively (Fig. 16Da). Population In-F, in this case, should be silent or weakly active to allow PF-PBSt to be active during flexion. Generation of the short flexor burst at the beginning of the phase is provided by the same circuitry involved in generating flexor-type PBSt activity (see Fig. 16Aa). Fig. 16Db illustrates activities of populations In-E, In-F, In-eF, and In-lF shaping biphasic PF-PBSt activity pattern and the resulting activity of Mn-PBSt.

8.1.4 Flexor-Type RF

For flexor-type RF activity pattern (type 1), Fig. 17A shows how the model was used to generate this profile. RF should be inhibited during the whole extensor phase and at the beginning of flexion. In our model, PF-RF activity during extension is determined by population In-eE. The strength of In-eE activity during extension depends on the relative strengths of input drives D_{eE} and D_{lE} to population In-eE and In-lE, respectively

(see Fig. 17Aa and Ba). If drive D_{eE} is strong and drive D_{lE} is weak or absent, then In-eE will be active and maintain its activity throughout the duration of extension, and therefore completely inhibit PF-RF activity during that phase (Fig. 17A). Note that during flexion, In-eE is inhibited by population Inpf-F (see Fig. 15), thus allowing it to be active only during extension. Also, population In-T contributes to shaping RF activity; if In-T is strongly activated by excitatory input drive D_T, then it completely inhibits In-lE which makes it possible for In-eE to maintain its activity for the whole extensor phase in order to inhibit PF-RF (Fig. 17A). On the other hand, during flexion, population PF-RF is inhibited by population In-eF (Fig. 17Aa) at the beginning of the phase, therefore producing an RF flexor burst late in the phase (Fig. 17Ab). Moreover, the stronger In-eF activity is, with respect to In-lF, the later RF's flexor burst starts and the shorter is its duration. Hence, onset of RF activity during flexion is determined by the interplay between input drives D_{eF} and D_{lF} to population In-eF and In-lF, respectively.

Note that population In-T plays a dual role in the model, simultaneously prohibiting RF and allowing PBSt activity during extension, or the opposite, such that RF and PBSt are never simultaneously active during extension. Also note that populations In-eF and In-lF, in addition to shaping RF activity during flexion, participate in shaping PBSt activity during the same phase; therefore mutual inhibition between these populations determines complimentary interactions between PBSt and RF during flexion, such that PBSt and RF activity does not overlap during flexion, where PBSt is active early in flexion and RF is active late in flexion.

8.1.5 Biphasic RF

Fig. 17B illustrates shaping of biphasic RF activity pattern (type 2) in the model. In this case of RF activity, PF-RF is inhibited at the beginning of extension and at the beginning of flexion, such that it is active late in both phases. Generating RF activity late in flexion is achieved with a similar process to that described for flexor-type RF (see description above). To generate the additional burst of activity of PF-RF in extension, input drive D_T to population In-T should be weak (or absent), so that population In-lE is released from the inhibition of In-T. In addition, drive D_{lE} to population In-lE should be strong enough for it to overcome the inhibition of population In-eE, and in turn inhibit In-eE in late extension. Similar to the pair In-eF and In-lF, the interplay of mutual inhibition between In-eE and In-lE, defined by the excitatory tonic drives to each of these populations, determines the duration of the extensor component of RF. If drive D_{lE} to In-lE is strong relative to drive D_{eE} to In-eE, then at some point during extension, population In-lE escapes the inhibition of In-eE and becomes active suppressing the activity of In-eE. This allows PF-RF (and hence Mn-RF) to exhibit a burst of activity at the end of the extensor phase. Fig. 17Bb shows activities of populations involved in the formation of biphasic PF-RF activity pattern and the resulting activities of PF-RF and Mn-RF populations.

8.2 Modeling PBSt and RF Activity during Fictive Locomotion

Fig. 18A-D shows results of simulations of different types of PBSt and RF activity during fictive locomotion in comparison with ENG records obtained in a fictive locomotion experimental setup. Upper panels in Fig. 18 (Aa, Ba, Ca, and Da) are of

flexor, extensor, PBSt and RF motoneuron pools' activities generated using our extended CPG model, and lower panels are of corresponding experimental recordings (Ab, Bb, Cb, and Db) exhibiting similar types of activity patterns of PBSt and RF. Traces in the simulation panels show averaged spiking frequency of neurons within analogous motoneuron populations. The first two traces are of activities of flexor (Mn-F) and extensor (Mn-E) motoneuron populations, respectively; the third and fourth traces are of activities of bifunctional motoneuron populations, Mn-PBSt and Mn-RF, respectively.

In Fig. 18Aa we have the simulation result of the case in which Mn-PBSt exhibits only a short burst at the beginning of flexion (type 1a) and Mn-RF expresses a biphasic pattern with one burst during late flexion and another short burst at the end of extension (type 2). The corresponding experimental recordings obtained during fictive locomotion, in which PBSt and RF exhibited similar patterns, are shown in Fig. 18Ab.

In Fig. 18Ba, the simulation shown is of Mn-PBSt exhibiting a longer flexor burst at the beginning of flexion (type 1b), and Mn-RF showing flexor type activity (type 1) with a single burst of activity at the end of flexion. The corresponding experimental recording is shown in Fig. 18Bb, however this recording did not include RF activity (we had no experiments in our database where PBSt and RF were simultaneously recorded while exhibiting long flexor-type and flexor-type activity, respectively).

Fig. 18Ca shows the result of a simulation in which extensor-type Mn-PBSt (type 2) is active for the full duration of extension, while flexor-type Mn-RF exhibits a flexor burst in late flexion (type 1). The corresponding experimental records show similar patterns for both PBSt and RF motoneurons (Fig. 18Cb).

In Fig. 18Da, the simulation is of biphasic Mn-PBSt (type 3) with low amplitude activity throughout extension and a short burst of activity at the beginning of flexion. Mn-RF, in this simulation, exhibits flexor-type activity (type 1). The experimental recording (Fig. 18Db) shows the same activity patterns for both PBSt and RF.

In summary, the extended model that was constructed in this study was able to reproduce all types of PBSt and RF activities and their combinations, observed during fictive locomotion in decerebrate immobilized cats (Fig. 9). Based on our simulations, we propose that the variety of activity patterns of PBSt and RF motoneurons, exhibited during fictive locomotion, is the result of variable activation levels of special interneuron populations involved in shaping PBST and RF profiles at the pattern formation level.

8.3 Modeling Deletions

8.3.1 Behavior of Flexor-Type PBSt during Resetting Extensor Deletions

In the process of developing the extended model, the challenge was not only to reproduce the full repertoire of PBSt and RF activity patterns but also to reproduce and explain their complex behavior during different types of deletions (Table 4). Specifically, the interesting problem was the behavior of flexor-type PBSt (types 1a and 1b) during resetting extensor deletions (Fig. 19C), where it can demonstrate either tonic, silent, or rhythmic activity during the deletion. To generate flexor-type activity patterns (type 1a or 1b), PF-PBSt should be inhibited during extension by In-E and in the latter part of flexion by population In-lF (see Fig. 16A and B). Activity onset of In-lF, and hence termination of PF-PBSt activity, in late flexion is determined by the relative strength of excitatory

input drives to populations In-eF and In-lF, which mutually inhibit each other (see Figs. 16A and B and 19A).

In all three cases presented in Fig. 19C, extensor deletions are of the resetting type, due to obvious phase shifts in post-deletion locomotor rhythms compared to pre-deletion rhythms. Shaded bars in Fig. 19C highlight behaviors of different motoneurons recorded during the deletions. Based on the organization of the two-level locomotor CPG model, resetting extensor deletions can be generated through a temporary spontaneous decrease of excitability of the extensor half-center of the RG level, i.e. population RG-E. In the model, this deletion type was reproduced by applying a temporary inhibitory tonic drive to population RG-E (designated by the horizontal bars at the top of Fig. 19Ba-c). Component circuitries shown in Fig. 19Aa-c demonstrate how the behavior of PF-PBSt, during a resetting extensor deletion, depends on the interplay between input drives D_{eF} and D_{lF} to populations In-eF and In-lF, respectively (left filled arrows), and tonic excitatory inputs that In-lF and PF-PBSt receive from PF-F and RG-F, respectively (right unfilled arrows) (see Figs. 14A and 5). Excitatory inputs to In-lF and PF-PBSt are tonic since populations PF-F and RG-F are tonically active during the deletion. Behavior of interneuron populations shown in Fig. 19Aa-c, during the deletions, is indicated by the filling of the circles representing these populations; empty for silent, black for strongly active, gray for weakly active, and half white half black for rhythmic. Fig. 19B shows simulation results demonstrating the different behaviors of PBSt during resetting extensor deletions; durations of the deletions are designated by shaded areas.

In the first case that we considered, population In-lF receives a weak excitatory input drive D_{lF} compared to drive D_{eF} to population In-eF (Fig. 19Aa), in order to

produce a long flexor-type PBSt (type 1b) (Fig. 16B). However, during the deletion, In-eF and In-lF are no longer rhythmically inhibited by Inrg-E, and In-lF now receives tonic drive from PF-F, similarly PF-PBSt receives tonic drive from RG-F. This leads to a loss of rhythmic activity in In-eF, In-lF and PF-PBSt; furthermore In-eF, which receives a stronger tonic drive (D_{eF}) relative to In-lF (D_{lF}), suppresses the activity of In-lF for the duration of the deletion. Therefore, PF-PBSt is no longer inhibited by In-lF and thus exhibits sustained activity, along with Mn-PBSt, during this deletion (Fig. 19Ba), thereby emulating and explaining the tonic activity of PBSt in the experimental record shown in Fig. 19Ca.

In the alternate situation, population In-lF receives a stronger input drive D_{lF} compared to drive D_{eF} to population In-eF (Fig. 19Ab), to generate a short flexor-type PBSt profile (type 1a) (Fig. 16A). During the deletion, after rhythmic inhibition is lost, In-lF becomes tonically active and inhibits In-eF, due to the stronger tonic drive (D_{lF}) to In-lF. Thus population In-lF completely inhibits PF-PBSt during the deletion, which results in a silent Mn-PBSt (Fig. 19Bb), and thus reproduces the corresponding behavior seen in the experimental records in Fig 19Cb.

Finally, in rare occasions, the interplay between tonic drives D_{eF} and D_{lF} creates a balance in mutual inhibition between populations In-eF and In-lF. This results in In-eF and In-lF acting like an independent oscillator during the deletion (Fig. 19Ac) with a period determined by the excitatory inputs to these populations and the weights of inhibitory connections between them (note, this oscillation period is not related to the locomotor period pre and post-deletion). Finally, this causes PF-PBSt, and by extension Mn-PBSt, to exhibit rhythmic activity during the deletion (Fig. 19Bc), therefore offering

an explanation for the rhythmic activity of PBSt displayed during the experimental recordings shown in Fig. 19Cc.

8.3.2 Behavior of Other Types of PBSt and RF during Resetting Deletions

The model was also able to reproduce all types of PBSt and RF behaviors during all types of deletions presented in Table 4. A selection of interesting examples is shown in Fig. 20. All deletions presented in Fig. 20 were resetting type deletions, due to a phase shift of post-deletion rhythms relative to pre-deletion rhythms. Deletions were simulated in the extended CPG model by applying an additional inhibitory drive to the rhythm generator half-center which is expected to be silent during the deletion (RG-F in Fig. 20A and C; RG-E in Fig. 20B and D), as indicated by horizontal bars above the activity traces. In Fig. 20A and B, Mn-PBSt had an extensor-type activity profile (type 2) before and after the deletion and Mn-RF (in Fig. 20A) demonstrated flexor-type activity (type 1). During the resetting flexor deletion simulated in Fig. 20Aa, Mn-PBSt became tonically active, whereas Mn-RF was silent. The behavior of both motoneuron populations corresponded to experimental data (Table 4). An example of an experimental recording for this situation is presented in Fig 20Ab, where PBSt was tonically active similar to extensor SmAB, and RF along with flexors Sart and TA were silent during the deletion. In Fig. 20Ba, of an extensor resetting deletion, extensor-type Mn-PBSt was silent during the deletion, which corresponded to the experimental data (Table 4). A corresponding example of such PBSt behavior during fictive locomotion is shown in Fig. 20Bb, in which flexors Sart and TA expressed sustained activity during the deletion, whereas extensors SmAB and GS, and PBSt were silent.

In Fig. 20C and D, Mn-PBSt had a biphasic activity profile (type 3) before and after the deletion. During a resetting flexor deletion (Fig. 20Ca), Mn-PBSt was tonically active, and thus corresponded to the available experimental data (Table 4). An example of such a deletion is shown in Fig. 20Cb, where biphasic PBSt was tonically active together with extensors SmAB and GS during the deletion, whereas flexors Sart and TA were silent. Interesting to note that in Fig. 20Cb the amplitude of PBSt activity during extension is reduced relative to flexion, and PBSt maintains such a low level of activity during the deletion. This supports our suggestion that the excitability of In-E (which determines the level of PBSt activity in the extensor phase; Fig. 16D) is determined by tonic drive D_T to population In-T, and therefore the activity level of In-E is not affected by this type of deletion (note that during this type of deletion, PF-PBSt receives inhibition only from In-E). These observations were explicitly reproduced by our model (Fig. 20Ca). In Fig. 20Da, during a resetting extensor deletion PBSt, which exhibited biphasic activity pre and post-deletion, became silent during the deletion. This behavior matched the experimental data (Table 4) and the corresponding example in Fig. 20Db, where flexor Sart had sustained activity during the deletion, whereas extensors SmAB and GS as well as biphasic PBSt were silent.

8.3.3 Behavior of PBSt and RF during Non-Resetting Deletions

During non-resetting deletions of either flexor or extensor activity, PF-PBSt continues to receive rhythmic inputs from both sides of the CPG, particularly from the RG level. Interneuron populations In-E, In-F, and In-lF responsible for shaping the activity of PF-PBSt also continue to receive rhythmic inputs during non-resetting

deletions. Moreover, during non-resetting extensor deletions, populations In-F and In-lF, which inhibit PF-PBSt during flexion, receive sustained excitatory input from population PF-F; during non-resetting flexor deletions, population In-E, which inhibits PF-PBSt during extension, receives sustained excitatory input from PF-E. In both cases, PBSt's behavior during the deletion is complex and may be dissimilar from the behavior of motoneuron pools that where co-active with PBSt pre-deletion. This is demonstrated for flexor-type PBSt (type 1b) (Fig. 21Aa and Ba), and extensor-type PBSt (type 2) (Fig. 21Ab and Bb) during non-resetting extensor and flexor deletions, respectively. Fig. 21B shows simulation results of PBSt behavior, shaded bars highlight the deletion episodes. Component circuitries (Fig. 21A) demonstrate how PBSt's behavior during each particular deletion depends on the interplay of continued rhythmic inputs to PF-PBSt and the interneuron populations from the RG level, and sustained inputs to the interneuron populations from the active side of the PF level.

Flexor-type PBSt activity (type 1b) is produced by inhibiting PF-PBSt during extension by population In-E and in late flexion by In-lF. In the model, a non-resetting extensor deletion is produced by temporarily applying an additional excitatory tonic drive to population PF-F (horizontal bar at the top of Fig. 21Ba). During the deletion, population In-E receives increased inhibition from Inpf-F and loses its excitatory input from PF-E, this decreases its ability to inhibit PF-PBSt, thus allowing PF-PBSt to be active in extensor intervals during the deletion. On the other hand, increased excitatory inputs to populations In-lF and In-F from PF-F, during the deletion, allows them to partially suppress PF-PBSt's activity in flexor intervals. A simulation (Fig. 21Ba) of this situation demonstrates how flexor-type PBSt can be expected to behave during this type

of deletion. This prediction was verified by an experimental recording (Fig. 21Ca) where PBSt exhibited a similar behavior and was partially rhythmic during the deletion, with higher activity levels occurring during anticipated extensor intervals.

Extensor-type PBSt activity (type 2) is produced by inhibiting PF-PBSt during flexion by population In-F and having In-E silent or weakly active. In the model, a non-resetting flexor deletion is produced by temporarily applying an additional excitatory tonic drive to population PF-E (horizontal bar at the top of Fig. 21Bb). During the deletion, population In-E receives increased excitatory input from PF-E which allows it to partially suppress PF-PBSt's activity in extensor intervals. Population In-F loses its excitatory input from PF-F, however, due to a strong input drive continues to be active and inhibits PF-PBSt in flexor intervals during the deletion. A simulation (Fig. 21Bb) of the corresponding situation reveals that extensor-type PBSt can be expected to remain rhythmically active in extensor intervals during this type of deletion, but with reduced activity levels. This prediction was again verified by an experimental recording of an identical situation (Fig. 21Cb) where PBSt had a similar activity profile to what the model has predicted.

In Fig. 22 we show an example of reproducing RF behavior during a non-resetting extensor deletion. In the model simulation (Fig. 22A), Mn-RF exhibited a biphasic activity profile (type 2) consisting of a flexor and an extensor burst, before and after the deletion. A non-resetting extensor deletion with sustained rhythmic activity of flexors was reproduced in the model by temporarily applying an additional inhibitory drive to population PF-E. During the deletion, biphasic Mn-RF lost its extensor burst and exhibited rhythmic flexion related activity. Mn-RF activity coincided with Mn-F

rhythmic activity during the deletion, only it started late relative to Mn-F but terminated at the same time. In the experimental recording shown in Fig. 22B, RF exhibited a biphasic activity pattern before and after the deletion, and during the non-resetting deletion of extensors SmAB and GS, along with rhythmic bursting of flexors Sart and TA, RF lost its extensor bursts and maintained rhythmic flexor activity. Towards the end of the deletion episode, a low amplitude extensor burst appeared which was observed in both extensors SmAB and GS as well as RF records (Fig 22B). To reproduce such a behavior in our model (Fig. 22A), the temporarily applied additional inhibitory drive to population PF-E was reduced towards the end of the deletion by 70%; in the figure, this is represented by a shading level change at the instance when this change was applied. This allowed the model to reproduce a similar behavior to that observed in the experimental recording including the low amplitude extensor and RF bursts at the end of deletion.

Chapter 9: Conc1uding Remarks

9.1 Candidate CPG Interneurons

Up until this point in time, no group of interneurons in the mammalian spinal cord has been discovered to be responsible or necessary for the generation of rhythmic locomotor activity. However, recently several research groups, using new genetic and electrophysiological techniques, have identified CPG interneuron candidates that might be involved in the locomotor rhythm generation and control. Several populations were found to be rhythmically active during locomotor activity and were genetically and electrophysiologically characterized such as V0-V3, EphA4 and HB9 interneurons (Guertin 2009). V0 interneurons include several types of neurons, of most interest are commissural interneurons (CIN) which can form excitatory and inhibitory reciprocal connections between the two sides of the spinal cord (Butt *et al.* 2002; Kiehn and Butt 2003; Lanuza *et al.* 2004). V1 interneurons may include inhibitory Ia and Renshaw cells (Gosgnach *et al.* 2006), and V2 interneurons were found to be associated with frequency and activity amplitude control in addition to bilateral coordination (Lundfald *et al.* 2007). V3 and EphA4 interneurons were linked to balanced, robust and coordinated locomotor rhythms (Butt *et al.* 2005; Zhang *et al.* 2008). Finally, HB9 excitatory interneurons are believed to form part of the rhythm generation or pattern formation networks of the locomotor CPG (Brownstone and Wilson 2008; Hinckley *et al.* 2005).

9.1.1 Commissural Interneurons

The axons of CINs cross the spinal cord midline, therefore they are easily identified anatomically and physiologically. Studies have shown that CINs function in

coordinating motoneuron activity on the two sides of the spinal cord, enabling alternating activity of the two hind-limbs during stepping (Kiehn and Butt 2003). Based on their axonal projections, CINs have been divided into short and long range groups. Short range CINs are segmental, projecting their axons within one spinal cord segment between the left and right sides of the spinal cord. Long range CINs are intrasegmental, they also project contralaterally but over one and up to six segments away from segment of origin. They are further subdivided into three groups: (1) ascending (aCINs); (2) descending (dCINs); and (3) having both ascending and descending axons (adCINs).

In rodents, where L2 spinal cord segment motoneuron activity is mostly flexor related and L4/L5 segment motoneuron activity is mostly extensor related, studies have shown that rostral dCINs, located in L2 and rhythmically active with flexor L2 motoneurons, bind or synchronize ipsilateral flexor activity with contralateral L4/L5 extensor activity (Butt *et al.* 2002; Butt and Kiehn 2003). Furthermore, segment L2 contains fewer motoneurons active during extension and L4/L5 contain fewer motoneurons active during flexion. Hence, L2 dCINs rhythmically active with extensor L2 motoneurons, are also suggested to bind ipsilateral L2 extensor activity with contralateral L4/L5 flexor activity. Considering that CINs can be either excitatory or inhibitory, in this suggested organization, dCINs would provide both excitatory and inhibitory drives serving an essential role in the creation of diagonal synergies across the spinal cord. Such that, when L2 exhibits flexor motoneuron activity, co-active ipsilateral dCINs projecting from L2 to contralateral L4/L5 not only excite extensor motoneurons in these segments, they also inhibit flexor motoneuron activity. Segmental CINs were also

found to play a role in left-right coordination, through both excitatory and inhibitory CIN types, guaranteeing contralateral flexor-extensor synchronization at each segment level.

These studies reveal the effects of CINs upon motoneurons in the contralateral side of the spinal cord, but expose nothing about any possible effects that they may have on contralateral CPG interneurons (Kiehn and Butt 2003). Moreover, as discussed in the introduction to this study, it is believed that each hind-limb is separately controlled by an independent CPG located in the ipsilateral side of the spinal cord. Therefore CINs, if they were found to affect contralateral CPG interneurons, will most likely be associated with the coordination of the two hind-limb CPGs, whether synchronizing them during galloping or ensuring that they are out of phase during walking or trotting. All available data regarding CINs thus far indicates that they do not form an integral part of the locomotor CPG and are neither involved in the rhythm generation process nor in pattern formation of motoneuron activity. Hence, studies that have looked into the function and activity of CINs neither offer supporting evidence for the CPG organization proposed in this study, nor do they reveal any contradictory findings that would challenge the work presented here.

9.1.2 Ipsilateral Projecting Excitatory Interneurons

Intracellular recordings in spinal cord regions where the locomotor CPG is believed to exist uncovered a group of excitatory interneurons identified by EphA4 genetic marker (Butt *et al.* 2005; Kiehn and Butt 2003). EphA4 positive interneurons have been shown to directly or indirectly excite ipsilateral motoneurons, moreover EphA4 interneurons were found to be rhythmically active with ipsilateral motoneurons

during locomotor activity (Butt *et al.* 2005). However, no experiments were conducted to determine whether EphA4 interneurons are in fact involved in the rhythm generation process or are merely expressing rhythmic activity due to rhythmic excitatory and or inhibitory inputs that they receive.

Another group of excitatory interneurons, expressing HB9 transcription factors, and exhibiting rhythmic activity during neurotransmitter induced locomotor activity, have been identified in the spinal cord of rodents (Brownstone and Wilson 2008; Hinckley *et al.* 2005; Kiehn *et al.* 2008). Morphological experiments have raised the possibility that HB9 interneurons are premotor and form part of the CPG network (Hinckley *et al.* 2005), but others (Brownstone and Wilson 2008) were unable to substantiate these claims and found no HB9 synaptic terminals on nearby motoneurons, instead they have suggested that HB9 neurons were not last order neurons. Nonetheless, HB9 rhythmic activity has been found to be in-phase with activity recorded at the ventral root of the corresponding spinal cord region.

No strong experimental evidence is available to determine with certainty the identity of neurons forming synaptic connections with HB9 neurons, which makes it difficult to establish the role of these neurons. Contradictory evidence has been presented concerning HB9 neurons forming synaptic connections with each other (Hinckley *et al.* 2005); or if HB9 neurons are not electronically coupled to each other, but rather to other non-HB9 neurons (Wilson *et al.* 2007). Furthermore, there is no solid evidence to suggest that HB9 interneurons are responsible for the generation of rhythmic activity. In fact it is possible that HB9 neurons receive rhythmic inputs from the locomotor CPG, thus co-activating them along with the corresponding segmental motoneurons (Hinckley *et al.*

2005). Yet others were able to observe rhythmic activity in synaptically isolated HB9 neurons in a spinal cord slice, suggesting that HB9 neurons are intrinsically rhythmic and capable of generating the locomotor rhythm on their own (Jiang *et al.* 1999). Based on the latter, Brownstone and Wilson (2008) have proposed that HB9 interneurons are part of an asymmetric flexor burst rhythm generator network, which projects onto a pattern formation network controlling the activity of flexor and extensor motoneurons.

It is difficult to argue for an asymmetric organization of the rhythm generator level considering the inconclusive evidence in favor of such an organization. Even though some available evidence points in the direction of an asymmetric organization, other evidence suggests otherwise. In particular an asymmetric organization of the RG fails to explain how blocking inhibition in the spinal cord leads to synchronized ipsilateral extensor-flexor activity (Beato and Nistri 1999; Bracci *et al.* 1996; Cowley and Schmidt 1995), an observation which is easily explained and reproduced by the half-center RG organization (Rybak *et al.* 2006a).

None of the rhythmically active interneurons uncovered thus far have demonstrated activity relating to bifunctional motoneurons or any of the proposed interneuron populations involved in shaping bifunctional motoneuron activity. While this offers no support for the CPG architecture proposed in this study, it also presents no evidence against it.

9.2 Summary and Future Directions

We have performed a comprehensive analysis of activity profiles of bifunctional motoneurons PBSt and RF during fictive locomotion experiments and their behavior

during spontaneous deletions. Such comprehensive analysis has not been performed prior to this study. Our results confirmed the suggestion previously proposed by Perret's group (Orsal *et al.* 1986; Perret 1983; Perret *et al.* 1988) that the different activity patterns of PBSt and RF observed during fictive locomotion are solely produced by the locomotor CPG and reflect the organization of neural circuitry within the CPG. This analysis allowed us to hypothesize the existence of inhibitory interneuron populations participating in shaping PBSt and RF activity patterns and propose an extended CPG model that is able to realistically reproduce the behavior of PBSt and RF during fictive locomotion and their behaviors during spontaneous deletions.

We demonstrated that a two-level locomotor CPG with a bipartite half-center rhythm generator and a special organization of neural circuits at the pattern formation level (between the rhythm generator and motoneuron pools) can account for and reproduce the complex patterns of bifunctional motoneurons, particularly PBSt and RF. The proposed CPG model was able to reproduce the full repertoire of PBSt and RF activity patterns observed during fictive locomotion. And, even though only a limited number of spontaneous deletion experimental recordings were used in the construction process of the CPG network, the model was in fact able to reproduce all activities of PBSt and RF during all deletion types presented in Table 4, which validates the CPG organization proposed in the current model.

The key elements of the proposed network are the principal neuron populations PF-PBSt and PF-RF that directly control the activation of PBSt and RF motoneuron pools, and additional interneuron populations In-F, In-eF, In-lF, In-E, In-eE, In-lE and In-T that shape the activity profiles of PF-PBSt and PF-RF during flexion and extension.

In the model, the excitability of these interneurons, or the drives they receive from the MLR, explicitly defines the activity profiles expressed by PBSt and RF motoneurons during a particular fictive locomotion experiment (from the repertoire of possible profiles). We suggest that these interneuron populations, during normal locomotion, receive excitatory inputs from sensory afferents and/or descending signals, which determine and shape the appropriate activity profiles of PBSt and RF that are required for a particular gait, speed of locomotion, or set of environmental conditions. Hence, we propose that the mechanism, by which the activity of PBSt and/or RF is varied from one type to another, is through varying the amount of excitatory drive that these inhibitory interneuron populations receive, thus providing a way for proprioceptive control of the activity of bifunctional motoneurons during real locomotion.

The proposed model cannot be fully verified due to the scarcity of data on the activity of various spinal interneurons including those that are expected to play a role in mediating inputs of sensory afferents to PBSt and RF motoneurons (e.g., Ia type interneurons). Interneuron populations forming the PF network and the organization of connections within this network cannot be confirmed at this point. Data from intracellular recordings of PBSt and RF motoneurons has not been widely used in this study due to the limited amount of this data and lack of experiments that would allow for well founded conclusions. Moreover, we are aware that the proposed network architecture may not represent the only possible solution, other possible architectures may be found that can produce similar outputs, therefore the proposed model remains hypothetical. Further experimental and modeling studies are necessary to refine the model and confirm or modify assumptions used in its construction. The behavior of PBSt and RF motoneurons

in addition to particular interneurons can be predicted using this CPG model under different conditions, thus offering testable predictions which can then be experimentally verified in fictive locomotion preparations to validate the model's accuracy. Furthermore, the model will have to be reevaluated, and if necessary modified, as more experimental data on CPG interneurons becomes available with time.

Table 1. Steady state activation and inactivation variables and time constants for voltage-dependent ionic channels

Ionic channels	$m_\infty(V)$, V is in mV $h_\infty(V)$, V is in mV	$\tau_m(V)$, ms $\tau_h(V)$, ms
Na	$m_{\infty Na} = (1 + \exp(-(V+35)/7.8))^{-1}$ $h_{\infty Na} = (1 + \exp((V+55)/7))^{-1}$	$\tau_{mNa} = 0$ $\tau_{hNa} = 30/(\exp((V+50)/15) + \exp(-(V+50)/16))$
Na$_P$	$m_{\infty NaP} = (1 + \exp(-(V+47.1)/3.1))^{-1}$ $h_{\infty NaP} = (1 + \exp((V+59)/8))^{-1}$	$\tau_{mNaP} = 0$ $\tau_{hNaP} = \tau_{hNaP\max} / \cosh((V+59)/16)$, $\tau_{hNaP\max} = 800$
K	$m_{\infty K} = (1 + \exp(-(V+28)/15))^{-1}$ $h_K = 1$	$\tau_{mK} = 7/(\exp((V+40)/40) + \exp(-(V+40)/50))$
K$_A$	$m_{\infty A1} = (1 + \exp(-(V+60)/8.5))^{-1}$ $h_{\infty A1} = (1 + \exp((V+78)/6))^{-1}$ $m_{\infty A2} = (1 + \exp(-(V+36)/20))^{-1}$ $h_{\infty A2} = (1 + \exp((V+78)/6))^{-1}$	$\tau_{mA1} = 1/(\exp((V+35.82)/19.69) + \exp(-(V+79.69)/12.7) + 0.37)$ $\tau_{hA1} = 1/(1 + \exp((V+46.05)/5) + \exp(-(V+238.4)/37.45))$ if $V < -63$, else $\tau_{hA1} = 19.0$ $\tau_{mA2} = 1/(\exp((V+35.82)/19.69) + \exp(-(V+79.69)/12.7) + 0.37)$ $\tau_{hA2} = 1/(1 + \exp((V+46.05)/5) + \exp(-(V+238.4)/37.45))$ if $V < -73$, else $\tau_{hA2} = 60.0$
Ca$_N$	$m_{\infty CaN} = (1 + \exp(-(V+30)/5))^{-1}$ $h_{\infty CaN} = (1 + \exp((V+45)/5))^{-1}$	$\tau_{mCaN} = 4$ $\tau_{hCaN} = 40$
Ca$_L$	$m_{\infty CaL} = (1 + \exp(-(V+40)/7))^{-1}$ $h_{CaL} = 1$	$\tau_{mCaL} = 40$

All expressions and parameters, except those for the Na$_P$ and K$_A$ channels, are taken from Booth *et al.* (1997). The expressions for the Na$_P$ channel are from Rybak *et al.* (2003). The expressions for K$_A$ channels are from Huguenard & McCormick (1991, 1992).

Table 2. Weights of synaptic connections in the network

Target population	Source population (weight of synaptic input to one neuron)
RG-E	RG-E (0.025); RG-F (0.025); Inrg-E (-0.225)
RG-F	RG-E (0.025); RG-F (0.025); Inrg-F (-0.225)
Inrg-E	RG-F (0.6)
Inrg-F	RG-E (0.6)
PF-E	RG-E (0.1); Inrg-E (-0.07); Inpf-E (-0.8)
PF-F	RG-F (0.1); Inrg-F (-0.07); Inpf-F (-0.8)
Inpf-E	PF-F (0.5)
Inpf-F	PF-E (0.5)
PF-PBSt	RG-E (0.1); RG-F (0.1); In-E (-0.4); In-F (-0.4); In-lF (-0.4)
PF-RF	PF-E (0.4); RG-F (0.15); In-eE (-1.0); In-eF (-0.8)
In-E	PF-E (0.1); Inrg-F (-0.1); Inpf-F (-0.15); In-T (-0.25)
In-F	PF-F (0.05); Inrg-E (-0.07); Inpf-E (-0.2)
In-eF	Inrg-E (-0.4); In-lF (-0.25)
In-lF	PF-F (0.1); Inrg-E (-0.2); In-eF (-0.25)
In-eE	PF-E (0.1); Inpf-F (-0.4); In-lE (-0.25); In-T (-0.25)
In-lE	Inrg-F (-0.25); In-eE (-0.25)
Ia-E	PF-E (0.55); Ia-F (-0.4); R-E (-0.4)
Ia-F	PF-F (0.55); Ia-E (-0.4); R-F (-0.4)
R-E	Mn-E (0.6); R-F (-0.3)
R-F	Mn-F (0.6); R-E (-0.3)
R-PBSt	Mn-PBSt (0.3)
R-RF	Mn-RF (0.3)
Mn-E	PF-E (1); Ia-F (-0.8); R-E (-0.05)
Mn-F	PF-F (1); Ia-E (-0.8); R-F (-0.05)
Mn-PBSt	PF-PBSt (1); R-PBSt (-0.05)
Mn-RF	PF-RF (1); R-RF (-0.05)

Values in brackets represent relative weights of synaptic inputs from the corresponding source populations. Negative value weights indicate inhibitory connections. Values of MLR drives to PF-E, PF-F, PF-PBSt, and PF-RF are $D_{PF-E} = D_{PF-F} = D_{PF-PBSt} = 0.1$, $D_{PF-RF} = 0.05$; for MLR drives to RG-E (D_{RG-E}), RG-F (D_{RG-F}), In-eE (D_{eE}), In-lE (D_{lE}), In-T (D_T), In-E (D_E), In-eF (D_{eF}), In-lF (D_{lF}), see figure legends.

Table 3. Activity of CPG populations in the basic model during spontaneous deletions

Population name	Deletion type				
	Extensor deletions			Flexor deletions	
	Tonic flexors		Rhythmic flexors	Tonic extensors	
	resetting	non-resetting		resetting	non-resetting
RG-E/Inrg-E	silent	rhythmic-E	rhythmic-E	tonic	rhythmic-E
RG-F/ Inrg-F	tonic	rhythmic-F	rhythmic-F	silent	rhythmic-F
PF-E/ Inpf-F	silent	silent	silent	tonic	tonic
PF-F/ Inpf-F	tonic	tonic	rhythmic-F	silent	silent

Table 4. Behavior of PBSt and RF during spontaneous deletions

	Deletion type				
	Extensor deletions			Flexor deletions	
	Tonic flexors		Rhythmic flexors	Tonic extensors	
	resetting	non-resetting		resetting	non-resetting
PBSt					
Flexor short (type 1a)	silent (7)	rhythmic[a] (1)	rhythmic[a] (1)	silent (4)	
Flexor long (type 1b)	tonic (4) or rhythmic[b] (1)	rhythmic (4)	rhythmic (6)	silent (4)	
Extensor (type 2)	silent (9)		silent (4)	tonic (8)	silent (1) or rhythmic[a] (1)
Biphasic, short flexor burst (type 3a)	silent (7)		silent (1)	tonic (5)	not found
Biphasic, long flexor burst (type 3b)	tonic(2)	not found			
RF					
Flexor (type 1)	tonic (5)	rhythmic (1)	rhythmic (3)	silent (7)	
Biphasic (type 2)	tonic (5)	rhythmic[c] (7)	rhythmic[c] (9)	not found	

[a] - The amplitude of rhythmic activity is markedly reduced
[b] - During this deletion, the frequency of PBSt oscillations differs from the frequency before/after deletion.
[c] - RF loses its extensor component.

Chapter 11: Figures
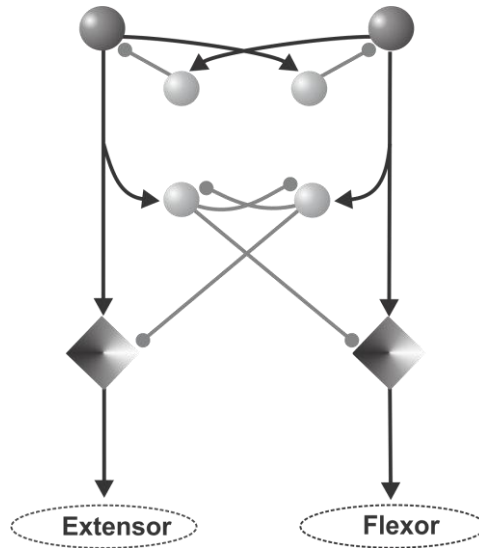
Figure 1. Classical half-center CPG model
Populations of interneurons are represented by spheres; motoneuron populations are represented by diamonds. Excitatory connections are shown as arrows; inhibitory connections are represented by lines with circles on the end.
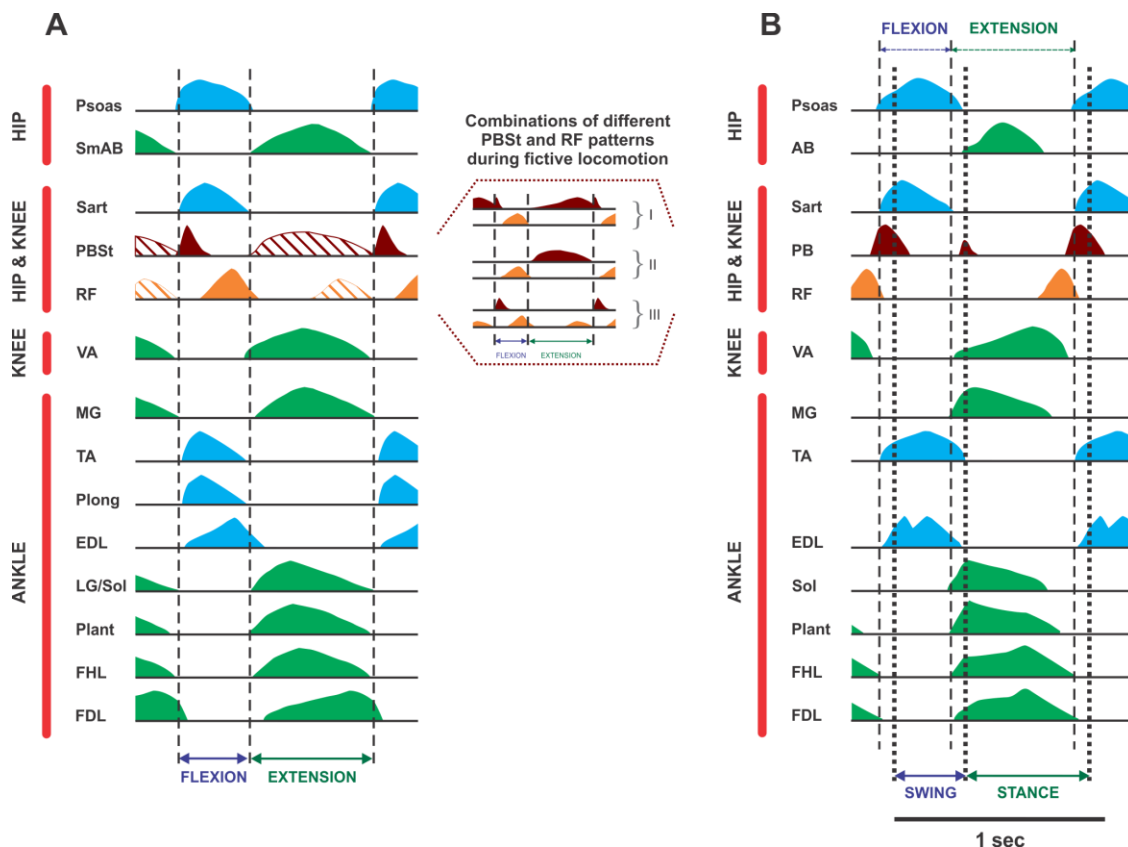
Figure 2. Normalized and averaged locomotor activity
A comparison of normalized and averaged motoneuron (A) and muscle (B) activity during fictive (A) and unrestrained (B) locomotion. Motoneurons and muscles are grouped based on the activity of which joint they control. Flexor motoneurons and muscles are in blue; extensor motoneurons and muscles are in green; PBSt and RF motoneurons and muscles are in brown and orange, respectively. A: Motoneuron ENG activity normalized and averaged over all experimental recordings available during fictive locomotion. Vertical dashed lines define the flexor and extensor phases, which were determined based on the onset of Sart activity, for flexion onset, and the onset of SmAB activity, for extension onset. Insert shows types of PBSt and RF activity patterns observed during fictive locomotion and their possible combinations. B: Muscle EMG activity normalized and averaged over all experimental recordings available during unrestrained locomotion. Vertical dotted lines indicate onsets of swing and stance phases; vertical dashed lines indicate onsets of flexor and extensor phases. (Markin *et al.* 2008)
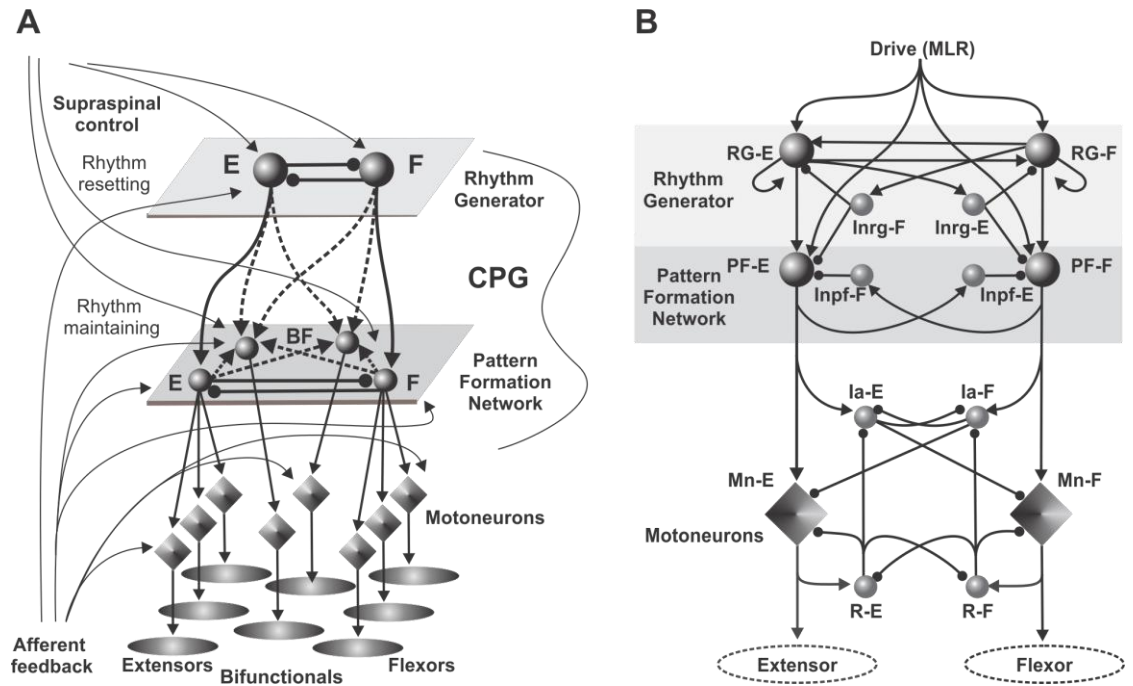
Figure 3. Two-level CPG concept and model
A: Schematic illustration of the two-level CPG concept. The locomotor CPG consists of a half-center rhythm generator (RG) and a pattern formation (PF) network. The RG defines the locomotor rhythm and the durations of flexor and extensor phases and controls the activity of the PF network. The PF network contains interneuron populations (grey spheres), which interact with each other and provide excitation to synergist or bifunctional motoneuron pools (diamonds) acting at different limb joints. The PF network mediates rhythmic input from the RG and distributes it to the motoneuron pools. **B**: Schematic of the basic two-level model of the locomotor CPG (Rybak *et al.* 2006a).
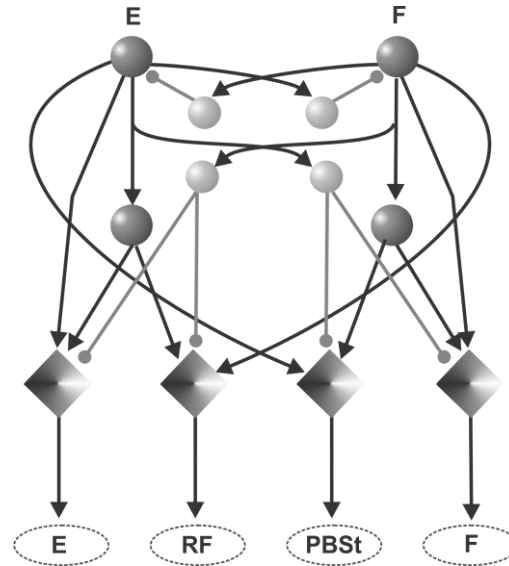
Figure 4. Perret CPG model
Schematic of the CPG model proposed by Perret and his colleagues (Perret 1983) to explain complex biphasic activity patterns of PBSt and RF.

Psoas	*Iliopsoas*
SmAB	*Semimembrinosus and anterior biceps*
Sart	*Sartorius*
PBSt	*Posterior biceps and semitendinosus*
RF	*Rectus femoris*
VA	*Vastus*
Plong	*Peroneus longus*
TA	*Tibialis anterior*
EDL	*Extensor digitorum longus*
GS	*Gastrocnemius*
Sol	*Soleus*
Plant	*Plantaris*
FDL	*Flexor digitorum longus*
FHL	*Flexor hallucis longus*
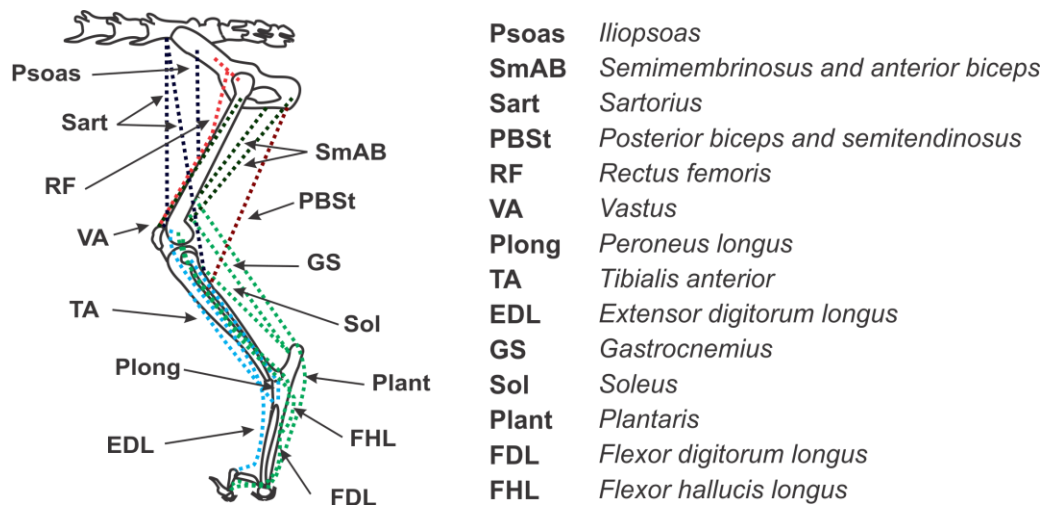
Figure 5. Major muscles controlling the cat hind limb
EDL - extensor digitorum longus; FDL - flexor digitorum longus; FHL - flexor hallucis longus; LG - lateral gastrocnemius; MG - medial gastrocnemius; PBSt - posterior biceps and posterior semitendinosus; Plant - plantaris; Plong - peroneus longus; IP - iliopsoas; Sart - sartorius; RF - rectus femoris; ABSm - anterior biceps and anterior semimembranosus; Sol - soleus; TA - tibialis anterior; VA - vastus.
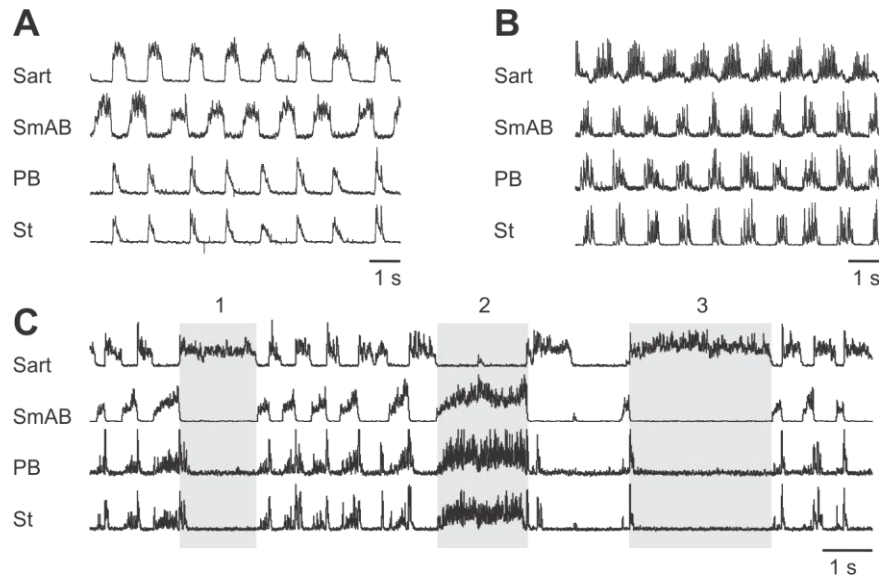
Figure 6. PB and St behavior during fictive locomotion experiments
PB and St ENGs were recorded separately in the same experiment. **A**: Both PB and St are simultaneously active in flexion. **B**: Both PB and St are simultaneously active in extension. **C**: Both PB and St are biphasic and demonstrate remarkably similar behaviors before, after, and during two extensor deletions (shaded areas 1 and 3) with tonically active flexor (Sart), and one flexor deletion (shaded area 2) with tonically active extensor (SmAB).
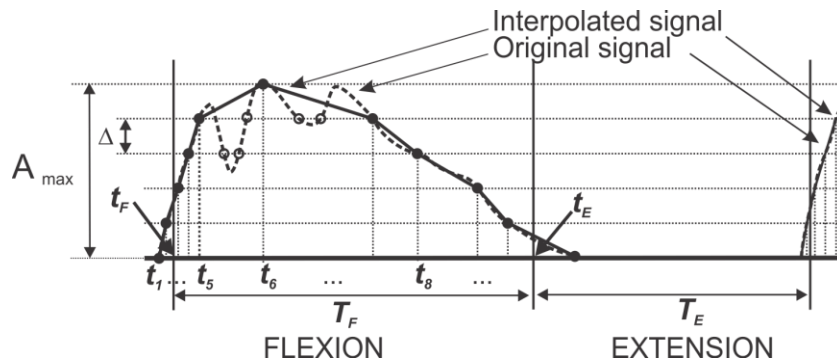
Figure 7. ENG signal interpolation
An example of an interpolation of an ENG pattern (*dashed line*) occurring mainly during the flexor phase. The interpolated signal (*solid line*) is formed through linear interpolation based on crossing points (*filled circles*) of original pattern and several amplitude levels. The interpolated signal in this case is made up of eleven crossing points $\{(t_1, A_1), (t_2, A_2), (t_3, A_3) \ldots (t_{11}, A_{11})\}$ between the original signal and six amplitude levels $(A_1, A_2 \ldots A_{max})$, where $A_1 = 0$; $A_{i+1} = A_i + \Delta$, $\Delta = A_{max}/5$, $i = 1, 2 \ldots 5$. All intermediate points (*open circles*) are ignored.
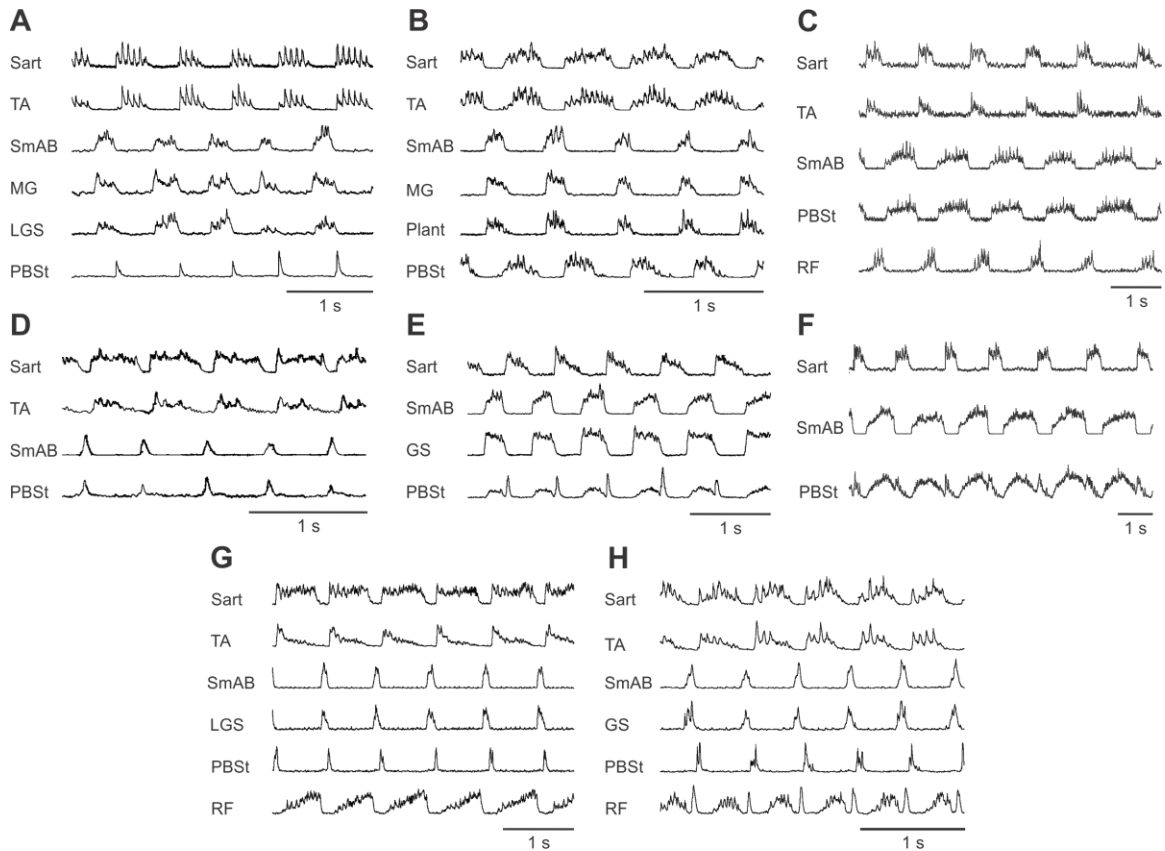
Figure 8. Profiles of PBSt and RF activity during fictive locomotion

The traces are rectified-integrated simultaneous ENG recordings from several flexors (top traces, Sart, TA), extensors (middle traces, SmAB, MG, GS, LGS, Plant) and bifunctionals (bottom traces, PBSt, RF) obtained in fictive locomotion experiments. **A**: PBSt demonstrates a short burst at the beginning of the flexor phase. **B**: PBSt is active during most of flexion. **C**: PBSt is active in extension during extensor dominated fictive locomotion, RF is active late in flexion. **D**: PBSt is active in extension during flexor dominated fictive locomotion. **E** and **F**: PBSt is active during both phases, exhibiting either a low (**E**) or high (**F**) level of activity during extension and a short burst of activity at the beginning of flexion. **G**: PBSt and RF are active in flexion; PBSt demonstrates a short activity burst at the beginning of flexion and RF becomes active shortly after the phase onset and demonstrates increased activity up to the end of flexion. **H**: PBSt is active at the beginning of flexion, and RF exhibits two activity bursts, one short burst at the end of extension and another one late in flexion.
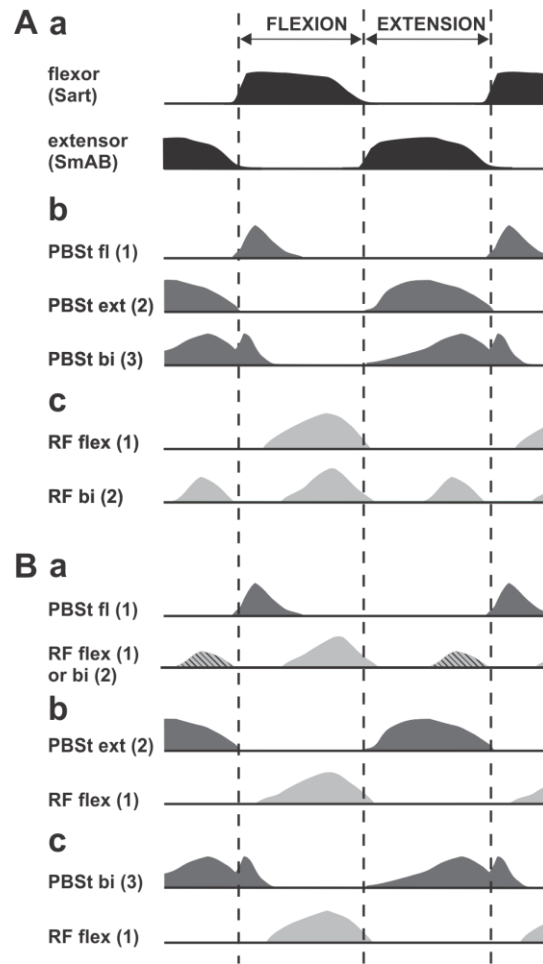
Figure 9. Normalized and averaged PBSt and RF activity during fictive locomotion
Normalized and averaged profiles of PBSt and RF activity with respect to the activity of typical flexor (Sart) and extensor (SmAB) motoneurons during fictive locomotion. **Aa**: Averaged and normalized activity of flexor (Sart) and extensor (SmAB). **Ab**: Three distinct patterns of PBSt activity: flexor-type (1), extensor-type (2), and biphasic (3). **Ac**: Two distinct patterns of RF activity: flexor-type (1) and biphasic (2). **Ba-c**: Averaged and normalized activity of PBSt and RF from experiments in which they were simultaneously recorded for flexor-type (**Ba**), extensor-type (**Bb**), and biphasic (**Bc**) PBSt profiles. In **Ba**, both flexor-type and biphasic RF activity patterns were observed when PBSt exhibited flexor-type activity.
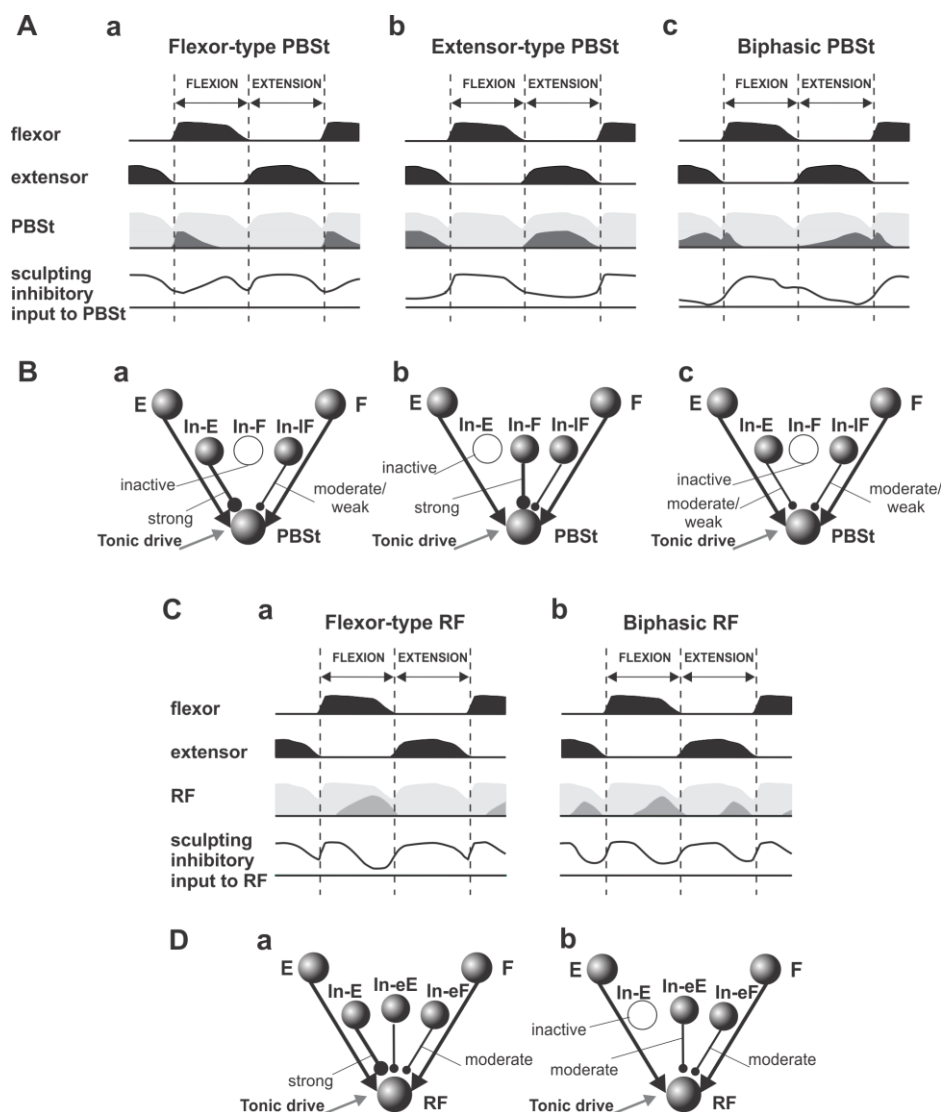
Figure 10. Shaping activity profiles of PBSt and RF
A and **C**: hypothetical activities of flexor and extensor parts of the CPG (first and second trace), sum of proposed excitatory inputs to PBSt and RF from flexor and extensor sides of the CPG in addition to tonic drive (third trace, lightly shaded area), desired PBSt and RF activity patterns (third trace, heavily shaded area), and sculpting inhibitory signals necessary to shape PBSt and RF activity for each activity type (last trace). **B** and **D**: neuron populations participating in shaping PBSt and RF activity are shown as shaded spheres; empty circles represent inactive neuron populations. Spheres marked with 'E' and 'F' schematically represent the flexor and extensor parts of the CPG. Inhibitory interneuron populations participating in shaping the activity of PBSt (In-E, In-F and In-lF) and RF (In-E, In-eE and In-eF) are shown in each diagram. Excitatory and inhibitory inputs to PBSt and RF populations are indicated by lines with arrows and small circles, respectively. Thicker lines with larger circles represent stronger inhibitory influences; thinner lines with smaller circles represent weaker/moderate inhibitory influences.
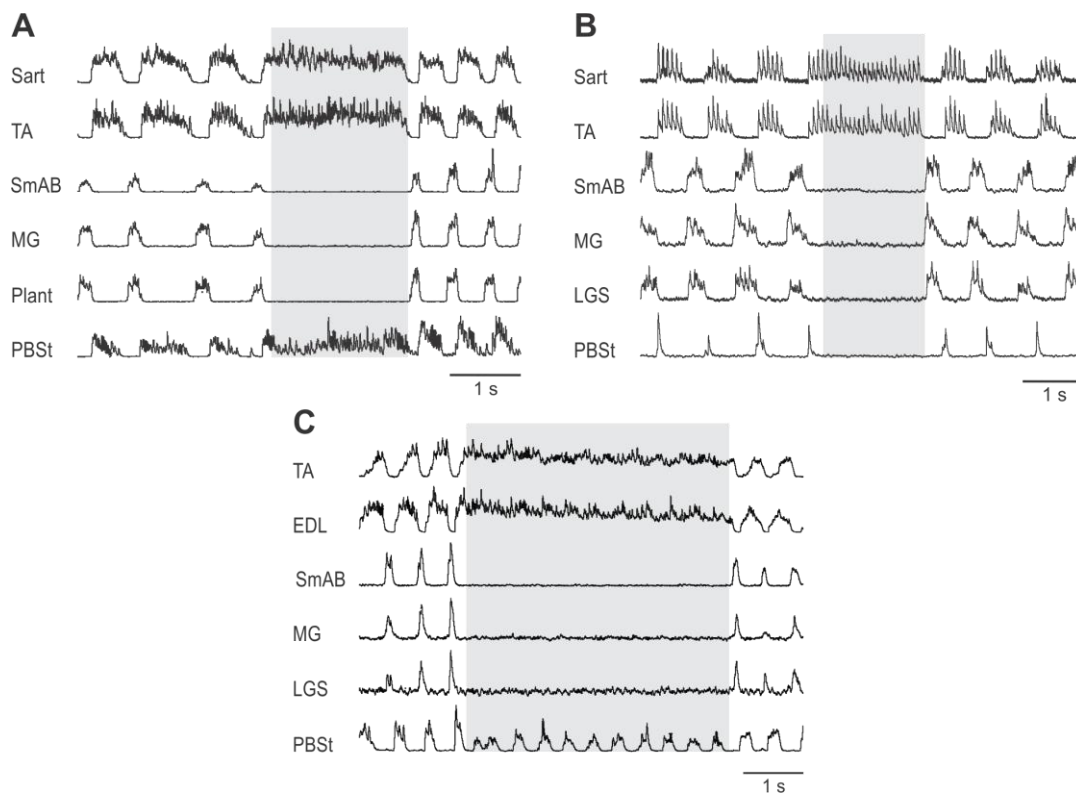
Figure 11. Flexor-type PBSt behavior during extensor activity deletion

Deletions of extensor activity (SmAB, MG, Plant, LGS) accompanied with sustained activity of flexors (Sart, TA, EDL). Shaded rectangles highlight deletion episodes. In all three recordings PBSt is of the flexor-type before and after the deletion. However during the deletions, PBSt demonstrates tonic activity similar to flexors in **A**; is silent similar to extensors in **B**; and expresses rhythmic activity in **C**. Note that the frequency of PBSt oscillations in **C** differs from the locomotor frequency before and after the deletion.
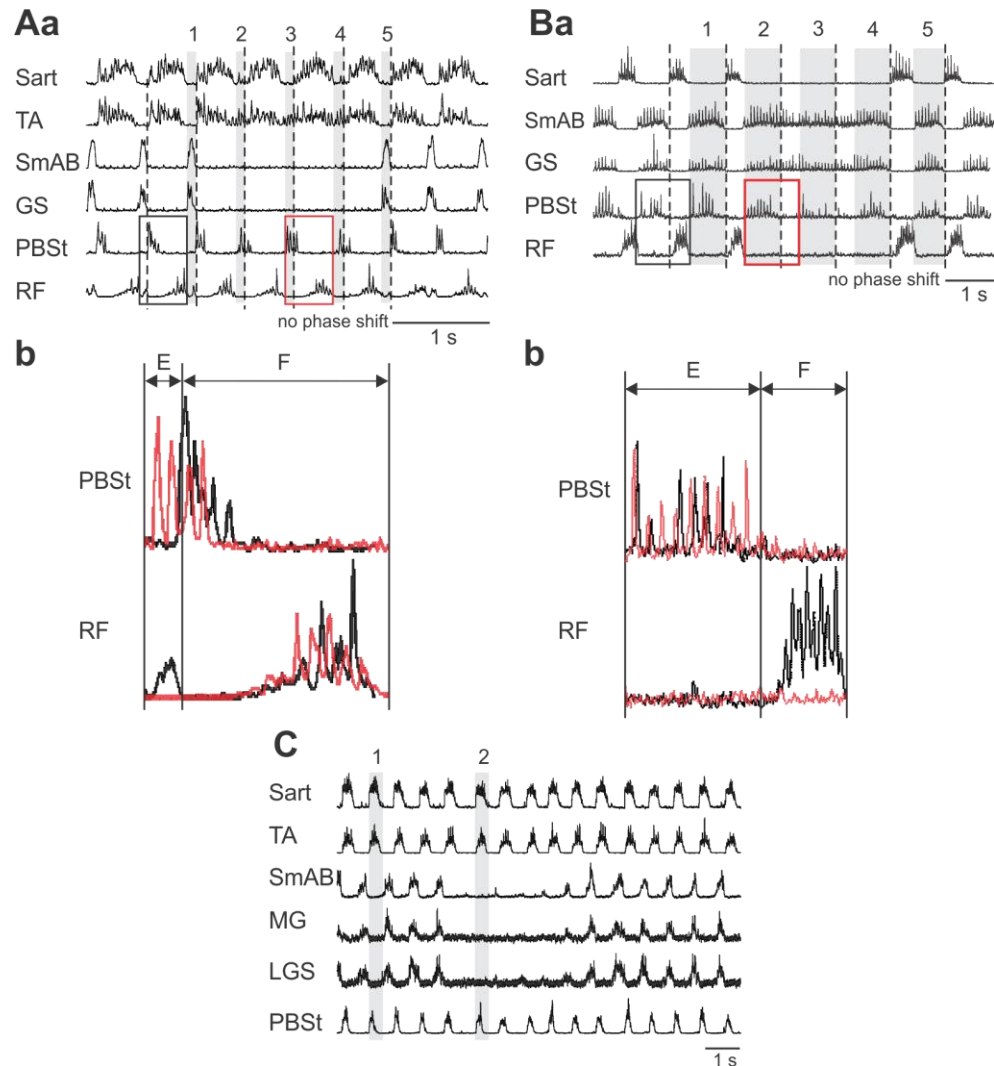
Figure 12. PBSt and RF behavior during deletions
Fictive locomotion recordings with episodes of deletions used to build PBSt and RF circuitry in the extended model (panels **Aa**, **Ba**, and **C**)). In **Aa** and **Ba** vertical dashed lines are plotted at intervals representing an average locomotor period calculated based on five step cycle periods preceding the deletions. During the deletions, these lines indicate approximately where the onsets of the flexor bursts would have occurred had there been no deletion. **Aa**: An example of the behavior of flexor type PBSt (type 1b) and biphasic RF (type 2) during non-resetting extensor deletions with sustained tonic activity of flexors. Note that TA demonstrates modulated tonic activity during the deletion while another flexor (Sart) maintains rhythmic activity. The extensors (SmAB and GS) are silent. During the deletion, PBSt and RF remain rhythmic. Shaded bars show the extensor phases before and after the deletion (bars 1 and 5) and the anticipated extensor intervals during the deletion (bars 2-4). **Ab**: Enlarged and overlapped traces of PBSt and RF ENGs for two locomotor cycles outlined in **Aa** by rectangles. The black traces correspond to a pre-deletion locomotor cycle; the red ones correspond to a supposed locomotor cycle during the deletion. In **Aa** and **Ab**, you can observe that: (1) during the deletion PBSt

becomes active in the anticipated extensor phases; (2) PBSt activity in the anticipated flexor phases is reduced; and (3) RF loses its extensor component during the deletion. **Ba**: An example of extensor-type PBST (type 2) and flexor-type RF (type 1) behavior during a non-resetting flexor deletion (Sart). The extensors (SmAB and GS) during the deletion become tonically active. The shaded bars indicate the extensor phases before and after the deletion and the assumed extensor phases during the deletion. **Bb**: Enlarged and overlapped traces of PBSt and RF ENGs for two locomotor periods before and during the deletion, outlined in **Ba** by rectangles. In **Ba** and **Bb**, it can be seen that RF becomes silent during the deletion while PBSt continues its activity during the anticipated extensor phases. **C**: An example of flexor-type PBSt (type 1b) behavior during spontaneous deletion of extensor activity (SmAB, LGS, and MG) with rhythmic flexors (Sart and TA). The shaded bars 1 and 2 illustrate the flexor phases before and during the deletion, respectively. During the deletion PBSt remains rhythmic and exhibits bursts of activity simultaneous with the flexors. No activity appears in the anticipated extensor intervals.
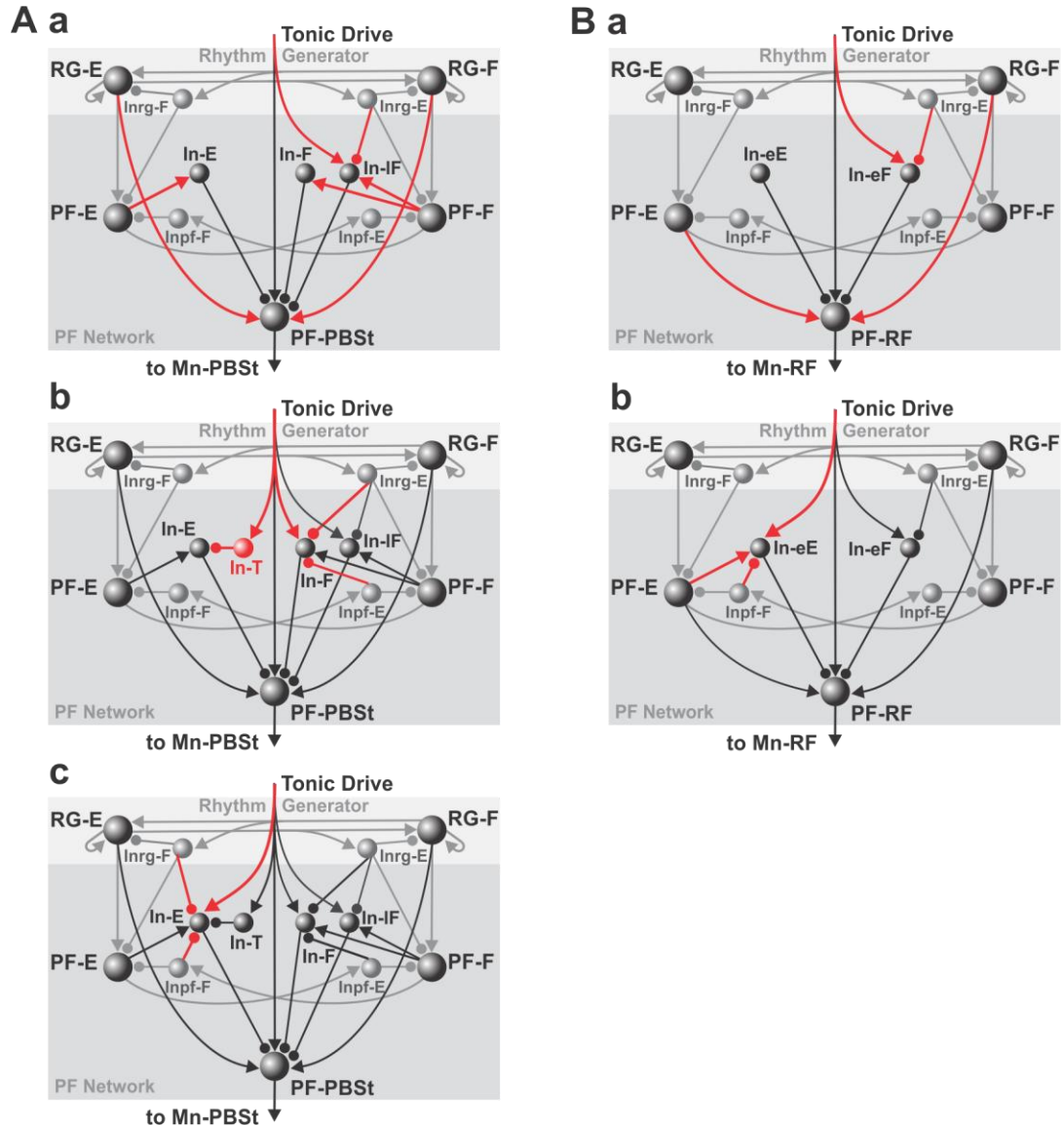
Figure 13. Construction of PF level networks controlling PBSt and RF activities
Construction is based on the analysis of fictive locomotion experiments with episodes of deletion shown in Fig. 12. The left column (panels **Aa**, **Ab**, and **Ac**) illustrates the sequential building of PBSt circuitry. The right column (panels **Ba** and **Bb**) shows the construction of RF circuitry. At each step of the circuitry construction, newly introduced network elements (populations and connections) are highlighted in red. See text for details.
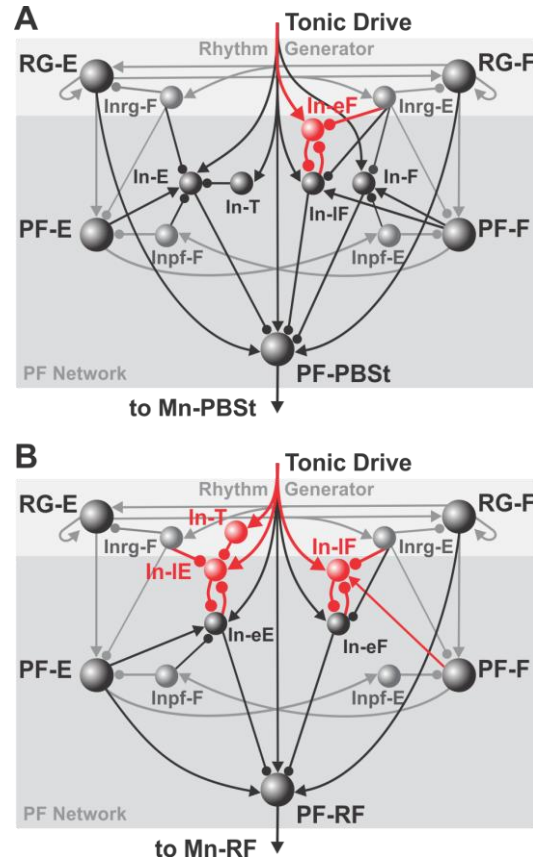
Figure 14. Extension of PF level networks controlling populations PF-PBSt and PF-RF

Additional proposed modifications of the PF level networks controlling PF-PBSt (**A**) and PF-RF (**B**) behavior in the extended model. Modifications made over the circuitries presented in Fig. 13 appear in red. See text for details.
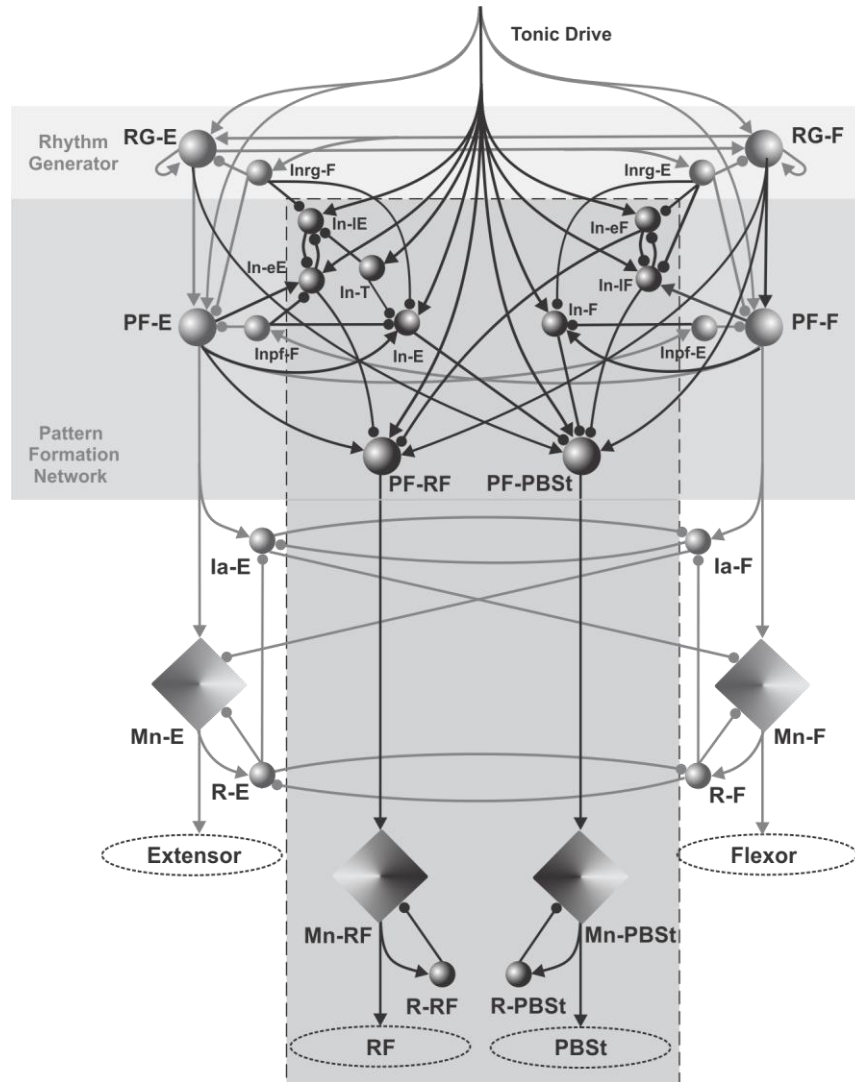
Figure 15. Schematic of the extended locomotor CPG model
The extended model includes all populations of the basic CPG model (see Fig. 3B) and hypothetical populations and connections incorporated into the PF network to control PBSt and RF activity (see Figs. 13 and 14). The extended model also includes two bifunctional motoneuron populations (Mn-PBSt and Mn-RF) and two populations of Renshaw cells, R-PBSt and R-RF, which receive collateral excitatory input from the corresponding motoneuron populations (Mn-PBSt and Mn-RF) and provide feedback inhibition to the homonymous motoneuron populations.
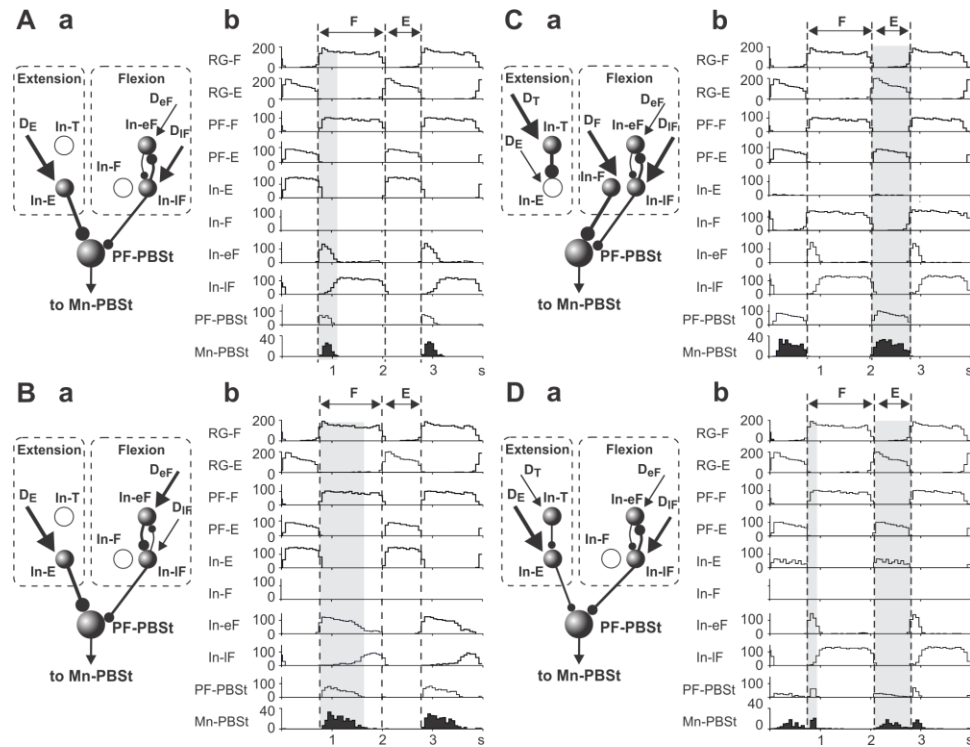
Figure 16. Shaping of PBSt activity patterns

Diagrams in the left column illustrate circuits that shape particular patterns of PBSt activity: short flexor profile, type 1a (**Aa**); long flexor profile, type 1b (**Ba**), extensor, type 2 (**Ca**); and biphasic, type 3 (**Da**). The dashed rectangle outlines designate populations participating in the shaping of PBSt activity during the extensor or flexor phase. The arrows of different sizes schematically show excitatory input drives of different strengths received by the interneuron populations, the larger the arrow size the stronger the input drive. Excitation level of each population is schematically represented by thickness of output connection, the greater the level of excitation, the thicker the connection. **Ab**, **Bb**, **Cb**, and **Db** show examples of corresponding computer simulations performed using the extended model. In these figures, the activity of each population is represented by a histogram of the average neuron activity in it. The alternating rhythmic bursts of the RG populations, RG-F and RG-E (the first two traces) define the duration of the extensor and flexor phases and the locomotor cycle period (indicated by dashed lines). The third and fourth trace represent activities of the PF-F and PF-E populations, closely following the activity of the corresponding RG populations. The next four traces represent the activity of the interneuron populations (In-E, In-F, In-eF and In-lF) shaping PF-PBSt's activity, and the last two traces show the activity of population PF-PBSt and the resulting activity of population Mn-PBSt. Shaded rectangles highlight the time intervals during which Mn-PBSt is active (for one locomotor cycle). In all four simulations drives to RG populations were: $D_{RG-E} = 0.17$ and $D_{RG-F} = 0.18$. Drives to interneuron populations shaping PBSt activity were: $D_T = 0$, $D_E = 0.25$, $D_F = 0$, $D_{eF} = 0.18$, $D_{lF} = 0.16$ in **Ab**; $D_T = 0$, $D_E = 0.25$, $D_F = 0$, $D_{eF} = 0.23$, $D_{lF} = 0.16$ in **Bb**; $D_T = 0.25$, $D_E = 0$, $D_F = 0.26$, $D_{eF} = 0.18$, $D_{lF} = 0.16$ in **Cb**; and $D_T = 0.05$, $D_E = 0.07$, $D_F = 0$, $D_{eF} = 0.18$, $D_{lF} = 0.16$ in **Db**.
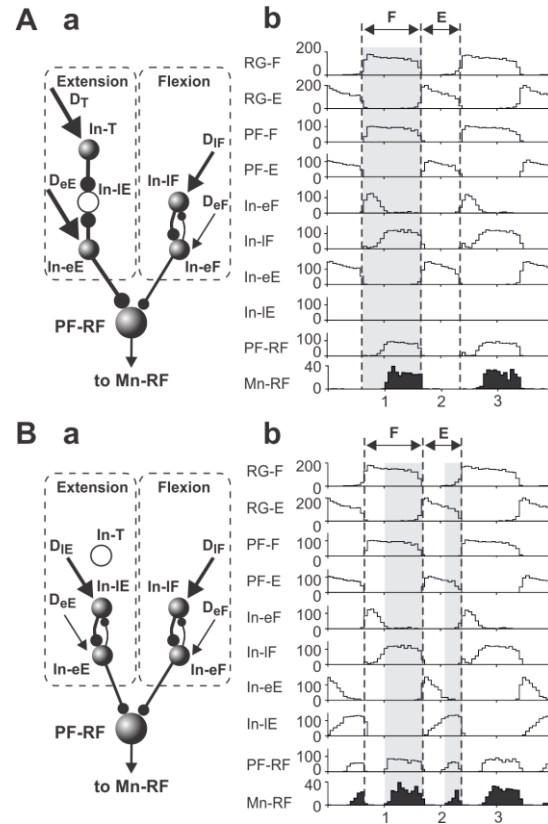
Figure 17. Shaping of RF activity patterns

Diagrams in the left column illustrate circuits that shape particular patterns of RF activity: flexor-type, type 1 (**Aa**); and biphasic, type 2 (**Ba**). **Ab** and **Bb** show examples of corresponding computer simulations performed using the extended model. The alternating rhythmic bursts of the RG populations, RG-F and RG-E are shown in the top two traces. The third and fourth trace represent activities of the PF-F and PF-E populations. The next four traces represent the activity of the interneuron populations (In-eF, In-lF, In-eE and In-lE) shaping PF-RF activity, and the last two traces show the activity of population PF-RF and resulting activity of population Mn-RF. Shaded rectangles highlight the time intervals during which Mn-RF is active (for one locomotor cycle). In both simulations, drives to RG populations were: $D_{RG-E} = 0.17$ and $D_{RG-F} = 0.18$. Drives to interneuron populations shaping RF activity were: $D_T = 0$, $D_{eE} = 0.25$, $D_{lE} = 0$, $D_{eF} = 0.18$, $D_{lF} = 0.16$ in **Ab**; $D_T = 0$, $D_{eE} = 0.135$, $D_{lE} = 0.18$, $D_{eF} = 0.18$, $D_{lF} = 0.16$ in **Bb**.
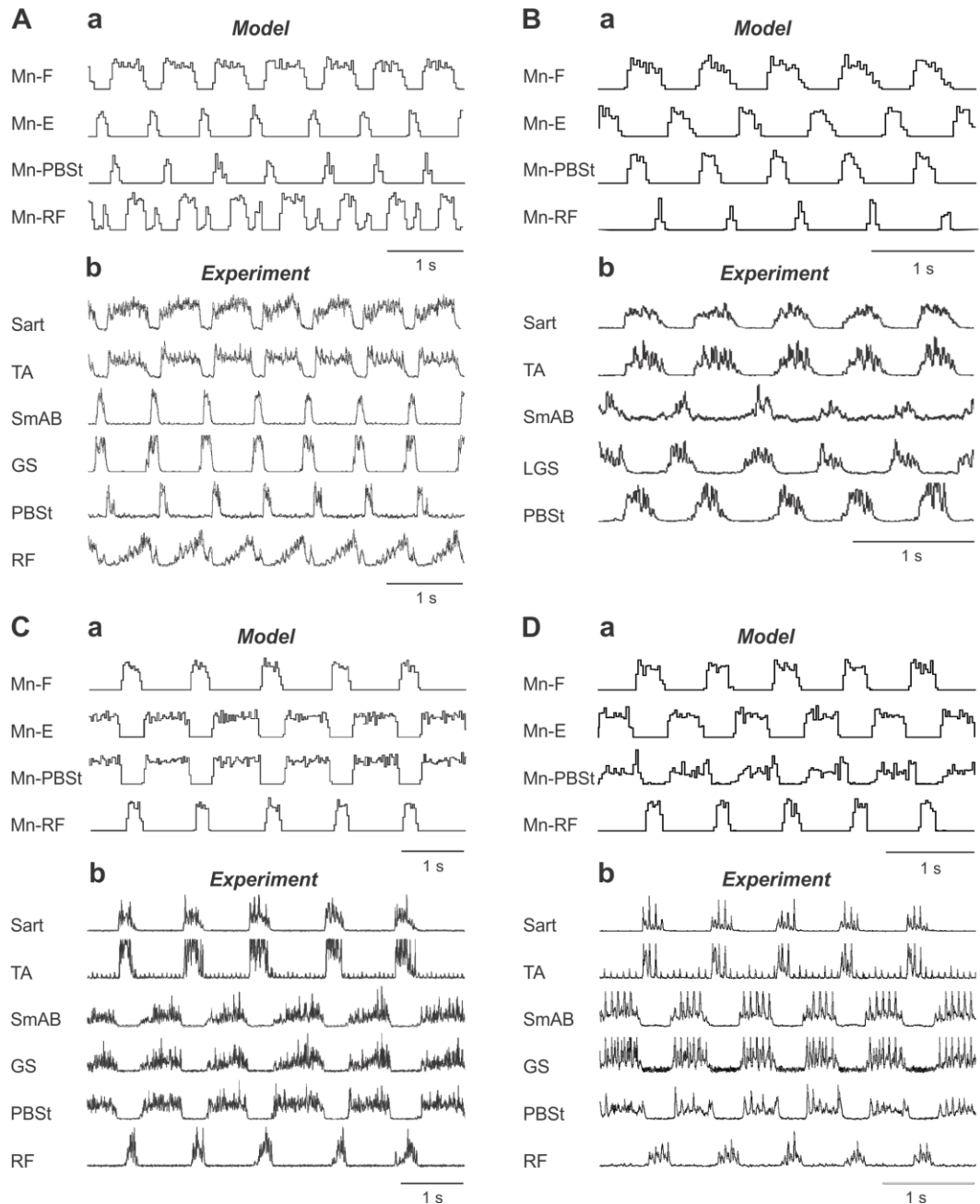
Figure 18. Extended CPG model reproducing PBSt and RF activity
Examples of simulations reproducing different types of PBSt and RF activity profiles using the extended CPG model, compared with the corresponding experimental recordings. In all simulations (**Aa**, **Ba**, **Ca** and **Da**), the first and second trace show the activity of the flexor and extensor motoneuron populations, respectively. The third and fourth trace show the activity of of bifunctional motoneuron populations Mn-PBSt and Mn-RF, respectively. Panel **Aa** shows the result of a simulation exhibiting short flexor-type PBSt (type 1a) and biphasic RF (type 2). For this simulation, $D_{RG-E} = 0.18$, $D_{RG-F} = 0.205$, $D_T = 0$, $D_E = 0.25$, $D_{eE} = 0.08$, $D_{IE} = 0.2$, $D_F = 0$, $D_{eF} = 0.2$, $D_{IF} = 0.16$. Panel **Ab** shows a corresponding experimental recording obtained during fictive

locomotion, in which PBSt and RF were recorded simultaneously. PBSt starts its activity together with flexors (Sart and TA) and is active during about 25% of the flexor phase (short flexor-type pattern of activity, type 1a). RF in this recording is biphasic (type 2) and demonstrates a short burst late in extension and a long bust in flexion starting immediately after PBSt activity terminates. Panel **Ba** shows the results of a simulation exhibiting long flexor-type PBSt (type 1b) and flexor-type RF (type 1). For this simulation, $D_{RG-E} = 0.165$, $D_{RG-F} = 0.15$, $D_T = 0$, $D_E = 0.25$, $D_{eE} = 0.16$, $D_{IE} = 0$, $D_F = 0$, $D_{eF} = 0.2$, $D_{IF} = 0.18$. Panel **Bb** shows a corresponding experimental recording in which long flexor-type PBSt (type 1b) starts its activity simultaneously with flexors (Sart and TA) and is active during most of flexion. Panel **Ca** shows the results of a simulation with extensor-type PBSt (type 2) and flexor-type RF (type 1) activity patterns. In this simulation, $D_{RG-E} = 0.165$, $D_{RG-F} = 0.15$, $D_T = 0.25$, $D_E = 0$, $D_{eE} = 0.16$, $D_{IE} = 0$, $D_F = 0.25$, $D_{eF} = 0.17$, $D_{IF} = 0.22$. Panel **Cb** presents a similar experimental case where PBSt is simultaneously active with extensors (SmAB and GS), while RF starts its activity delayed compared to flexors (Sart and TA) and is active up to the end of the flexor phase (type 1). Panel **Da** shows the results of a simulation of biphasic PBSt (type 3) and flexor-type RF (type 1). In this simulation, $D_{RG-E} = 0.175$, $D_{RG-F} = 0.17$, $D_T = 0$, $D_E = 0.08$, $D_{eE} = 0.16$, $D_{IE} = 0$, $D_F = 0$, $D_{eF} = 0.17$, $D_{IF} = 0.22$. Panel **Db** shows a corresponding experimental record in which PBSt is active in both phases (type 3). In the extensor phase, PBSt is active for the entire duration of the phase at a low amplitude activity level, simultaneously with extensors (SmAB and GS). In the flexor phase, PBSt exhibits a short burst that starts simultaneously with flexors (Sart and TA), and the RF flexor burst starts immediately after PBSt activity terminates.
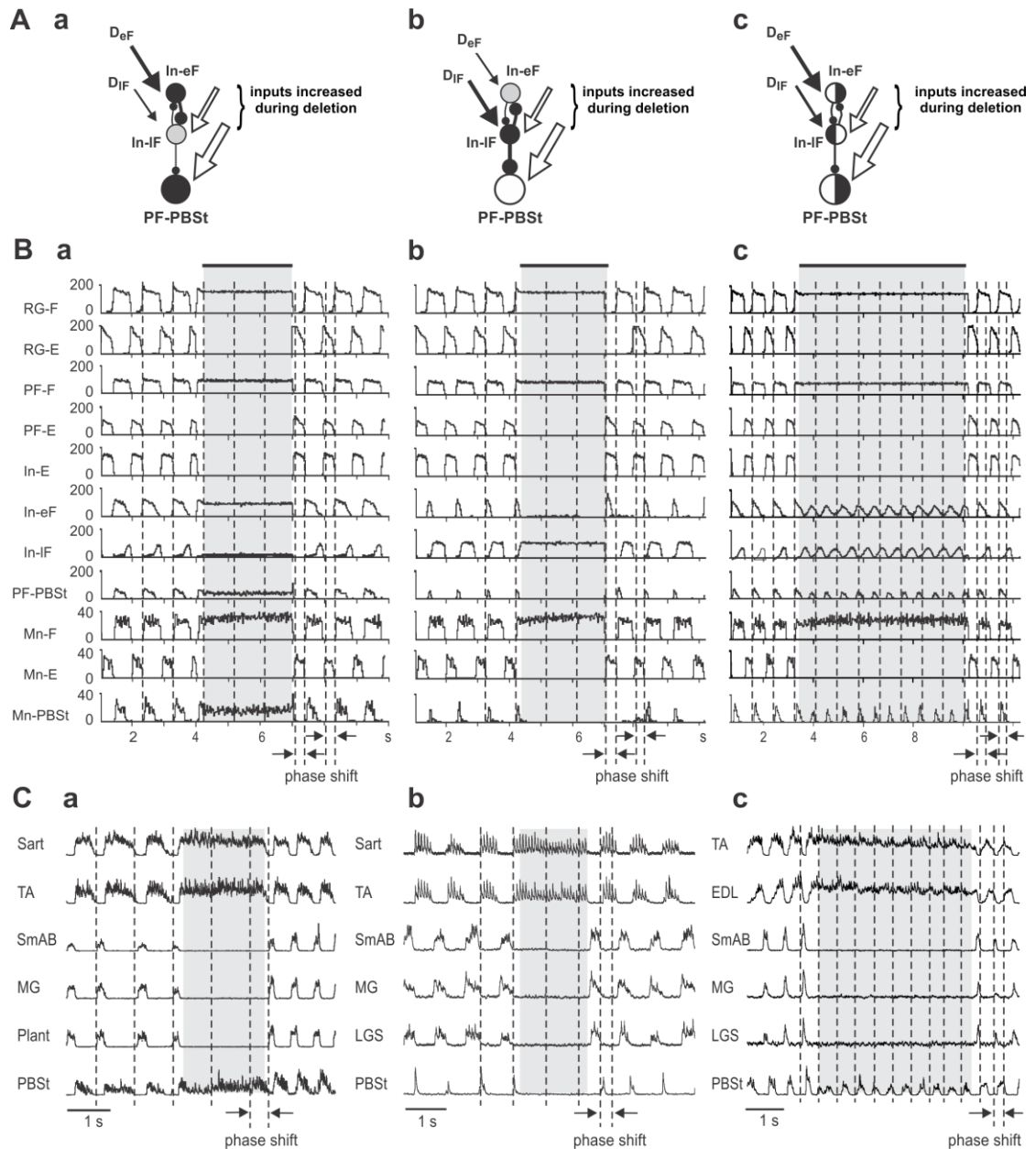
Figure 19. Simulations of flexor-type PBSt behavior during resetting extensor deletions

In the model, all deletions were produced by temporarily applying an inhibitory input drive to the extensor side of the CPG at the RG level (RG-E). **A**: Circuits shaping PBSt activity during deletions for: PBSt with long flexor burst before and after the deletion (**Aa**), short flexor burst before and after the deletion (**Ab**), and a flexor burst lasting about 50% of the phase, before and after the deletion (**Ac**). The solid arrows of different sizes schematically show excitatory input drives of different strengths received by the interneuron populations, the larger the arrow size the stronger the input drive. Excitation level of each population is schematically represented by the thickness of the output connection, the greater the level of excitation, the thicker the connection. Unfilled arrows

illustrate additional activation of neuron populations during deletions. Black circles represent populations highly activated during deletions; grey circles illustrate low level of activity in the particular populations; unfilled circles designate inactive populations. Circles that are half black half white represent populations that are rhythmically active during the deletions. **B**: The results of simulations of PBSt behavior during deletions. In the model, all deletions were produced by temporarily applying an inhibitory input drive ($D_{add} = 0.4$) to population RG-E, as indicated by the horizontal black bars at the top of traces. Shaded rectangles highlight the behaviors of neuron populations during the deletions. The first eight traces are of different CPG populations at the RG and PF levels. The last three traces illustrate the activities of flexor and extensor motoneuron populations and Mn-PBSt, respectively. In all three simulations, $D_{RG-F} = 0.17$, $D_{RG-E} = 0.16$, $D_F = 0$, $D_E = 0.25$, $D_T = 0$. $D_{eF} = 0.18$, $D_{lF} = 0.145$ in **Ba**; $D_{eF} = 0.14$, $D_{lF} = 0.18$ in **Bb**; and $D_{eF} = 0.18$, $D_{lF} = 0.155$ in **Bc**. **Ca-c**: Experimental recordings corresponding to PBSt behavior shown in **Ba-c**. The vertical dashed lines are plotted at intervals representing an average locomotor period. An obvious phase shift of the post-deletion rhythm with respect to the pre-deletion rhythm (see arrows at the bottom) indicates that all deletions are of the resetting type.
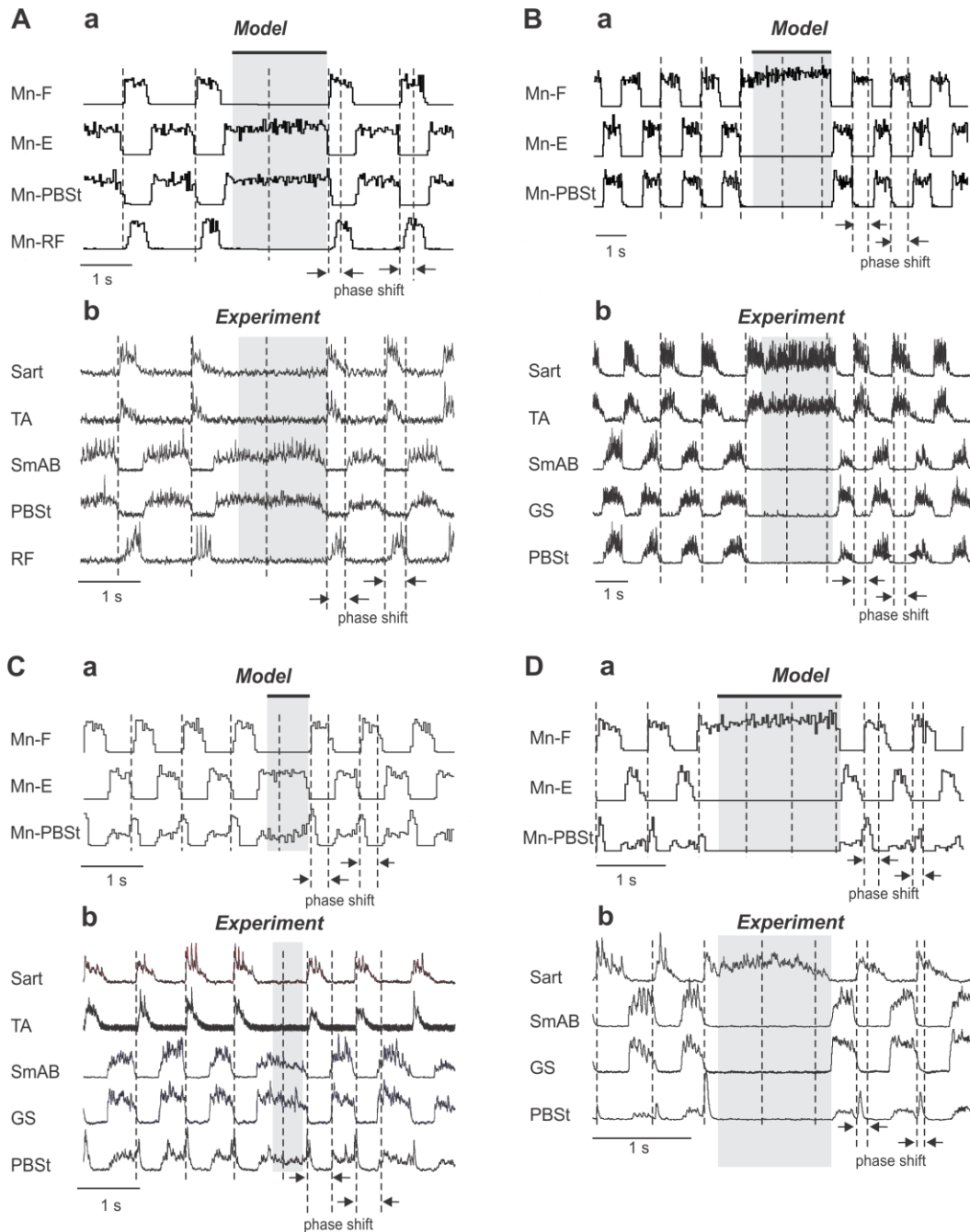
Figure 20. **Simulations of PBSt and RF behavior during resetting deletions**
Examples of simulations and experimental records with extensor-type (**A** and **B**) and biphasic (**C** and **D**) PBSt profiles during flexor (**A** and **C**) and extensor (**B** and **D**) resetting deletions with sustained activity of antagonist motoneuron pools. In the model, all deletions were produced by temporarily applying an inhibitory input drive ($D_{add} = 0.3$) to the flexor (**A** and **C**) or extensor (**B** and **D**) side of the CPG's RG level, as indicated by the horizontal black bars above the traces. Shaded rectangles highlight behaviors of neuron populations during deletions. All deletions presented in this figure exhibited an obvious phase shift of the post-deletion rhythm (see arrows at the bottom of all panels)

indicating that all these deletion are of the resetting type. **Aa**: The results of a simulation of extensor-type PBSt and flexor-type RF during a resetting flexor deletion. In this simulation, $D_{RG-F} = 0.15$, $D_{RG-E} = 0.165$, $D_F = 0.25$, $D_E = 0$, $D_T = 0.25$, $D_{eF} = 0.16$, $D_{lF} = 0.23$, $D_{eE} = 0.15$, $D_{lE} = 0$. During the deletion, Mn-PBSt exhibited tonic activity, whereas Mn-RF was silent. **Ab**: The corresponding experimental records during fictive locomotion. Before, after, and during the deletion PBSt was simultaneously active with extensor (SmAB) demonstrating sustained activity during the deletion. RF showed a delayed flexor burst before and after the deletion and was silent during the deletion similar to flexors (see Sart and TA). **Ba**: The results of a simulation of extensor-type PBSt during a resetting extensor deletion. In this simulation, $D_{RG-F} = 0.15$, $D_{RG-E} = 0.15$, $D_F = 0.25$, $D_E = 0$, $D_T = 0.25$, $D_{eE} = 0.18$, $D_{lE} = 0.22$. During this deletion, Mn-PBSt was silent. **Bb**: The corresponding experimental recordings. Before and after the deletion PBSt was simultaneously active with extensors (SmAB and GS). During the deletion, flexors (Sart and TA) were tonic, and extensors as well as PBSt were silent. **Ca**: The results of a simulation of biphasic PBSt behavior during a resetting flexor deletion. In this simulation, $D_{RG-F} = 0.19$, $D_{RG-E} = 0.18$, $D_F = 0$, $D_E = 0.07$, $D_T = 0$, $D_{eE} = 0.18$, $D_{lE} = 0.2$. During the deletion, Mn-PBSt exhibited tonic activity. **Cb**: The corresponding experimental records during fictive locomotion. Before and after the deletion PBSt was active during both phases, exhibiting a low amplitude activity during the whole extensor phase and a short burst at the beginning of flexion. During the deletion, extensors (SmAB and GS) were tonically active, flexors (Sart and TA) were silent, and PBSt demonstrated tonic activity. Note the low amplitude of this activity. **Da**: The results of a simulation of biphasic PBSt behavior during a non-resetting extensor deletion. In this simulation, $D_{RG-F} = 0.21$, $D_{RG-E} = 0.19$, $D_F = 0$, $D_E = 0.09$, $D_T = 0$, $D_{eE} = 0.18$, $D_E = 0.17$. During the deletion, Mn-PBSt was silent. **Db**: The corresponding experimental recordings. Before and after the deletion PBSt was biphasic, exhibiting a low amplitude activity during the whole extensor phase and a short burst at the beginning of flexion. During the deletion, flexors (Sart and TA) had sustained activity, and PBSt was silent along with extensors (SmAB and GS).
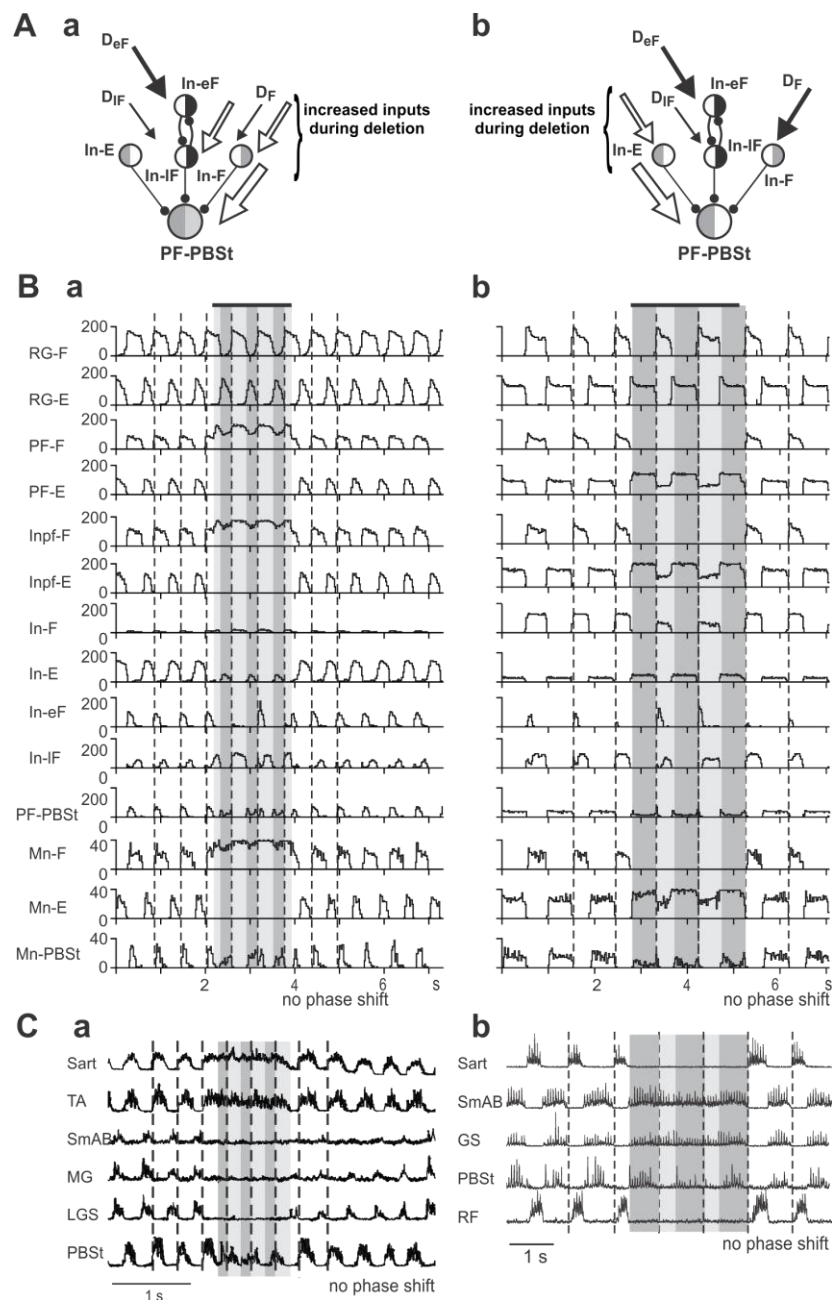
Figure 21. **Simulations of PBSt behavior during non-resetting deletions**
Simulations of the behavior of flexor and extensor-types PBSt during non-resetting extensor (**Aa** and **Ba**) and flexor (**Ab** and **Bb**) deletions. In the model, these deletions were produced by temporarily increasing the excitability of populations PF-F (**Aa** and **Ba**) and PF-E (**Ab** and **Bb**). Vertical dashed lines in **B** and **C** are plotted at intervals representing an average locomotor period calculated over five step cycles preceding the deletions. During the deletions, these lines indicate approximately where the onset of flexor bursts would have occurred had there been no deletion. A lack of phase shift indicates that these deletions are non-resetting. Dark rectangles highlight suggested extensor intervals during the deletion. **A**: Circuits shaping PBSt activity, flexor-type (**Aa**)

and extensor-type (**Ab**) PBSt. Arrows of different sizes schematically represent excitatory input drives of different strengths received by the interneuron populations, the larger the arrow size the stronger the input drive. Excitation level of each population is schematically represented by thickness of the output connection, the greater the level of excitation, the thicker the connection. Unfilled arrows illustrate additional activation of neuron populations during the deletions. Half-filled circles represent populations continuing rhythmic activity during the deletion. The left side of the circles corresponds to the suggested extensor intervals, the right side corresponds to the flexor interval, during the deletion. Black color indicates strong activity during the corresponding phase; grey, low or moderate activity level; and white, no activity. **B**: The results of the simulations of PBSt's behavior during the deletions. The black horizontal bar indicates when the additional drive was applied to produce the deletion. The top eleven traces are of various CPG interneuron populations, and the last three traces illustrate the activity of flexor, extensor, and PBSt motoneuron populations, respectively. In **Ba**, the deletion of extensor activity was produced by applying additional excitatory drive $D_{add} = 0.2$ to population PF-F. Other drives were set at, $D_{RG-F} = 0.15$, $D_{RG-E} = 0.19$, $D_F = 0.07$, $D_E = 0.25$, $D_T = 0$, $D_{eF} = 0.18$, $D_{lF} = 0.15$, $D_{eE} = 0.22$, $D_{lF} = 0$. In **Ba**, the deletion of flexor activity was produced by applying additional excitatory drive $D_{add} = 0.1$ to population PF-E. Other drives were set at, $D_{RG-F} = 0.15$, $D_{RG-E} = 0.165$, $D_F = 0.25$, $D_E = 0.1$, $D_T = 0.1$, $D_{eF} = 0.12$, $D_{lF} = 0.18$, $D_{eE} = 0.15$, $D_{lF} = 0$. **Ca** and **Cb**: Experimental recordings corresponding to PBSt behavior simulated in **Ba** and **Bb**, respectively.
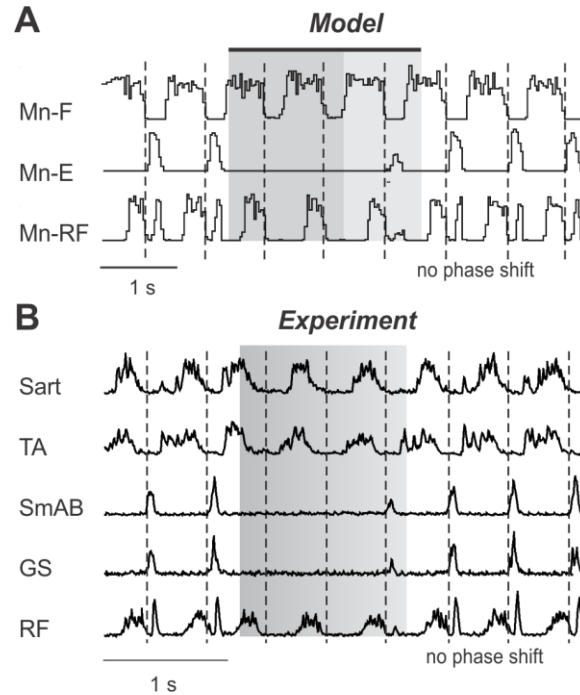
Figure 22. Simulation of biphasic RF behavior during a non-resetting extensor deletion

A: Simulation of biphasic RF (type 2) behavior during a non-resetting extensor deletion with rhythmically active flexors. In this simulation, $D_{RG-F} = 0.16$, $D_{RG-E} = 0.175$, $D_F = 0$, $D_E = 0.25$, $D_T = 0$, $D_{eF} = 0.2$, $D_{IF} = 0.2$, $D_{eE} = 0.12$, $D_{IF} = 0.25$. The deletion of extensor activity was produced by applying a temporary inhibitory drive to population PF-E (initially, $D_{add} = 0.7$) indicated by the black bar at the top of traces. During the deletion, Mn-RF maintained rhythmic activity but lost the extensor component it its activity profile. Shaded rectangles highlight the behavior of motoneuron populations during the deletion. The change in the shading level schematically shows a reduction of the additional inhibitory drive to the PF-E population by 70%. See text for details. **B**: The corresponding experimental recording during fictive locomotion. Before and after the deletion RF was active during both phases, exhibiting a short burst at the end of the extensor phase and a long flexor burst starting late in flexion. During the deletion extensors (SmAB and GS) were silent, flexors (Sart and TA) continued to be rhythmic, and RF also demonstrated rhythmic activity, however it lost its extensor component. Note the weak bursts of activity in extensors (SmAB and GS) and the weak extensor burst of RF at the end of the deletion. Vertical dashed lines show how no phase shift occurred during this deletion and therefore is non-resetting.

List of References

Andersson, O, Forssberg, H, Grillner, S and Wallen, P (1981). "Peripheral feedback mechanisms acting on the central pattern generators for locomotion in fish and cat." *Can J Physiol Pharmacol* **59**(7): 713-726.

Av-Ron, E (1994). "The role of a transient potassium current in a bursting neuron model." *J Math Biol* **33**(1): 71-87.

Barajon, I, Gossard, J P and Hultborn, H (1992). "Induction of fos expression by activity in the spinal rhythm generator for scratching." *Brain Res* **588**(1): 168-172.

Bard, P and Macht, M B (1958). Neurophysiological Basis of Behavior, 55. Churchill, London, G. E. W. Wolstenholme and C. M. O'Connor

Beato, M and Nistri, A (1999). "Interaction between disinhibited bursting and fictive locomotor patterns in the rat isolated spinal cord." *J Neurophysiol* **82**(5): 2029-2038.

Bellingham, M C (1998). "Driving respiration: the respiratory central pattern generator." *Clin Exp Pharmacol Physiol* **25**(10): 847-856.

Berkowitz, A (2002). "Both shared and specialized spinal circuitry for scratching and swimming in turtles." *J Comp Physiol A Neuroethol Sens Neural Behav Physiol* **188**(3): 225-234.

Berkowitz, A (2008). "Physiology and morphology of shared and specialized spinal interneurons for locomotion and scratching." *J Neurophysiol* **99**(6): 2887-2901.

Bjursten, L M, Norrsell, K and Norrsell, U (1976). "Behavioural repertory of cats without cerebral cortex from infancy." *Exp Brain Res* **25**(2): 115-130.

Booth, V, Rinzel, J and Kiehn, O (1997). "Compartmental model of vertebrate motoneurons for Ca2+-dependent spiking and plateau potentials under pharmacological treatment." *J Neurophysiol* **78**(6): 3371-3385.

Bracci, E, Ballerini, L and Nistri, A (1996). "Localization of rhythmogenic networks responsible for spontaneous bursts induced by strychnine and bicuculline in the rat isolated spinal cord." *J Neurosci* **16**(21): 7063-7076.

Brownstone, R M and Wilson, J M (2008). "Strategies for delineating spinal locomotor rhythm-generating networks and the possible role of Hb9 interneurones in rhythmogenesis." *Brain Res Rev* **57**(1): 64-76.

Burke, R E, Degtyarenko, A M and Simon, E S (2001). "Patterns of locomotor drive to motoneurons and last-order interneurons: clues to the structure of the CPG." *J Neurophysiol* **86**(1): 447-462.

Buschges, A, Akay, T, Gabriel, J P and Schmidt, J (2008). "Organizing network action for locomotion: insights from studying insect walking." *Brain Res Rev* **57**(1): 162-171.

Butera, R J, Jr., Rinzel, J and Smith, J C (1999). "Models of respiratory rhythm generation in the pre-Botzinger complex. I. Bursting pacemaker neurons." *J Neurophysiol* **82**(1): 382-397.

Butt, S J, Harris-Warrick, R M and Kiehn, O (2002). "Firing properties of identified interneuron populations in the mammalian hindlimb central pattern generator." *J Neurosci* **22**(22): 9961-9971.

Butt, S J and Kiehn, O (2003). "Functional identification of interneurons responsible for left-right coordination of hindlimbs in mammals." *Neuron* **38**(6): 953-963.

Butt, S J, Lundfald, L and Kiehn, O (2005). "EphA4 defines a class of excitatory locomotor-related interneurons." *Proc Natl Acad Sci U S A* **102**(39): 14098-14103.

Carlson-Kuhta, P, Trank, T V and Smith, J L (1998). "Forms of forward quadrupedal locomotion. II. A comparison of posture, hindlimb kinematics, and motor patterns for upslope and level walking." *J Neurophysiol* **79**(4): 1687-1701.

Carr, P A, Huang, A, Noga, B R and Jordan, L M (1995). "Cytochemical characteristics of cat spinal neurons activated during fictive locomotion." *Brain Res Bull* **37**(2): 213-218.

Christie, K J and Whelan, P J (2005). "Monoaminergic establishment of rostrocaudal gradients of rhythmicity in the neonatal mouse spinal cord." *J Neurophysiol* **94**(2): 1554-1564.

Cina, C and Hochman, S (2000). "Diffuse distribution of sulforhodamine-labeled neurons during serotonin-evoked locomotion in the neonatal rat thoracolumbar spinal cord." *J Comp Neurol* **423**(4): 590-602.

Clarac, F (2008). "Some historical reflections on the neural control of locomotion." *Brain Res Rev* **57**(1): 13-21.

Cowley, K C and Schmidt, B J (1995). "Effects of inhibitory amino acid antagonists on reciprocal inhibitory interactions during rhythmic motor activity in the in vitro neonatal rat spinal cord." *J Neurophysiol* **74**(3): 1109-1117.

Dai, X, Noga, B R, Douglas, J R and Jordan, L M (2005). "Localization of spinal neurons activated during locomotion using the c-fos immunohistochemical method." *J Neurophysiol* **93**(6): 3442-3452.

Darbon, P, Yvon, C, Legrand, J C and Streit, J (2004). "INaP underlies intrinsic spiking and rhythm generation in networks of cultured rat spinal cord neurons." *Eur J Neurosci* **20**(4): 976-988.

Delcomyn, F (1980). "Neural basis of rhythmic behavior in animals." *Science* **210**(4469): 492-498.

Dimitrijevic, M R, Gerasimenko, Y and Pinter, M M (1998). "Evidence for a spinal central pattern generator in humans." *Ann N Y Acad Sci* **860**: 360-376.

Duysens, J (1977). "Reflex control of locomotion as revealed by stimulation of cutaneous afferents in spontaneously walking premammillary cats." *J Neurophysiol* **40**(4): 737-751.

Duysens, J (2006). "How deletions in a model could help explain deletions in the laboratory." *J Neurophysiol* **95**(1): 562-563; author reply 563-565.

Edgerton, V R, Grillner, S, Sjostrom, A and Zangger, P (1976). Central generation of locomotion in vertebrates. Neural Control of Locomotion, 439-464. New York, Plenum Press

Eidelberg, E, Walden, J G and Nguyen, L H (1981). "Locomotor control in macaque monkeys." *Brain* **104**(Pt 4): 647-663.

Ekeberg, Ö (1993). "A combined neuronal and mechanical model of fish swimming." *Biological Cybernetics* **69**(5): 363-374.

Ekeberg, Ö, Lansner, A and Grillner, S (1995). "The neural control of fish swimming studied through numerical simulations." *Adapt. Behav.* **3**(4): 363-384.

Engberg, I and Lundberg, A (1969). "An electromyographic analysis of muscular activity in the hindlimb of the cat during unrestrained locomotion." *Acta Physiol Scand* **75**(4): 614-630.

Forssberg, H, Grillner, S and Halbertsma, J (1980). "The locomotion of the low spinal cat. I. Coordination within a hindlimb." *Acta Physiol Scand* **108**(3): 269-281.

Freusberg, A (1874). "Reflexbewegungen beim Hunde." *Pflügers Arch.* **9**: 358–391.

Garcia-Rill, E and Skinner, R D (1987). "The mesencephalic locomotor region. II. Projections to reticulospinal neurons." *Brain Res* **411**(1): 13-20.

Gerasimenko, Y, Roy, R R and Edgerton, V R (2008). "Epidural stimulation: comparison of the spinal circuits that generate and control locomotion in rats, cats and humans." *Exp Neurol* **209**(2): 417-425.

Getting, P A (1975). "Tritonia swimming: triggering of a fixed action pattern." *Brain Res* **96**(1): 128-133.

Gosgnach, S, Lanuza, G M, Butt, S J, Saueressig, H, Zhang, Y, Velasquez, T, Riethmacher, D, Callaway, E M, Kiehn, O and Goulding, M (2006). "V1 spinal neurons regulate the speed of vertebrate locomotor outputs." *Nature* **440**(7081): 215-219.

Graham Brown, T (1910). "Studies in the reflexes of the guinea-pig. V. Some experiments on the influence exercised by the higher centres upon the scratch-reflex." *Q. J. Exp. Physiol.* **3**: 319–353.

Graham Brown, T (1911a). "The intrinsic factors in the act of progression in mammals." *Proc. R. Soc. B.* **84**: 308-319.

Graham Brown, T (1911b). "Studies in the physiology of the nervous system. VII. Movements under narcosis in the pigeon. Movements under narcosis in the rabbit–progression–scratching–flexion." *Q. J. Exp. Physiol.* **4**: 151–182.

Graham Brown, T (1913). "The phenomenon of "narcosis progression" in mammals." *Proc. R. Soc. B.* **86**: 140-164.

Graham Brown, T (1914). "On the nature of the fundemental activity of the nervous centres: together with an analysis of the conditioning of rhythmic activity in progression, and a theory of the evolution of function in the nervous system." *J. Physiol* **48**: 18-41.

Grillner, S (1969). "The influence of DOPA on the static and the dynamic fusimotor activity to the triceps surae of the spinal cat." *Acta Physiol Scand* **77**(4): 490-509.

Grillner, S and Zangger, P (1974). "Locomotor movements generated by the deafferented spinal cord." *Acta Physiol Scand* **91**: 38A-39A.

Grillner, S (1975). "Locomotion in vertebrates: central mechanisms and reflex interaction." *Physiol Rev* **55**(2): 247-304.

Grillner, S and Zangger, P (1975). "How detailed is the central pattern generation for locomotion?" *Brain Res* **88**(2): 367-371.

Grillner, S and Zangger, P (1979). "On the central generation of locomotion in the low spinal cat." *Exp Brain Res* **34**(2): 241-261.

Grillner, S (1981). Control of locomotion in bipeds, tetrapods, and fish. Handbook of Physiology. Section I: The Nervous System. (Brooks V, Ed), 1179-1236. Bethesda, MD, American Physiology Society

Grillner, S and Wallen, P (1982). "On peripheral control mechanisms acting on the central pattern generators for swimming in the dogfish." *J Exp Biol* **98**: 1-22.

Grillner, S and Zangger, P (1984). "The effect of dorsal root transection on the efferent motor pattern in the cat's hindlimb during locomotion." *Acta Physiol Scand* **120**(3): 393-405.

Grillner, S (1985). "Neurobiological bases of rhythmic motor acts in vertebrates." *Science* **228**(4696): 143-149.

Grillner, S and Wallen, P (1985). "Central pattern generators for locomotion, with special reference to vertebrates." *Annu Rev Neurosci* **8**: 233-261.

Grillner, S, Deliagina, T, Ekeberg, O, el Manira, A, Hill, R H, Lansner, A, Orlovsky, G N and Wallen, P (1995). "Neural networks that co-ordinate locomotion and body orientation in lamprey." *Trends Neurosci* **18**(6): 270-279.

Grillner, S, Parker, D and el Manira, A (1998). "Vertebrate locomotion--a lamprey perspective." *Ann N Y Acad Sci* **860**: 1-18.

Grillner, S and Wallen, P (2002). "Cellular bases of a vertebrate locomotor system-steering, intersegmental and segmental co-ordination and sensory control." *Brain Res Brain Res Rev* **40**(1-3): 92-106.

Grillner, S (2003). "The motor infrastructure: from ion channels to neuronal networks." *Nat Rev Neurosci* **4**(7): 573-586.

Grillner, S, Wallen, P, Saitoh, K, Kozlov, A and Robertson, B (2008). "Neural bases of goal-directed locomotion in vertebrates--an overview." *Brain Res Rev* **57**(1): 2-12.

Guertin, P, Angel, M J, Perreault, M C and McCrea, D A (1995). "Ankle extensor group I afferents excite extensors throughout the hindlimb during fictive locomotion in the cat." *J Physiol* **487 (Pt 1)**: 197-209.

Guertin, P A (2009). "The mammalian central pattern generator for locomotion." *Brain Res Rev* **62**(1): 45-56.

Guertin, P A and Steuer, I (2009). "Key central pattern generators of the spinal cord." *J Neurosci Res* **87**(11): 2399-2405.

Gurfinkel, V S and Shik, M L (1973). The control of posture and locomotion. Motor control, 217–234. New York, Plenum Press

Halbertsma, J M (1983). "The stride cycle of the cat: the modelling of locomotion by computerized analysis of automatic recordings." *Acta Physiol Scand Suppl* **521**: 1-75.

Hinckley, C A, Hartley, R, Wu, L, Todd, A and Ziskind-Conhaim, L (2005). "Locomotor-like rhythms in a genetically distinct cluster of interneurons in the mammalian spinal cord." *J Neurophysiol* **93**(3): 1439-1449.

Hooper, S L and DiCaprio, R A (2004). "Crustacean motor pattern generator networks." *Neurosignals* **13**(1-2): 50-69.

Huguenard, J R and McCormick, D A (1991). Vclamp and Cclamp. A Computational Simulation of Single Thalamic Relay and Cortical Pyramidal Neurons. Neural Simulation Instruction Manual. Stanford, CA, Stanford Univ.

Huguenard, J R and McCormick, D A (1992). "Simulation of the currents involved in rhythmic oscillations in thalamic relay neurons." *J Neurophysiol* **68**(4): 1373-1383.

Hultborn, H and Nielsen, J B (2007). "Spinal control of locomotion--from cat to man." *Acta Physiol (Oxf)* **189**(2): 111-121.

Jankowska, E, Jukes, M G, Lund, S and Lundberg, A (1967a). "The effect of DOPA on the spinal cord. 6. Half-centre organization of interneurones transmitting effects from the flexor reflex afferents." *Acta Physiol Scand* **70**(3): 389-402.

Jankowska, E, Jukes, M G, Lund, S and Lundberg, A (1967b). "The effect of DOPA on the spinal cord. 5. Reciprocal organization of pathways transmitting excitatory action to alpha motoneurones of flexors and extensors." *Acta Physiol Scand* **70**(3): 369-388.

Jankowska, E (1992). "Interneuronal relay in spinal pathways from proprioceptors." *Prog Neurobiol* **38**(4): 335-378.

Jiang, Z, Carlin, K P and Brownstone, R M (1999). "An in vitro functionally mature mouse spinal cord preparation for the study of spinal motor networks." *Brain Res* **816**(2): 493-499.

Jordan, L M (1991). Brainstem and spinal cord mechanisms for the initiation of locomotion. Neurobiological Basis of Human Locomotion, p. 3-19. Tokyo, Japan Scientific Press

Jordan, L M, Brownstone, R M and Noga, B R (1992). "Control of functional systems in the brainstem and spinal cord." *Curr Opin Neurobiol* **2**(6): 794-801.

Jordon, L M (1991). Brainstem and spinal cord mechanisms for the initiation of locomotion. Neurobiological basis of human locomotion, 3-20. Tokyo, Japan Sci. Soc. Press

Kiehn, O and Kjaerulff, O (1996). "Spatiotemporal characteristics of 5-HT and dopamine-induced rhythmic hindlimb activity in the in vitro neonatal rat." *J Neurophysiol* **75**(4): 1472-1482.

Kiehn, O and Butt, S J (2003). "Physiological, anatomical and genetic identification of CPG neurons in the developing mammalian spinal cord." *Prog Neurobiol* **70**(4): 347-361.

Kiehn, O (2006). "Locomotor circuits in the mammalian spinal cord." *Annu Rev Neurosci* **29**: 279-306.

Kiehn, O, Quinlan, K A, Restrepo, C E, Lundfald, L, Borgius, L, Talpalar, A E and Endo, T (2008). "Excitatory components of the mammalian locomotor CPG." *Brain Res Rev* **57**(1): 56-63.

Kjaerulff, O, Barajon, I and Kiehn, O (1994). "Sulphorhodamine-labelled cells in the neonatal rat spinal cord following chemically induced locomotor activity in vitro." *J Physiol* **478 (Pt 2)**: 265-273.

Kjaerulff, O and Kiehn, O (1996). "Distribution of networks generating and coordinating locomotor activity in the neonatal rat spinal cord in vitro: a lesion study." *J Neurosci* **16**(18): 5777-5794.

Kriellaars, D J (1992). Generation and peripheral control of locomotor rhythm. Winnipeg, University of Manitoba.

Kriellaars, D J, Brownstone, R M, Noga, B R and Jordan, L M (1994). "Mechanical entrainment of fictive locomotion in the decerebrate cat." *J Neurophysiol* **71**(6): 2074-2086.

Kristan, W B and Weeks, J C (1983). Neurons controlling the initiation, generation and modulation of leech swimming. <u>Neural origin of rhythmic movements.</u> Cambridge, Cambridge University Press

Krouchev, N, Kalaska, J F and Drew, T (2006). "Sequential activation of muscle synergies during locomotion in the intact cat as revealed by cluster analysis and direct decomposition." *J Neurophysiol* **96**(4): 1991-2010.

Kudo, N and Yamada, T (1987). "N-methyl-D,L-aspartate-induced locomotor activity in a spinal cord-hindlimb muscles preparation of the newborn rat studied in vitro." *Neurosci Lett* **75**(1): 43-48.

Lafreniere-Roula, M and McCrea, D A (2005). "Deletions of rhythmic motoneuron activity during fictive locomotion and scratch provide clues to the organization of the mammalian central pattern generator." *J Neurophysiol* **94**(2): 1120-1132.

Langlet, C, Leblond, H and Rossignol, S (2005). "Mid-lumbar segments are needed for the expression of locomotion in chronic spinal cats." *J Neurophysiol* **93**(5): 2474-2488.

Lanuza, G M, Gosgnach, S, Pierani, A, Jessell, T M and Goulding, M (2004). "Genetic identification of spinal interneurons that coordinate left-right locomotor activity necessary for walking movements." *Neuron* **42**(3): 375-386.

Lee, R H and Heckman, C J (2001). "Essential role of a fast persistent inward current in action potential initiation and control of rhythmic firing." *J Neurophysiol* **85**(1): 472-475.

Lundberg, A (1981). Half-centres revisited. <u>Regulatory Functions of the CNS. Motion and Organization Principles</u>, 155-167. Budapest, Pergamon Akadem Kiado

Lundfald, L, Restrepo, C E, Butt, S J, Peng, C Y, Droho, S, Endo, T, Zeilhofer, H U, Sharma, K and Kiehn, O (2007). "Phenotype of V2-derived interneurons and their relationship to the axon guidance molecule EphA4 in the developing mouse spinal cord." *Eur J Neurosci* **26**(11): 2989-3002.

MacGregor, R I (1987). <u>Neural and Brain Modelling</u>. New York, Academic Press.

Markin, S N, Griffel, B, Lemay, M A, Prilutsky, B I, McCrea, D A and Rybak, I A (2007). <u>Analysis of hindlimb motoneuron activity during fictive locomotion in cat and</u>

identification of possible motor synergies controlled by locomotor CPG. Society for Neuroscience Meeting, San Diego.

Markin, S N, Lemay, M A, Ollivier-Lanvin, K, Prilutsky, B I, McCrea, D A and Rybak, I A (2008). Comparison of hindlimb motoneuron activities during fictive and normal locomotion in the cat. Society for Neuroscience Meeting, Washington D.C.

McCrea, D A (2001). "Spinal circuitry of sensorimotor control of locomotion." *J Physiol* **533**(Pt 1): 41-50.

McCrea, D A and Rybak, I A (2007). "Modeling the mammalian locomotor CPG: insights from mistakes and perturbations." *Prog Brain Res* **165**: 235-253.

McCrea, D A and Rybak, I A (2008). "Organization of mammalian locomotor rhythm and pattern generation." *Brain Res Rev* **57**(1): 134-146.

McKenna, K E, Chung, S K and McVary, K T (1991). "A model for the study of sexual function in anesthetized male and female rats." *Am J Physiol* **261**(5 Pt 2): R1276-1285.

Miller, S and Scott, P D (1977). "The spinal locomotor generator." *Exp Brain Res* **30**(2-3): 387-403.

Minassian, K, Persy, I, Rattay, F, Pinter, M M, Kern, H and Dimitrijevic, M R (2007). "Human lumbar cord circuitries can be activated by extrinsic tonic input to generate locomotor-like activity." *Hum Mov Sci* **26**(2): 275-295.

Mori, S (1987). "Integration of posture and locomotion in acute decerebrate cats and in awake, freely moving cats." *Prog Neurobiol* **28**(2): 161-195.

Mori, S, Sakamoto, T and Takakusaki, K (1991). Interactions of posture and locomotion in cats: its automatic and volitional control aspects. Neurobiological basis of human locomotion, 21-32. Tokyo, Scientific societies press

Nadelhaft, I and Vera, P L (1995). "Central nervous system neurons infected by pseudorabies virus injected into the rat urinary bladder following unilateral transection of the pelvic nerve." *J Comp Neurol* **359**(3): 443-456.

Nakamura, Y and Katakura, N (1995). "Generation of masticatory rhythm in the brainstem." *Neurosci Res* **23**(1): 1-19.

Nishimaru, H, Takizawa, H and Kudo, N (2000). "5-Hydroxytryptamine-induced locomotor rhythm in the neonatal mouse spinal cord in vitro." *Neurosci Lett* **280**(3): 187-190.

Noga, B R, Shefchyk, S J, Jamal, J and Jordan, L M (1987). "The role of Renshaw cells in locomotion: antagonism of their excitation from motor axon collaterals with intravenous mecamylamine." *Exp Brain Res* **66**(1): 99-105.

Noga, B R, Kriellaars, D J, Brownstone, R M and Jordan, L M (2003). "Mechanism for activation of locomotor centers in the spinal cord by stimulation of the mesencephalic locomotor region." *J Neurophysiol* **90**(3): 1464-1478.

Orlovsky, G N (1969). "Spontaneous and induced locomotion of the thalamic cat." *Biophysics* **14**: 1154–1162.

Orlovsky, G N, T., D and Grillner, S (1999). Neural control of locomotion: from mollusc to man. New York, Oxford University Press.

Orsal, D, Perret, C and Cabelguen, J M (1986). "Evidence of rhythmic inhibitory synaptic influences in hindlimb motoneurons during fictive locomotion in the thalamic cat." *Exp Brain Res* **64**(1): 217-224.

Orsal, D, Cabelguen, J M and Perret, C (1990). "Interlimb coordination during fictive locomotion in the thalamic cat." *Exp Brain Res* **82**(3): 536-546.

Pearson, K G and Duysens, J (1976). Function of segmental reflexes in the control of stepping in cockroaches and cats. Neural Control of Locomotion. New York, Plenum Press

Perreault, M C, Angel, M J, Guertin, P and McCrea, D A (1995). "Effects of stimulation of hindlimb flexor group II afferents during fictive locomotion in the cat." *J Physiol* **487 (Pt 1)**: 211-220.

Perret, C and Cabelguen, J M (1980). "Main characteristics of the hindlimb locomotor cycle in the decorticate cat with special reference to bifunctional muscles." *Brain Res* **187**(2): 333-352.

Perret, C (1983). "Centrally generated pattern of motoneuron activity during locomotion in the cat." *Symp Soc Exp Biol* **37**: 405-422.

Perret, C, Cabelguen, J M and Orsal, D (1988). Analysis of the pattern of activity in "knee flexor" motoneurons during locomotion in the cat. Stance and Motion: Facts and Concepts, 133–141. New York, Plenum Press

Philippson, M (1905). "L'autonomie et la centralisation dans le système nerveux des animaux [Autonomy and centralization in the animal nervous system]." *Trav. Lab. Physiol. Inst. Solvay* **7**: 1-208.

Pratt, C A and Jordan, L M (1987). "Ia inhibitory interneurons and Renshaw cells as contributors to the spinal mechanisms of fictive locomotion." *J Neurophysiol* **57**(1): 56-71.

Pratt, C A, Buford, J A and Smith, J L (1996). "Adaptive control for backward quadrupedal walking V. Mutable activation of bifunctional thigh muscles." *J Neurophysiol* **75**(2): 832-842.

Robertson, R M and Pearson, K G (1985). "Neural circuits in the flight system of the locust." *J Neurophysiol* **53**(1): 110-128.

Rossignol, S (1996). Neural control of stereotypic limb movements. Handbook of physiology. Section 12: Exercise: Regulation and integration of multiple systems. (Rowell LB, Sheperd JT, eds), 173-216, American Physiological Society

Rossignol, S, Barriere, G, Frigon, A, Barthelemy, D, Bouyer, L, Provencher, J, Leblond, H and Bernard, G (2008). "Plasticity of locomotor sensorimotor interactions after peripheral and/or spinal lesions." *Brain Res Rev* **57**(1): 228-240.

Rybak, I, Shevtsova, N, Lafreniere-Roula, M and McCrea, D (2006a). "Modelling spinal circuitry involved in locomotor pattern generation: insights from deletions during fictive locomotion." *J Physiol* **577**(Pt 2): 617-639.

Rybak, I, Stecina, K, Shevtsova, N and McCrea, D (2006b). "Modelling spinal circuitry involved in locomotor pattern generation: insights from the effects of afferent stimulation." *J Physiol* **577**(Pt 2): 641-658.

Rybak, I A, Paton, J F and Schwaber, J S (1997). "Modeling neural mechanisms for genesis of respiratory rhythm and pattern. II. Network models of the central respiratory pattern generator." *J Neurophysiol* **77**(4): 2007-2026.

Rybak, I A, Shevtsova, N A, St-John, W M, Paton, J F and Pierrefiche, O (2003). "Endogenous rhythm generation in the pre-Botzinger complex and ionic currents: modelling and in vitro studies." *Eur J Neurosci* **18**(2): 239-257.

Safronov, B V and Vogel, W (1995). "Single voltage-activated Na+ and K+ channels in the somata of rat motoneurones." *J Physiol* **487 (Pt 1)**: 91-106.

Schroder, H D (1985). "Anatomical and pathoanatomical studies on the spinal efferent systems innervating pelvic structures. 1. Organization of spinal nuclei in animals. 2. The nucleus X-pelvic motor system in man." *J Auton Nerv Syst* **14**(1): 23-48.

Selverston, A I (2005). "A neural infrastructure for rhythmic motor patterns." *Cell Mol Neurobiol* **25**(2): 223-244.

Sherrington, C S (1906). "Observations on the scratch-reflex in the spinal dog." *J Physiol* **34**(1-2): 1-50.

Sherrington, C S (1910a). "Flexion-reflex of the limb, crossed extension-reflex, and reflex stepping and standing." *J Physiol* **40**(1-2): 28-121.

Sherrington, C S (1910b). "Note on the scratch-reflex of the cat." *Q. J. Exp. Physiol.* **3**: 213-220.

Sherrington, C S (1910c). "Remarks on reflex mechanisms of the step." *Brain* **33**: 1-25.

Sherrington, C S (1913). "Further observations on the production of reflex stepping by combination of reflex excitation with reflex inhibition." *J Physiol* **47**(3): 196-214.

Shik, M L, Orlovsky, G N and Severin, F V (1966a). "Organization of locomotor synergy." *Biophysics* **11**: 879-886.

Shik, M L, Severin, F V and Orlovskii, G N (1966b). "Control of walking and running by means of electric stimulation of the midbrain." *Biofizika* **11**(4): 659-666.

Shik, M L, Severin, F V and Orlovskii, G N (1967). "Structures of the brain stem responsible for evoked locomotion." *Fiziol Zh SSSR Im I M Sechenova* **53**(9): 1125-1132.

Shik, M L and Orlovsky, G N (1976). "Neurophysiology of locomotor automatism." *Physiol Rev* **56**(3): 465-501.

Shurrager, P S and Dykman, R A (1951). "Walking spinal carnivores." *J Comp Physiol Psychol* **44**(3): 252-262.

Sirota, M G and Shik, M L (1973). "The cat locomotion elicited through the electrode implanted in the midbrain." *Sechenov Physiol. J* **59**: 1314-1321.

Smith, J C and Feldman, J L (1987). "In vitro brainstem-spinal cord preparations for study of motor systems for mammalian respiration and locomotion." *J Neurosci Methods* **21**(2-4): 321-333.

Smith, J C, Ellenberger, H H, Ballanyi, K, Richter, D W and Feldman, J L (1991). "Pre-Botzinger complex: a brainstem region that may generate respiratory rhythm in mammals." *Science* **254**(5032): 726-729.

Smith, J L and Carlson-Kuhta, P (1995). "Unexpected motor patterns for hindlimb muscles during slope walking in the cat." *J Neurophysiol* **74**(5): 2211-2215.

Smith, J L, Carlson-Kuhta, P and Trank, T V (1998). "Forms of forward quadrupedal locomotion. III. A comparison of posture, hindlimb kinematics, and motor patterns for downslope and level walking." *J Neurophysiol* **79**(4): 1702-1716.

Stecina, K, Quevedo, J and McCrea, D A (2005). "Parallel reflex pathways from flexor muscle afferents evoking resetting and flexion enhancement during fictive locomotion and scratch in the cat." *J Physiol* **569**(Pt 1): 275-290.

Stein, P S (1971). "Intersegmental coordination of swimmeret motoneuron activity in crayfish." *J Neurophysiol* **34**(2): 310-318.

Stein, P S and Grossman, M L (1980). "Central program for scratch reflex in turtle." *J. Comp. Physiol.* **140**: 287-294.

Stein, P S (2005). "Neuronal control of turtle hindlimb motor rhythms." *J Comp Physiol A Neuroethol Sens Neural Behav Physiol* **191**(3): 213-229.

Stein, P S (2008). "Motor pattern deletions and modular organization of turtle spinal cord." *Brain Res Rev* **57**(1): 118-124.

Streit, J, Tscherter, A and Darbon, P (2005). Rhythm generation in spinal culture. Is it the neuron or the network? Neurons, Networks, Motor Behavior, 61-73. Cambridge, MA, MIT Press

Stuart, D G (2007). "Reflections on integrative and comparative movement neuroscience." *Integr. Comp. Biol.*: icm037.

Stuart, D G and Hultborn, H (2008). "Thomas Graham Brown (1882--1965), Anders Lundberg (1920-), and the neural control of stepping." *Brain Res Rev* **59**(1): 74-95.

Sugaya, K, Roppolo, J R, Yoshimura, N, Card, J P and de Groat, W C (1997). "The central neural pathways involved in micturition in the neonatal rat as revealed by the injection of pseudorabies virus into the urinary bladder." *Neurosci Lett* **223**(3): 197-200.

Syed, N I, Bulloch, A G and Lukowiak, K (1990). "In vitro reconstruction of the respiratory central pattern generator of the mollusk Lymnaea." *Science* **250**(4978): 282-285.

Szekely, G, Czeh, G and Voros, G (1969). "The activity pattern of limb muscles in freely moving normal and deafferented newts." *Exp Brain Res* **9**(1): 53-72.

Truitt, W A and Coolen, L M (2002). "Identification of a potential ejaculation generator in the spinal cord." *Science* **297**(5586): 1566-1569.

Viala, D, Buisseret-Delmas, C and Portal, J J (1988). "An attempt to localize the lumbar locomotor generator in the rabbit using 2-deoxy-[14C]glucose autoradiography." *Neurosci Lett* **86**(2): 139-143.

Vizzard, M A, Erickson, V L, Card, J P, Roppolo, J R and de Groat, W C (1995). "Transneuronal labeling of neurons in the adult rat brainstem and spinal cord after injection of pseudorabies virus into the urethra." *J Comp Neurol* **355**(4): 629-640.

Wieder, J A, Brackett, N L, Lynne, C M, Green, J T and Aballa, T C (2000). "Anesthetic block of the dorsal penile nerve inhibits vibratory-induced ejaculation in men with spinal cord injuries." *Urology* **55**(6): 915-917.

Wilson, J M, Cowan, A I and Brownstone, R M (2007). "Heterogeneous electrotonic coupling and synchronization of rhythmic bursting activity in mouse Hb9 interneurons." *J Neurophysiol* **98**(4): 2370-2381.

Yakovenko, S, McCrea, D A, Stecina, K and Prochazka, A (2005). "Control of locomotor cycle durations." *J Neurophysiol* **94**(2): 1057-1065.

Zhang, Y, Narayan, S, Geiman, E, Lanuza, G M, Velasquez, T, Shanks, B, Akay, T, Dyck, J, Pearson, K, Gosgnach, S, Fan, C M and Goulding, M (2008). "V3 spinal neurons establish a robust and balanced locomotor rhythm during walking." *Neuron* **60**(1): 84-96.

Vita

Khaldoun Hamade (06/25/1981) graduated with high distinction and received a Bachelor of Science in Biology from the American University of Beirut (Lebanon) in 2002. Since 2004 he was a Ph.D candidate in Biomedical Engineering at Drexel University, School of Biomedical Engineering Sciences and health systems, Philadelphia, PA (USA), under the supervision of I. A. Rybak, Ph.D.

Khaldoun received a Neuroengineering Research Award on July 2009, during the Drexel Neuronengineering: Planning for the Future research event (Philadelphia, PA).

Khaldoun gained research experience, under the supervision of I. A. Rybak, Ph.D, as a research assistant and graduate research fellow working on modeling of the locomotor CPG (2006-2010). He was also a research assistant, under the supervision of Dr. Bishara Atiyeh and Dr. Abdo Jurjus, studying the effectiveness of different skin burn medications (2003-2004).

Select Publications:

K. Hamade, N. Shevtsova, S. Markin, S. Chakrabarty, D. McCrea, I. Rybak. How a bipartite CPG can control the activity of bifunctional motoneurons: a modeling study with insights from deletions during fictive locomotion. Society for Neuroscience 2008 meeting, Washington DC. November 2008

N. Shevtsova, S. Chakrabarty, K. Hamade, S. Markin, D. McCrea, I. Rybak. Computational model of mammalian locomotor CPG reproducing firing patterns of flexor, extensor and bifunctional motoneurons during fictive locomotion. Society for Neuroscience 2007 meeting, San Diego, Ca. November 2007

B. Atiyeh, S. Hayek, R. Atiyeh, I. Abdallah, K. Hamade, A. Jurjus. Cicatrisation des Plaies et Onguent pour les Brulures Exposees Humides (MEBO) (Wound Healing and Moist Exposed Burn Ointment). Journal des Plaies et Cicatrisation 9:7-13,2005